Control and Prevention of Ice Formation on the Surface of an Aluminum Alloy

Rahimi, Maral

DOI (link to publication from Publisher):
10.5278/vbn.phd.engsci.00173

Publication date:
2016

Document Version
Publisher's PDF, also known as Version of record

CONTROL AND PREVENTION OF ICE FORMATION ON THE SURFACE OF AN ALUMINUM ALLOY

BY
MARAL RAHIMI

DISSERTATION SUBMITTED 2016

AALBORG UNIVERSITY
DENMARK

CONTROL AND PREVENTION OF ICE FORMATION ON THE SURFACE OF AN ALUMINUM ALLOY

by

Maral Rahimi

AALBORG UNIVERSITY
DENMARK

Dissertation submitted

Dissertation submitted:	December, 2016
PhD supervisor:	Prof. Alireza Afshari Aalborg University, Copenhagen, Denmark
Assistant PhD supervisor:	Associate Prof. Peter Fojan Aalborg University, Denmark
PhD committee:	Senior Researcher Eva B. Møller (chairman) Aalborg University, Denmark
	Professor Erik Dahlquist Mälardalen University, Sweden
	Associate Professor Rafael Taboryski Technical University of Denmark, Denmark
PhD Series:	Faculty of Engineering and Science, Aalborg University

ISSN (online): 2246-1248
ISBN (online): 978-87-7112-845-1

Published by:
Aalborg University Press
Skjernvej 4A, 2nd floor
DK – 9220 Aalborg Ø
Phone: +45 99407140
aauf@forlag.aau.dk
forlag.aau.dk

Printed in Denmark by Rosendahls, 2016

PREFACE

This PhD thesis represents the work done during my PhD study at the Department of Energy and Environment, the Danish Building Research Institute (SBi), Aalborg University, Denmark and the Department of Physics and Nanotechnology at Aalborg University, Denmark. The final year of my PhD studies was spent in the Department of Chemistry at Technical University of Denmark (DTU), Denmark

The PhD dissertation includes 5 supporting papers which are incorporated in Chapter 3 of the thesis. Four of the supporting papers are published in international peer-reviewed journals, and one is published in a peer-reviewed conference proceeding.

The first part of this PhD study addresses the effects of aluminium surface morphology and chemical modification on wettability and was carried out in the laboratories of the BioPhysics' Group, the Department of Physics and Nanotechnology, Aalborg University. The second part of the study focuses on the effect of surface modification on initial ice formation on aluminum surfaces and was carried out in the Air Quality Laboratory at the Danish Building Research Institute/Aalborg University. The final part of the study, addressing the effect of surface chemistry on ice nucleation and freezing delay, was carried out in the laboratories of the Group of Polymers and Functional Interfaces at the Department of Chemistry, Technical University of Denmark.

STRUCTURE OF THESIS

Chapter 1 is allocated to the introduction. In the introduction section, the problems related to ice formation in air-to-air heat exchangers are presented. The relevant theories on surface characterization and morphology, including surface roughness energy and wettability and their effect on ice nucleation, formation, structure, growth and freezing delay are introduced. Moreover, state of the art results within this area are discussed and compared with the acquired results of this study.

Chapter 2 is allocated to the material and methodology of the study and covers sample surface preparation, modifications, and the implemented experimental procedures together with descriptions of experimental setups.

Chapter 3 presents the obtained experimental results. The results are further discussed and put into perspective. In order to prevent duplication of already published manuscripts, the research papers are attached to the thesis and form the basis for the discussion.

Chapter 4 summarizes the conclusions obtained from the studies. It also includes suggestions for future work to advance the knowledge in the field of ice prevention on heat exchangers.

ENGLISH SUMMARY

In cold climates, mechanical ventilation systems with heat recovery, e.g. air-to-air exchangers, are often used to reduce energy demand for heating by recovering the heat from the exhausted air. This, however, creates a risk of ice accretion on the fins of the heat exchanger as warm and humid exhausted air cools down. Due to the reduction in heat exchanger efficiency due to ice formation, this phenomenon has been studied for many decades. There are two approaches to controlling ice formation on heat exchangers: active and passive. The active methods, e.g. bypass, recirculation, preheating etc., require energy and consequently reduce the overall efficiency of the system. They are not addressed in this work and have already been studied extensively by many researchers. The passive methods, which are related to the surface characteristics of the heat exchanger fins and their effect on the initial phases of ice formation, are the main focus of this PhD study. Since aluminum alloys are commonly used to build air-to-air heat exchangers, their surface characteristics play a crucial role in ice nucleation, formation and accretion. This study is specifically focused on aluminum alloy 8011.

Aluminum and its alloys are expected to possess a high energy surface; however, measurements show that the actual surface exhibits a rather high contact angle of about 78 degrees, which is presumably related to surface contamination. In this PhD study, several types of surface modifications were developed that allowed us to obtain stable hydrophilic and hydrophobic surfaces with the contact angles varying from 12° to more than 120°. The effects of these modifications on surface morphology and wettability—the main parameters determining ice nucleation, formation, accretion and freezing delay—were studied comprehensively. In particular, it was found in the first part of study that flat hydrophobic surfaces exhibit slower ice growth and denser ice layers, making this type of treatment preferable for aluminum heat exchangers. Moreover, observations show that the bare aluminum surfaces are characterized by faster ice growth and less dense ice layer as compared to hydrophilically and hydrophobically modified aluminum surfaces. This commonly observed phenomenon can be attributed to the heterogeneous character of bare aluminum surfaces, leading to a broad distribution of surface energies on the microscopic scale. Upon even minor cooling below the freezing point, this leads to the nucleation of widely separated water droplets/ice crystals on high-energy nucleation centers and the formation of low-density feather-like ice structures, hence this significantly deteriorates the performance of heat exchangers with aluminum fins.

Furthermore, the freezing delay and wettability of chemically modified aluminum surface as a function of the substrate temperature was studied. Comparison of the observed behavior with the predictions of the heterogeneous ice nucleation theory showed that a slightly hydrophilic substrate modified with (3-aminopropyl) triethoxy silane (APTES) exhibited longer freezing delays as compared to both more hydrophilic and more hydrophobic substrates. This is attributed to a particular surface chemistry of the APTES modification that prevents ice formation at the interface of the substrate due to presence of high local ion concentration (amino groups), hence leading to significant freezing point suppression. Furthermore, the results suggest that surface topography and wettability determine the freezing kinetics of a droplet placed on a precooled sample. Therefore, surface chemistry which may change these surface characteristics can be used as a tool to control the actual wetting properties of a cold surface in a humid atmosphere.

On the basis of the findings and observations of this study, we find that tailoring the surface characteristics through the application of different chemical or mechanical methods is an effective method for changing the icing properties of a surface. Future studies might focus on studying the effect of different surface coatings with ion concentration on ice formation kinetics.

DANSK RESUME

I kolde klimaer anvendes ofte mekanisk ventilation med varmegenvinding, for eksempel luft-til-luft varmevekslere, for at reducere energibehovet til opvarmning ved at genvinde varmen i udsugningsluften. Dette indebærer imidlertid en risiko for isdannelse på varmegenvinderen, idet den varme og fugtige indeluft afkøles. Fænomenet har været undersøgt i årtider da isdannelsen har en negativ indvirkning på varmegenvinderens effektivitet. Forebyggelse og bekæmpelse af isdannelse på varmegenvindere kan ske via to metoder betegnet henholdsvis som aktive metoder og passive metoder. De aktive metoder, for eksempel bypass, recirkulation og forvarmning, kræver energitilførsel, som dermed reducerer den samlede effektivitet af systemet. Aktive metoder er ikke behandlet i dette arbejde; metoderne har varit grundigt undersøgt tidligere. Fokus for dette ph.d.-studium er passive metoder, som er relateret til varmegenvinderens overfladeegenskaber og overfladernes virkning på de indledende faser af isdannelse. Da aluminiumlegeringer almindeligvis anvendes til fremstilling af luft-til-luft varmegenvindere, spiller deres overfladekarakteristika en afgørende rolle for isdannelsen. Denne undersøgelse er specielt fokuseret på aluminiumslegering 8011.

Aluminium og aluminiumlegeringer forventes at besidde en høj overflade energi mens målingerne viser en temmelig høj kontaktvinkel for vand på ca. 78 grader, hvilket formentlig er relateret til snavs på overflade.

Aluminium og aluminiumlegeringer må antages at have en høj overfladeenergi, men målingerne viser imidlertid, at den aktuelle overflade har en forholdsvis stor kontaktvinkel på ca. 78°, som formodentlig må tilskrives overfladeforurening.

I dette ph.d.-studium blev der udviklet flere forskellige overflademodifikationer, som tillod stabile, hydrofile og hydrofobe overflader med kontaktvinkler varierende fra 12° til mere end 120°. Der er gennemført omfattende undersøgelser af effekten af modifikationerne på overflademorfologien og befugtningsevnen, som er vigtige parametre for nuklering, isdannelse, tilvækst og kinetik. Det blev fundet, at på flade, hydrofobe overflader forekommer istilvækst langsommere, og giver et tættere islag end hydrofile overflader. Denne type av behandling er således at foretrække for aluminiumvarmegenvindere. Desuden blev det observeret, at en bar aluminiumoverflade er kendetegnet ved en hurtigere istilvækst og et mindre tæt islag sammenlignet med en hydrofil og hydrofobt modificeret aluminiumoverflade. Dette almindeligt observerede fænomen kan tilskrives den heterogene karakter af en bar aluminiumoverflade, hvilket fører til en bred fordeling af overfladeenergi i mikroskopisk skala. Dette fører til kimdannelse af adskilte vanddråber/iskrystaller på højenergi partikeldannende centre selv ved mindre afkøling under frysepunktet og dannelse af lavdensitets fjerlignende isstrukturer. Dette fører til en betydelig forringelse af effektiviteten af aluminiumvarmegenvindere.

Endvidere blev nedfrysning kinetikken og befugtningsgraden af kemiskmodificeret aluminiumsoverflade som en funktion af substratet temperatur undersøgt. En sammenligning mellem den observerede adfærd og forudsigelser baseret på en teori for såkaldt heterogen isnukleering viste, at et svagt hydrofil substrat modificeret med (3-aminopropyl) triethoxysilan (APTES) havde længere frysningsforsinkelser end både mere hydrofile og mere hydrofobe substrater. Dette blev tilskrevet en bestemt type overfladekemi - APTES - som forhindrer isdannelse ved grænsefladen af substratet på grund af tilstedeværelsen af en høj lokal ionkoncentration (aminogrupper) hvilkeførte til en betydelig frysepunktsænkning. Endvidere blev det fastslået at overfladentopografien og befugtningsgraden kan bestemme indefrysningskinetikken for en dråbe som anbringes på en i forvejen afkølet prøve. Derfor kan overfladekemien anvendes som et redskab til at styre befugtningsegenskaber på en kold overflade i en fugtig atmosfære.

Ændring overfladeegenskaber ved forskellige kemiske eller mekanisk metode er en effektiv metode til at ændre icing egenskaber af overfladen. Det kan foreslås, at fremtidige studier bør fokusere på studieraf effekten af forskellige overfladebelægning med ion koncentration på is dannelsens kinetik.

Desuden blev frysningsforsinkelse og befugtningsevnen af en kemisk modificeret aluminiumsoverflade som funktion af underlagets temperatur undersøgt. Sammenligning af observationer og forventninger ud fra heterogen isdannelsesteori viste, at et svagt hydrofilt underlag modificeret med (3-aminopropyl) triethoxysilan (APTES) demonstrerede længere frysningsforsinkelse i forhold til både mere hydrofile og mere hydrofobe underlag. Dette skyldes APTES-modifikationens

særlige overfladekemi, som forhindrer isdannelse på grænsefladen til underlaget på grund af tilstedeværelse af en lokalt høj ionkoncentration (aminogrupper), som medfører en betydelig sænkning af frysepunktet. Endvidere tyder resultaterne på, at overfladens topografi og befugtningsevne er bestemmende for frysningskinetikken for en dråbe anbragt på en i forvejen afkølet overflade. Overfladekemien, der således er i stand til at ændre egenskaberne af en overflade, kan anvendes som redskab til at kontrollere de faktiske befugtningsegenskaber af en kold overflade i fugtige omgivelser.

Resultater og iagttagelser fra denne undersøgelse viser, at ved at skræddersy overfladebeskaffenheden ved hjælp af forskellige mekaniske og kemiske metoder, kan en overflades frysningsegenskaber ændres. Det foreslås, at fremtidige studier fokuserer på effekten af forskellige overfladebelægninger på dannelsen af is.

LIST OF PUBLICATIONS

I Effects of Aluminium Surface Morphology and Chemical Modification on Wettability

M. Rahimi, P. Fojan, L. Gurevich, and A. Afshari.

Applied Surface Science 296, 2014, 124–132.

II Control and Prevention of Ice Formation and Accretion on Heat Exchangers for Ventilation Systems

M. Rahimi, and A. Afshari.

Conference: Healthy Building Conference Europe 2015, May, Eindhoven.

III Aluminium Alloy 8011: Surface Characteristics

M. Rahimi, P. Fojan, L. Gurevich, and A. Afshari.

Applied Mechanics and Materials 719-720, 2015, 29-37.

IV The Effect of Surface Modification on Initial Ice Formation on Aluminum Surfaces

M. Rahimi, A. Afshari, P. Fojan, L. Gurevich.

Applied Surface Science 355, 2015, 327–333

V Effect of Aluminum Substrate Surface Modification on Wettability and Freezing Delay of Water Droplet at Subzero Temperatures

M. Rahimi, A. Afshari, E, Thormann.

ACS Applied Materials & Interfaces journal 8(17), 2016, 11147-11153

This thesis has been submitted for assessment in partial fulfilment of the PhD degree. The thesis is based on the published scientific papers which are listed above. Parts of the papers are used directly or indirectly in the extended summary of the thesis. As part of the assessment, co-author statements have been made available to the assessment committee and are also available at the Faculty. The thesis is not in its present form acceptable for open publication but only in limited and closed circulation as copyright may not be ensured.

ACKNOWLEDGEMENTS

I would like to first express my sincere appreciation to my supervisors, Professor Alireza Afshari and Associate Professor Peter Fojan. Their great guidance, visions, kind support and encouragement made this work possible.

I have to especially thank Associate Professor Leonid Gurevich and Associate Professor Esben Thormann. Your insights, kind help and support have been crucial for this work and it has been amazing to work, to learn and to develop from your guidance. I could not have completed such a professional piece of work without your involvement.

I also express my acknowledgement to my fellow colleagues who have helped me a lot and provided me with a friendly work environment during these years at SBi, the Danish Building Research Institute, the Department of Physics and Nanotechnology, Aalborg University and at DTU chemistry, the Group of Colloids and Soft Interfaces. Special regards goes to Gokce Engudar, whom I shared my office with at DTU, for our many talks, your thoughts, well-wishes and for just being there whenever I needed a friend.

Moreover, I thankfully acknowledge the financial support provided by the Government of Greenland and COWIfonden to this work.

I would like to express my thanks to my family, my Mom Azar, my dad Askar and my brother Behrouz for their always unconditional love and support.

Siamak, I cannot thank you enough for how you have encouraged and supported me throughout this experience. You knew it would be a long and sometimes difficult process, but you never gave up supporting me.

To my beloved daughter Aneli, who was born during my PhD process and her presence in my life is full of joy and heartwarming, thanks for always being such a good and lovely girl.

Copenhagen, November 2016

Maral Rahimi

TABLE OF CONTENTS

NOMENCLATURE

f	Surface area fraction
ΔG	Gibbs free energy change (J/mol)
H_{ice}	Height of the ice layer
ΔH	Volumetric enthalpy change (MJ/m^3)
I	Nucleation rate
I_0	Kinetic constant per unit surface (nucleation/m2 s)
k	Boltzmann constant (1.38066×10^{-23} J/K)
m	Mass (kg)
$\dot{m}$	Mass flow rate [kg/m^2 s]
P	Pressure (Pa)
q	Heat
R	Surface roughness
RH	Relative Humidity (%)
r	Embryo Radius (m)
r*	Critical Embryo Radius (m)
S	Sample area in mm^2
t	Time
T_k	Surface temperature in Kelvin
T	Temperature (K)
V	Volume (m^3)

GREEK SYMBOLS

γ	Interfacial Tension (mJ/m^2)
θ	Contact Angle (degree)
ρ	Density (kg/m^3)

SUBSCRIPTS

adv	Advancing
air	Air
Al	Aluminum substrate
Hetero	Heterogeneous nucleation
Homo	Homogeneous nucleation
Hyst	Hysteresis
I	Ice
M	Melting
r	Rough surfaces
rec	Receding
s	Smooth Surface
v	Volume
W	water

ABBREVIATIONS

AFM	Atomic force microscopy
APTES	3-aminopropyltriethoxy silane
CA	Contact Angle
PEG	Hyper-branched polyethylene glycol
PFOS	Perfluorooctylsilane
RMS	Root mean square

CHAPTER 1. INTRODUCTION

According to the European Energy Efficiency Directive and the International Energy Agency the building sector accounts for around 40% of the total European energy use. The main purposes for energy use in the building sector are heating and cooling, ventilation, lighting and the production of hot sanitary water together with other installed equipment and removable devices that require energy. The heating of buildings accounts for approximately more than 50% of the total energy use of residential buildings [1,2].

Due to its large share of the world's total end use of energy, there is a need to save and recover the energy consumed in the building sector. In order to reduce the energy consumption in residential buildings, the buildings must be well-insulated and airtight. Consequently, in maintaining a sufficient indoor air quality in the buildings, energy efficient ventilation must be used to remove polluted air and introduce outdoor air during occupied periods. This ventilation system also requires energy to run fans in order to deliver required airflow through the distribution systems. Improving the efficiency of ventilation systems by recovering the thermal energy content of exhaust air is a method used for reducing energy demand in the building sector. This can be done by including heat exchangers and heat pumps to ventilation systems. Heat recovery of ventilation systems by means of heat exchangers is a common and effective technique. Air-to-air heat exchangers are commonly used for heat recovery in residential buildings. This is due to its desirable performance such as allowing temperature-driven heat transfer between the participating airstreams and allowing partial-pressure-driven moisture transfer between the two streams. Moreover, it has the ability to block the cross-stream transfer of air when needed. Heat is recovered from the exhaust air and transferred to the supply air in the air-to-air heat exchanger as illustrated in Figure 1-1 [2–4]

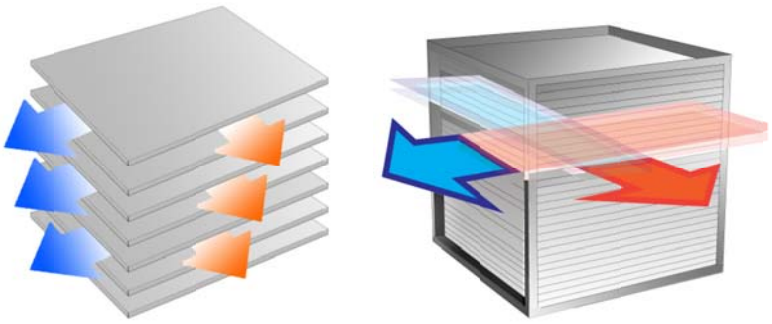

Figure 1-1 Schematic view of air-to-air heat exchanger

Aluminum alloys are the main materials used for the production of heat exchangers and play an important role in modern industry. They are widely used because of their relatively low cost, light weight, high heat conductivity and good corrosion resistance. However, the risk of ice formation and growth on its surface increases in cold working conditions when temperature drops below the dew point of water. Ice formation can cause serious malfunctions of the equipment. Aluminum alloy surface characteristics such as roughness, contact angle and wettability play a significant role in the control and prevention of ice formation and consequently in its applications in cold working conditions [5–7]. In addition to the effects of surface characteristics on ice nucleation, formation, growth and accretion, these phenomena are also dependent on the psychrometric parameters such as humidity, temperature, air velocity etc.

1.1 ICE FORMATION AND ACCRETION ON HEAT EXCHANGERS

In this section, the ice formation problem and the related factors and theory to its nucleation, formation and prevention are explained and elaborated on. Ice formation and accretion on air-to-air heat exchangers' fins provide a significant challenge in cold climates. This is due to the fact that by increasing the heat exchanger efficiency in order to reduce the energy uses in the buildings, the temperature of the exhaust air and the surface of the heat exchanger fins become lower than both the water dew-point and the freezing temperature. This will lead to condensation of moisture content of exhaust air and then to freeze and ice formation on the surface of the heat exchanger fins [8]. The formed ice layer can cause malfunction and reduce efficiency. This is due to the reduction of heat transfer rates caused by the disappearance of the direct contact of air flow with the surface and the ice layer thus functioning as an insulator. Moreover, it may cause the partial or complete clogging of the air passage of the heat exchangers and consequently decrease the airflow. This will lead to higher-pressure drop and reduce the amount of thermal energy available for recovery, and at worst, it may stop the function of the heat exchanger [3,9,10]. Therefore, in order to maintain the efficiency and working condition of heat exchangers, removal, control, prevention and de-icing methods of accumulated ice on heat exchangers fins must be applied [11].

The common sources of moisture in residential buildings that may cause ice formation problems in ventilation system in cold periods include human evaporation, humidifiers, whirlpools, hot tubs, washing, cooking, bathing etc.[12].

Increasing the efficiency of heat exchangers increases the risk of ice formation due to reduction in the exhaust air temperature. The risk can also be increased by increasing the mass flow rate ratio of supply air to the exhaust air (mass flow rate of supply air/mass flow rate of exhaust air) [10]. On a cold day, the exhaust air at room temperature, which contains moisture, is cooled down when its heat content is transferred to the supply air. Condensation occurs as soon as its temperature decreases and reaches the dew point, and by decreasing the temperature to below the freezing point, ice formation will occur on the heat exchanger surface. This procedure is illustrated as point 1 to point 3 in a classical psychometric Mollier diagram in Figure 1-2, which is a graphical representation of the relationship between air temperature, moisture content and enthalpy of air.

Point 1 represents warm humid exhaust air in the heat exchanger at room condition of for example temperature of 25°C and the relative humidity of around 50% and the dew point of 6°C. By decreasing the temperature from 1 to 2, the water vapor content of air will remain constant until it reaches the dew point 2, then condensation on the surface will occur. The exhaust air temperature will decrease until the temperature reaches the cold heat exchanger fins surface temperature, as seen in example point 3. By continuing the temperature drop and reaching the freezing point, ice formation will occur on the surface. The formed ice layer grows by migration of the moisture molecules of the supply air passing in to the formed ice layer on the surface. This leads to ice layer growth and densification.

1.2 ICE CONTROL AND PREVENTION METHODS

Since ice formation may cause malfunction and reduce the heat recovery effectiveness of the heat exchanger, different techniques and methods have been investigated and applied in order to control and prevent ice formation and maintain heat exchanger efficiency [3]. The existing methods are categorized in two main categories; passive methods and active methods. Basically, the passive methods aim to prevent and delay ice formation by means of tailoring the cooled surface characteristics with no additional energy applied, while the active methods control ice formation and remove the formed ice by supplying additional energy. These two methods are described below.

1.2.1 ACTIVE METHODS

Active methods control the ice formation and remove the formed ice. This means that ice formation on the surface must be detected and certain measures must be taken to control its growth or to remove it from the surface. This may be done

through the application of three common sensing techniques which include installing a temperature sensor in the supply air or in the exhaust air located in the cold corner of the heat exchanger, and by sensing the pressure drop across the heat exchanger. The common active methods used for the control and removal of ice are: preheating of supply air, variation of the mass flow ratio, bypassing the supply air and exhaust air recirculation. All these techniques reduce the overall efficiency of the heat exchanger [3,9,10,13].

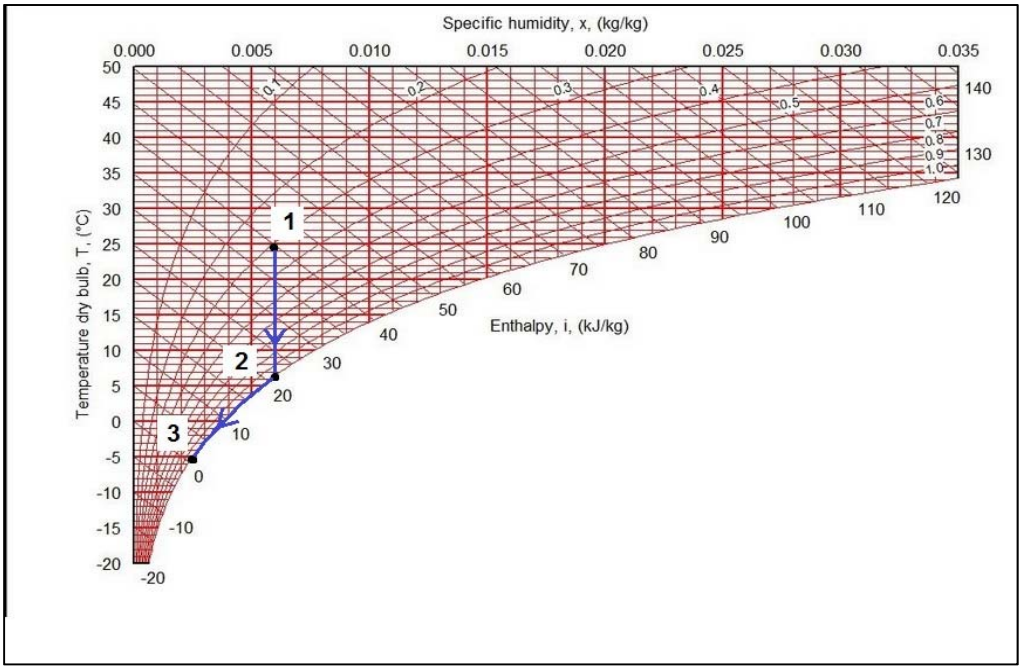

Figure 1-2 Psychrometric representation of the air water content condensation and ice formation on heat exchanger fins by Mollier diagram [13]

1.2.1.1 Preheating of supply air

This is a common technique for ice formation control [14]. As soon as the installed temperature sensors in the supply air passage sense that the supply air temperature is below the frosting threshold and there is added risk of condensation and ice formation, the heating elements of the heat exchangers begin heating the supply air. Another control strategy for activating the preheating technique is to use a pressure drop sensor across the exchanger core. This method requires auxiliary energy such as gas or electricity and significantly reduces the energy efficiency of heat exchangers. Therefore, this technique is not economical in regions with long periods of cold temperatures [3,13,15,16]

1.2.1.2 Variation of the mass flow ratio

Variation of the mass flow ratio (*m* supply air/*m* exhaust air) is another technique for controlling the ice formation on the heat exchanger's fins. When the sensors detect the added risk of ice formation, the flow ratio of cold supply air to warm exhaust air (*m* supply air/*m* exhaust air) is reduced and consequently, the thermal energy of warm exhaust air will compensate for the low thermal energy level of supply air and prevent and control ice formation [9,16]. The disadvantage of

this method is that it creates an unbalanced flow rate in the system which, over a long period of application, may cause infiltration in the building and a reduction of the building's air quality [15].

1.2.1.3 Bypassing the supply air

This is another common technique for the control and prevention of ice formation. In using this technique a set point for the exhaust air temperature or supply air is selected to inform the controller of the heat exchanger system when to activate the bypass. This set point is selected according to the calculation of the dew point and the risk of condensation on the heat exchanger. It means that the heat exchanger will be de-iced by fully closing the supply air flow in the heat exchanger, thus allowing the exhaust air to continue to flow. The warm exhaust air flow will then warm up the heat exchanger and de-ice it. By regulating the set point, a bypassing switch may be continuously regulated for optimum energy use. When no risk of condensation or ice formation exists, bypassing remains out of the operation [3,10]. Bypassing may be applied to fully or partially de-ice the heat exchanger. In case of partial de-icing, dampers are installed in the cold supply air, which would be open under normal working conditions. In case the installed sensors detect a risk of ice formation in a certain location of the heat exchanger, individual dampers are alternately closed for a certain period of time, which will prevent the cold supply air from entering into that particular part of the exchanger. The warm exhaust air flow then de-ices the heat exchanger [13].

1.2.1.4 Exhaust air recirculation

Using this active technique when the risk of ice formation is detected, the supply air flow will be stopped and only the exhaust air flow is recirculated in the system to warm the heat exchangers for a fixed duration of time at set time intervals. Since the recirculation of exhaust air may cause a reduction in air quality, the defrosting time should not exceed 20% of the total operating time. In order to prevent this and compensate the air quality of the system in the normal operating time, the airflow rate must be increased; this, however, may reduce the efficiency of the heat exchanger [9,15]. In comparing defrosting techniques, Philips et al., showed that this technique is particularly suitable for extremely cold climates [9].

1.2.2 PASSIVE METHODS

Passive methods of ice formation control on heat exchanger fins are related to the methods that do not require energy and consequently reduce the energy efficiency of heat exchangers. Moreover, implementing these methods will improve the effectiveness of the heat exchanger in cold working condition; this is due to the ability of these methods to partially control and delay the ice formation by changing the surface characteristics of the heat exchanger fins. The surface characteristics of the heat exchanger fins such as surface wettability, roughness and surface energy play a significant role in ice nucleation and ice formation. However, it should be noted that the effect of these methods is restricted to the initial stages of ice formation. This is due to the fact that in a freezing condition by inevitable nucleation of ice on the surface the direct contact between modified fin surface and humid exhaust air will be disappear. Therefore the surface effects on control and prevention of ice formation becomes weaker as ice grow [17,18]. Though the effectiveness of passive methods is restricted to the initial stages of ice formation, their application may reduce the energy required for the regeneration of heat exchangers significantly [19].

Along with the fundamental interest in research on surface modification, this has led to a recent increase in the interest in passive methods. For example, some studies focus on the effect of surface characteristics in real heat exchanger applications, such as Qi, 2013 [20] and Rahman and Jacobi, 2012 [21], while other studies merely focus on the effect of surface characteristics on plate samples representing the surfaces of heat exchanger fins in an effort to investigate the effect of surface characteristics on wettability and ice formation [22–24].

Previous studies have mainly focused on changing the surface wettability to become more hydrophobic or more hydrophilic [22,25]. Surface wettability may be changed by modifying the surface characteristics by tailoring the surface roughness or tailoring surface chemistry.

Many recent studies have focused on the effect of superhydrophobic surfaces and have reported the anti-icing effects of superhydrophobic surfaces, these include Cao et al., 2009, Farhadi et al.,2011and Kulinich et al., 2011[26–28].

On the other hand, other studies have shown that superhydrophobic surfaces do not have always the anti-ice effects and thus may not be the best choice for freezing delay [29,30]. Oberli et al., 2014 observed that superhydrophobic surfaces may slow the rate of water condensation on its surface and consequently delay water freezing, however, this does not eliminate it completely [30]. These authors also found that some superhydrophobic surfaces may have strong ice adhesion and do not have the anti-ice effect. Moreover, Jung et al., 2011 studied water freezing delays on untreated and coated surfaces ranging from hydrophilic to superhydrophobic, and they observed the longest freezing delay for hydrophilic surfaces [31].

In the present study, the effects of different surface modifications of aluminum alloy 801 is investigated in order to find the most suitable and effective aluminum surface characteristics for freezing delay and the delay of ice formation for heat exchanger production.

Moreover, the effects of aluminum surface characteristics, such as wettability and roughness, on ice nucleation, formation and growth is presented, discussed and explained in this study through detailed and state of the art investigations within this area.

1.3 ICE NUCLEATION AND GROWTH

In forming a better understanding of the ice formation problem, the mechanism of ice nucleation and growth on a surface is described and elaborated in this section. Ice nucleation begins when the surface temperature drops below the dew point. This is caused by a decrease in the water content temperature of the exhaust air which is in direct contact with the surface.

Hayashi et al., (1977) originally classified three stages of ice growth to describe the evolution of an ice layer, and this theory is now widely accepted by other researchers for example by Wang et al., 2006, Prolss et al., 2006, Cheng et al., 2002 [32][33][34]. Hayashi et al., (1977) investigated ice formation through the deposition and ice nucleation of water content of air stream on cold surfaces. Other researches, such as Tao et al.,(1994) have investigated ice growth stages according to condensation and the freezing of water content of humid air on cold surfaces [35].

The three stages introduced by Hayashi are: (1) crystal growth stage (2) ice layer growth stage, and (3) ice layer full growth stage [36]. In the first stage, which is rather short, the ice nucleation formation requires overcoming to the free energy of nucleation which is related to the interfacial energy. During this stage, the nuclei size will increase and initially ice crystals are formed on the surface. These ice crystals cover the cold surface and are formed far apart from each other in a vertical direction [17,36]. In this stage, the ice crystal surface temperature becomes higher than the cooled substrate temperature as its surface area increases. Consequently, increased energy removal is required to maintain its growth. When this amount becomes higher than the energy removal required for starting a nucleation on a new site, the initial crystal stops growing and forms branches around the top of each ice crystal. This process will continue and new nuclei will form on each branch; when having reached its maximum size, a new nucleation starts and branches together to form a forest of ice trees. At this stage, the ice is characterized as "ice layer growth" and this will continue until a uniform ice layer has been formed. After this stage, during "Full layer ice growth", the ice layer will not change its shape until the surface temperature of the ice has reached water triple point temperature; this is caused by an increase in the thermal resistance of the ice. This temperature will cause for continuous cycles of the ice melting and refreezing on its surface. This cycle abruptly increases the ice layer density as the molten water penetrates the ice layer and freezes there. This will continue until thermal equilibrium is reached throughout the ice layer [36–38]

Figure 1-3 shows the early stages of ice formation and growth on a cold surface following the condensation of air water content on the cold plate, adapted from Tao et al. (1993) and (1994). The first initial stage shows the condensation of water from ambient flow on the cold surface as small droplet of subcooled liquid phase. In time and as the temperature drops, the subcooled liquid phase droplets starts to crystalize and form a certain ice layer thickness, as explained previously [35,39].

According to t Tao et al. (1993) and (1994) investigation, the ice growth stage after the freezing of the water droplets is identical to the stages suggested by Hayashi et al., (1977) [35,36,39].

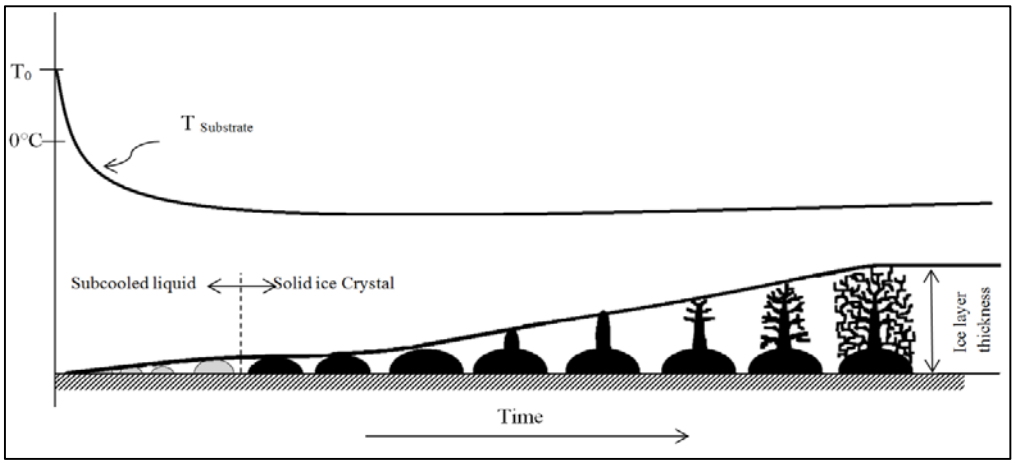

Figure 1-3 Definition of early stages of ice growth on a cold plate – adapted from Tao et al. (1993)[39].

1.4 ICE LAYER GROWTH AND DENSIFICATION MECHANISM

Ice layer growth involves the transfer of heat (q) and mass (m) from a humid air stream to the formed ice layer when the humid air is in contact with ice layer. The schematic illustration of ice growth and densification is shown in Figure 1-4. Part of the transferred mass in the form of moisture deposits on the surface of the ice layer and increases its thickness. The other part diffuses into a porous structure of ice which deposits there by phase changing and causes an increase in the ice density ‘‘densification process’’. Moreover, during the mass transfer the sensible heat (q), which is related to changes in the temperature of moist air, is also transferred from the humid air stream to the ice layer because of their temperature difference. The latent heat of the phase change of moist to the ice on the ice surface and in the ice structure is also transferred to the ice layer by conduction [5,37,40,41].

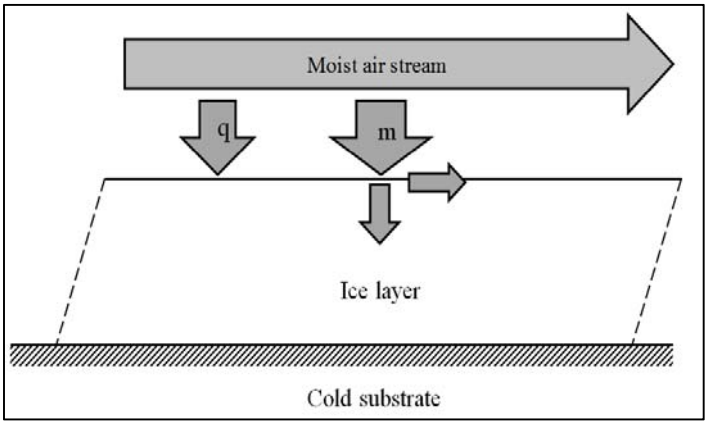

Figure 1-4 A schematic illustration of ice growth and densification through heat (q) and mass (m) transfer from humid air stream adopted from [5,41]

The most crucial ice properties affecting the performance of equipment affected by ice formation are ice layer thickness, thermal conductivity and ice density. Therefore, in order to maintain the performance of the equipment, these properties should be study and ice control and prevention methods must be applied.

1.5 ICE STRUCTURE

According to results of the investigation on icing conditions, by Hayashi et al. (1976) and Lee et al., (2004) the structure and density of formed ice on a cold surface depends on the surface wetting characteristics (hydrophilicity and hydrophobicity) and the psychrometric conditions, such as the air humidity, cold plate temperature and Reynolds number of air flow [23,42]. Lee et al., (2004) developed frost maps for two different surfaces having two different hydrophilic characteristics, aluminum samples and hydrophilic coating samples with dynamic contact angles of 88° degree and 23° degree. A summary of their observations and findings regarding the dependency of ice structure to surface characteristics and environment are illustrated in Figure 1-5 [23]. They characterized three types of ice structures: feather type ice crystals, grass type ice crystals and plate type ice crystals. For different surface wettability –hydrophilic and hydrophobic surfaces, changing the air humidity will cause for different ice structures being formed on top of the surface at identical surface temperatures [23]. Their finding in this study were along the same lines as the observations of Hayashi et al. (1976) [42].

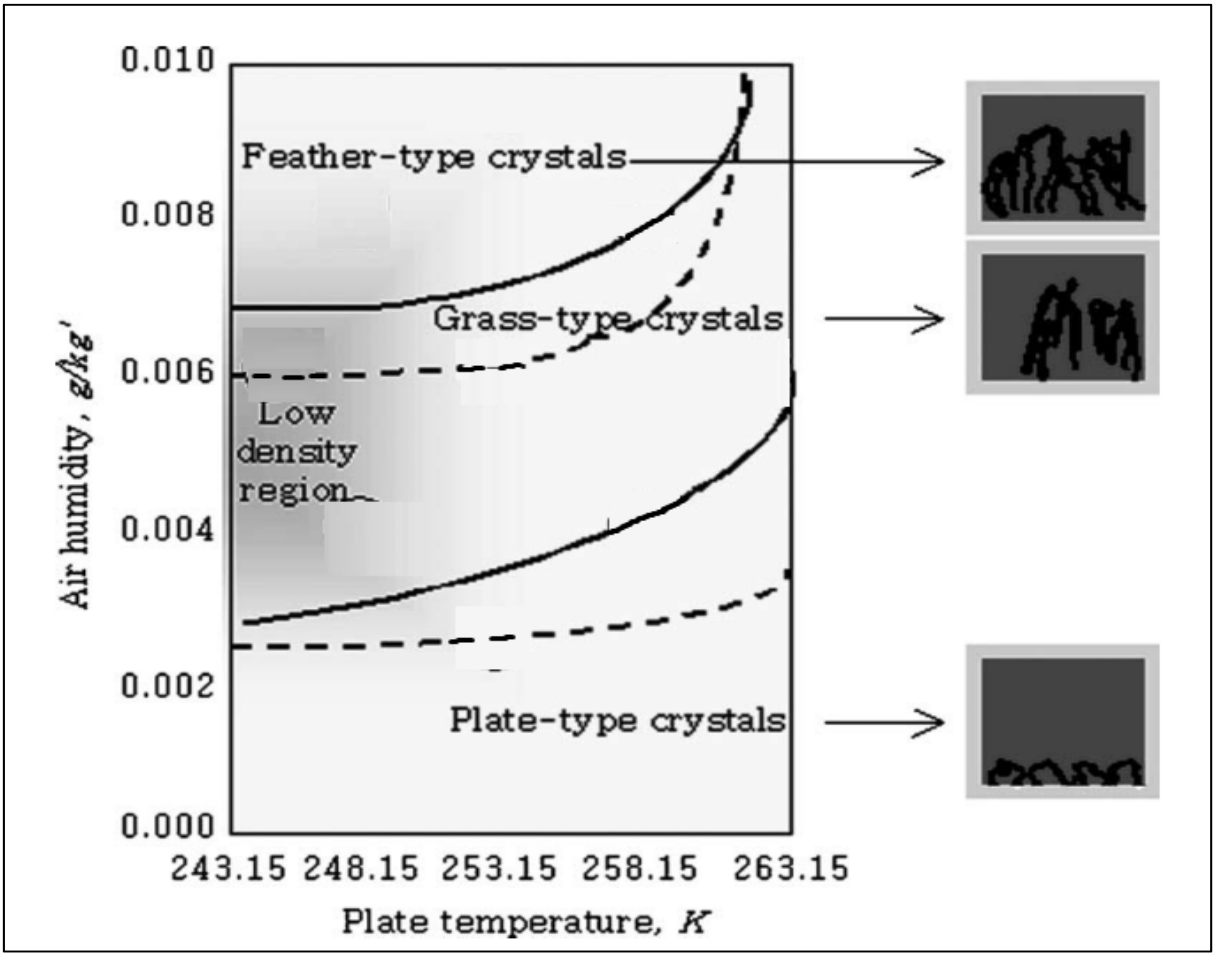

Figure 1-5 Map of the ice structure on a hydrophobic surface with a dynamic contact angle of 88°(dashed line) and a hydrophilic surface with a dynamic contact angle of 23° (sold line) according to cold surface temperature and air humidity [23]

1.6 SURFACE CHARACTERISTICS

Psychrometric parameters, such as air temperature, velocity, humidity and surface temperature, play an important role in ice formation, its structure and growth; however, this process is also affected by substrate surface conditions, such as surface wettability, surface roughness and surface chemistry which are also crucial parameters of ice nucleation, formation and freezing delay [5,17,22,43–45]. In order to understand how the surface condition affects icing it is necessary to understand the surface characteristics and how these may be modified and tailored to prevent and delay ice formation.

Therefore, this work focuses on the effect of surface characteristics on ice nucleation, formation, structure and growth. Moreover, in this section surface wettability, roughness and the common techniques for measuring these are explained in order to provide a better understanding of their effect on ice formation and accumulation.

1.6.1 SURFACE WETTABILITY

A surface wettability is characterized by the contact angle of a droplet on the solid surface. It can be explained according to the Young equation (1). The droplet shape is determined by the interfacial tension (γ) between the phases (gas, liquid and solid) in contact [46]. Figure 1-6 shows a schematic illustration of a formed spherical water droplet on an aluminum surface with the contact angle of Θ.

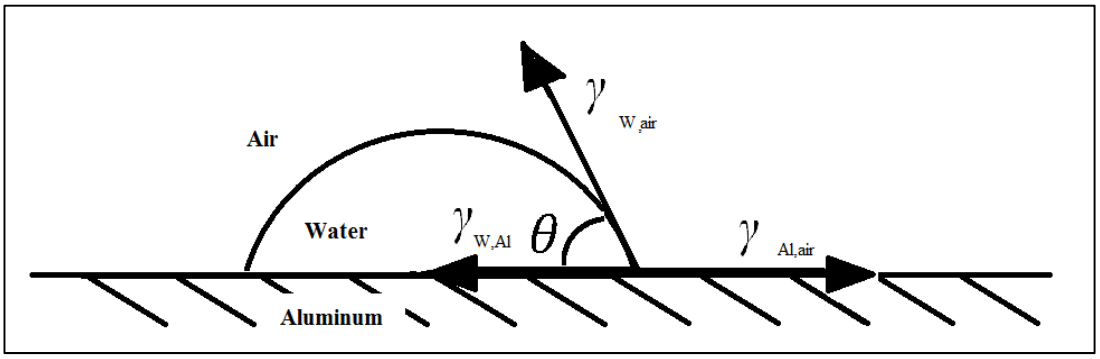

Figure 1-6 Schematics illustration of a spherical water droplet on a planar aluminum surface. Θ is the contact angle, γ is the surface tension between the gas and the liquid phase, $\gamma_{W,Al}$ is the surface tension between water and aluminum (liquid-solid), and $\gamma_{Al,air}$ is the surface tension between aluminum and air (solid-gas).

As illustrated in Figure 1-6, the contact angle Θ for a water droplet on an aluminum substrate is related to the surface tensions between the gas, aluminum substrate and the liquid phases:

$$\cos\theta = \frac{\gamma_{Al,air} - \gamma_{W,Al}}{\gamma_{W,air}} \qquad 1$$

Where $\gamma_{Al,\,air}$ is the interfacial tension between aluminum substrate and air, $\gamma_{W,Al}$ is related to the interfacial tension between water and aluminum and $\gamma_{W,\,air}$ is related to interfacial tension between water and air [46] .

On a real surface, which contains imperfections, the actual contact angle is not identical to the static contact angle. Since the liquid droplet moves on the substrate in order to wet the fresh solid surface, measuring a single static contact angle becomes more complicated. In case the three-phase contact line is in motion, the contact angle produced is called a “dynamic” contact angle. The observed contact angle is different for a liquid droplet advancing on a dry surface (advancing contact

angle, θ_{adv}) or receding on a previously wetted surface (receding contact angle, θ_{rec}). The difference between the advancing and a receding contact angles is the contact angle hysteresis (θ_{hyst}).

Any deviations from the ideal surface condition, such as surface heterogeneity, contamination or roughness, can cause contact angle hysteresis or increases it. Moreover, the dynamic contact angles can be measured at various rates of speed. At low speed, it should be close to or identical to a properly measured static contact angle [47,48].

Two classical theories explain the relation between contact angle and surface wettability and surface morphology: the Wenzel and the Cassie–Baxter model [49,50]. These models are applicable when the droplet size is significantly larger than the wavelength of the surface roughness or chemical inhomogeneity [51,52].

The Wenzel model assumes that the droplet penetrating through the surface roughness remains in direct contact with the surface. According to this model and its equation (2), the hydrophilicity or hydrophobicity of a hydrophilic or hydrophobic surface will be increased by increasing the surface roughness and vice versa by decreasing the surface roughness [49].

$$\cos \theta_r = R \cos \theta_s \qquad 2$$

where R is the surface roughness and θ_s and θ_r are the contact angles on perfectly smooth and rough surfaces of the same composition, respectively.

The Cassie/Baxter model treats the solid surface as being composed of different components materials with specific wetting properties[50]. These components occupy different surface area fractions and exhibit different contact angles of a liquid. These properties modify the wettability of the surface and consequently the contact angle on such a microscopically mosaic surface. For example, when a surface is composed of two materials, where material 1 and 2 occupy the surface area fractions f1 and f2 and exhibit the contact angles Θ1 and Θ2, respectively, the contact angle of a liquid on such a surface can be expressed as equation (3)[50].

$$\cos \theta_R = f_1 \cos \theta_1 + f_2 \cos \theta_2 \qquad 3$$

In case component 2 is air, the contact angle of air θ_2 is 180◦ and the contact angle of liquid on such a substrate is:

$$\cos \theta_R = f_1 \cos \theta_1 - f_2 \qquad 4$$

The aforementioned phenomenon occurs on a rough surface where the grooves of the surface are entrapping air as the second phase material. Consequently, the entrapped air below the liquid reduces the interfacial contact area between the solid surface and the liquid and may cause an increase in contact angle [53].

When the measured contact angle of a water sessile drop on a solid surface is smaller than 90°, and the surface has a strong affinity to water, the term ‘‘hydrophilic surface’’ have been used in literature for introducing the wetting characteristics of the aforementioned surface. For surfaces with a measured contact angle of water sessile drop on the solid surface of more than the 90°, and when the surface repels water, the term ‘‘hydrophobic surface’’ have been used. Both surface types and a schematic view of sessile liquid drop shape on top of these surfaces are illustrated in Figure 1-7 [54].

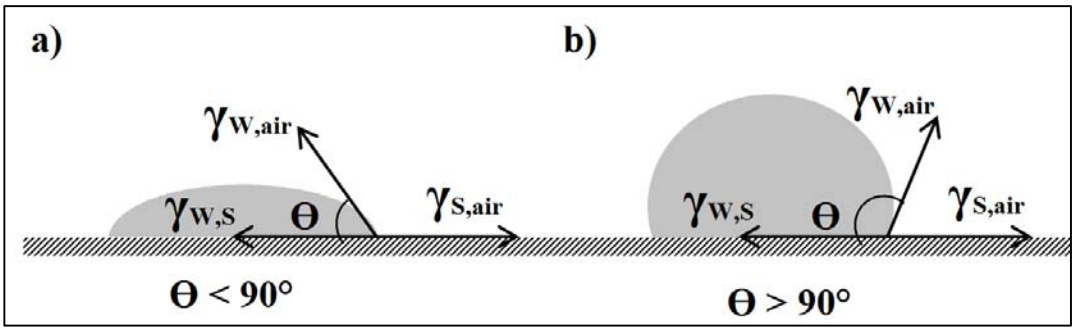

Figure 1-7 Illustration of contact angles formed by sessile liquid drops on a) a hydrophilic substrate and b) a hydrophobic substrate

1.6.2 CONTACT ANGLE MEASUREMENTS METHODS

There are two techniques for measuring the contact angle: the direct optical method and the indirect force method. In the indirect force method, the weight change of a thin, smooth, vertical plate which is brought in contact with a liquid is measured by balance. The measured force is a combination of gravity, buoyancy and the capillary force, which is related to the liquid surface tension, the perimeter of contact line, considered as the perimeter of the cross-section and contact angle of a solid sample [48].

The direct optical techniques, which is the most commonly used technique, is a direct measurement of the angle at the three-phase contact point on a sessile drop profile [46,48]. Moreover, different methods are available for using the sessile drop method of contact angle measurement on a real surface with local defects in order to measure the advancing and receding contact angle and their hysteresis.

In the first method the contact angle between the droplet and the surface is measured constantly while the droplet volume is increasing at a constant rate of μL/min. Just before the wetting line starts to advance, the advancing contact line is determined (θ_{adv}). For receding contact angles the volume of the advancing droplet is decreasing at a constant rate and the receding contact angle (θ_{rec}) will be determined as the contact angle of the droplet and the surface just before the wetting line recedes. The contact angle hysteresis (θ_{hyst}) will be calculated as the difference between the θ_{adv} and θ_{rec}[46].

The second method is evaporation of sessile drops which can explain the effect of surface roughness and heterogeneity on the θ_{rec} and θ_{hyst}. This method is commonly used in experiments because it allows for small sized droplets to be measured. In this experimental method, the sessile drop will be placed on the surface with a constant rate and the θ_{adv} will be measured as the previous methods. The difference is that for the θ_{rec} measurement the droplet will be placed on the surface to be evaporated and the contact angle changes are observed and recorded continuously until it evaporates completely [48,55–57].

According to the observation of Bourg and Shanahan, 1995 and Shanahan and Bourg, 1994, the sessile drop evaporation can be divided into four stages. In the first stage, the measured contact angle and height of the droplet decrease slightly in time while the diameter of the droplet remains constant. In the second stage, the measured contact angle and height of the droplet decrease intensely while the diameter of the droplet remains constant. In the third stage, the contact angle almost remains constant, this angle is the receding contact angle, and, in time, the height and the diameter of the droplet decrease. In the fourth and final stage, all factors constantly decrease until the droplet has evaporated completely [56,58]. The schematic of these stages is illustrated in Figure 1-8.

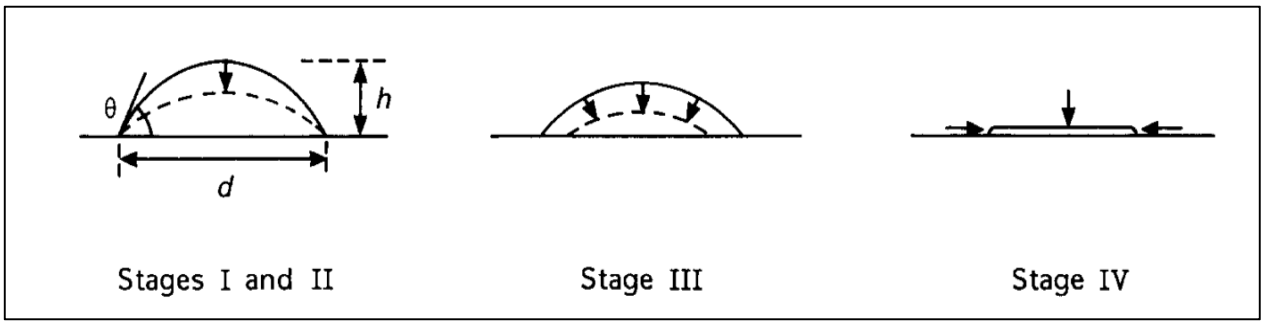

Figure 1-8 Schematic representation of sessile drop evaporation stages and its effect on contact angle by M., Shanahan, M., Bourg, 1994 [58]

It should be mentioned that the surface heterogeneity, contamination, roughness and chemistry can cause a three phase contact line pinning phenomenon. This phenomenon causes for the constant decrease of the contact angle and height of droplet until the droplet has reached a stage of total evaporation, thus making it impossible to measure the receding contact angle and consequently, the contact angle hysteresis on the surface [46,58–60]. Shanahan and Bourgès-Monnier (1994) and Bormashenko et al.,(2011) observed and reported the pinning of three-phase contact line after the initial stage of sessile drop evaporation on a rough polymer surface, aluminum and steel surfaces [58,60]. If the pinning point phenomenon occurs, the advancing contact angle and the static contact angle can be measured.

According to the observation of Bourg and Shanahan, 1995 and Shanahan and Bourg, 1994 [56,58] on the smooth surface in the first and second stage of the evolution of measured contact angle, contact angle of the droplet decreases slightly in time and in the third stage the contact angle almost remains constant. In the fourth stage it decreases until the droplet has evaporated completely. These stages are illustrated in Figure 1-9 by solid line. Moreover the contact angle measurement on rough surface has constant decrease of the contact angle until the droplet has reached a stage of total evaporation as due to pinning phenomenon and illustrated in Figure 1-9 by dashed line.

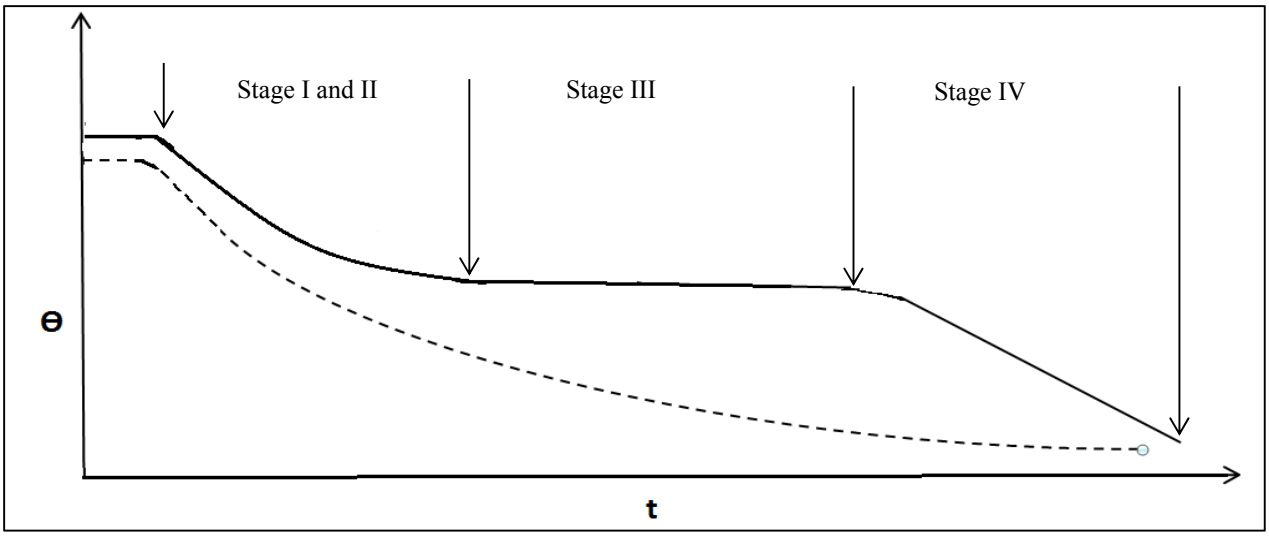

Figure 1-9 Evolution in contact angles of sessile drop evaporation contact angle measurement: solid and dashed lines denote smooth and rough surface, respectively.

1.6.3 SURFACE ROUGHNESS

As discussed and explained in equation (1), surface roughness plays a crucial role in surface wettability and consequently, in its icing-related properties. There are different definitions of the surface roughness. According to the Wenzel model, the roughness factor R, representing the surface roughness, is equal to the ratio of actual surface area and the geometrical plane surface area [49,61]. For an ideal solid surface, the actual surface area is always greater than the geometric surface area and consequently, the roughness factor is greater that one [49].

According to equation (2), measuring the contact angle on a perfectly smooth and rough solid surface renders it possible to calculate the roughness factor of the purposed solid surface as illustrated in equation 5 below:

$$R = \cos\theta_r / \cos\theta_s \quad (5)$$

Moreover, the surface morphology may be visualized using atomic force microscopy (AFM), and the data acquired from the surface scanning may be used for calculating the roughness factor. The roughness value acquired by the AFM is equal to the imaging area divided by the geometrical plane surface area. The geometrical plane surface area is the scan field and the imaging area can be calculated by means of triangulation of roughness factor by AFM software [62].
So when the imaging area is identical to the actual surface area, the R roughness factor of the Wenzel model will be identical to the roughness of AFM. This is related to many factors such as filed of scan and the number of pixels and quality of the tip [62].

1.7 ICE NUCLEATION THEORY

After studying ice formation, its prevention and control methods and its growth and structure in a macroscopic scale, the icing phenomenon and problem in a microscopic scale must be elaborated, including its nucleation, freezing delay and its related theory.

The nucleation of ice nuclei occurs when the substrate temperature or the surrounding environment temperature, which is in contact with the humid air or the water droplet, is below the freezing point. This phenomenon may occur on the contact area of water and cooled solid surface when the water stays on the surface. According to classical nucleation theory, the affecting factor on ice nucleation is defined by the Gibbs energy barrier which is related to the interfacial tension between ice and water and the contact area of a water droplet and a solid surface [63].

Fletcher, 1970 [63] showed that the maximum free energy for the homogeneous nucleation of ice embryo ΔG^*_{Homo} with the critical sphere of radius r* is according to the equation (6) and (7).

$$\Delta G^*_{Homo} = \frac{16\pi\gamma^3_{IW}}{3(\Delta G_V)^2} \quad (6)$$

$$r^* = -\frac{2\gamma_{IW}}{\Delta G_V} \quad (7)$$

Where the ΔG_V is the free energy difference per unit of volume between ice and water which can be define as equation (8).

$$\Delta G_V = \frac{T_m - T}{T_m}\Delta H_v \quad (8)$$

where T_m is the ice melting temperature at 1atm and 273.15K, T is the supercooling temperature (in K), and ΔHv = 287 MJ/m3 is the water volumetric enthalpy of fusion [64].

γ_{IW} is the ice, water interfacial tension which is temperature dependent and can be calculated at different temperatures. Different calculation methods are mentioned by e.g. Floriano, Angell, 1990 and Leyendekkers and Hunter, 1985 [65][66].

Heydari et al., 2013 calculated γ_{IW} the ice, water interfacial tension in the temperature range of $-36\ °C \leq T \leq 0\ °C$ by the suggested equation of Pruppacher et al., 1998 as equation (9) which is also used in this study [44,67].

$$\gamma_{IW} = 28.0 + 0.25\,(T - 273.15) \quad (9)$$

with γ_{IW} in mJm^{-2} and T in K.

Moreover, Fletcher, 1958 and 1970 [63,68] showed that the free energy barrier to heterogeneous nucleation of critical embryo (ΔG^*_H) with the critical radius of (r^*) is according to the equation (10) .

$$\Delta G^*_{Hetro} = \Delta G_{Homo}{}^* f(m,x) \quad (10)$$

Where $f(m,x)$ which is related to the geometrical factor of embryo and its wetting characteristics is explain by equation (11) and is always less than unity [44,68]:

$$f(m,x) = \frac{1}{2}\left[1 + \left(\frac{1-mx}{g}\right)^3 + x^3\ \left[2 - 3\left(\frac{x-m}{g}\right) + \left(\frac{x-m}{g}\right)^3\right] + [3m^2x^2(\frac{x-m}{g} - 1)]\right] \quad (11)$$

The function g is defined as equation (12):

$$g = (1 + x^2 - 2mx)^{\frac{1}{2}} \quad (12)$$

Where $x=r/r^*$ is the relation between the radius of nucleus (r) and critical embryo (r^*), the value of x the characteristic dimension will change between 0 to ∞ from homogenies nucleation to nucleation on a plane surface. Hao et al, 2014 considered the $x \approx R/r^*$ in their calculation where R is the surface roughness value in nm measured by AFM. This consideration is also applied in the calculation of the free energy of ice nucleation in this study [64].

$m = \cos \Theta_{IW}$ is the contact angle of ice embryo on the nucleating particle in water which can be explained by interface parameters between the existing phases. As indicated by classical heterogeneous nucleation theory, ice nucleation depends not only on surface roughness but also on contact angle (i.e., wettability). The Θ_I contact angle of ice embryo on the nucleating particle or substrate that needs to be calculated for the further calculation of heterogeneous nucleation can be calculated according to the Jung et al., 2011 derivation of Young's equation where (W,I and S refer to water, ice and substrate) as the equations (13) and (14) [31].

$$\gamma_I \cos\theta_I = \gamma_W \cos\theta + \gamma_{IW} \cos\theta_{IW} \quad (13)$$

According to the Young equation, assuming that the ice contact angle in air and the water contact angle in air on the same substrate are identical, allows for the ice-water contact angle to be defined by equation (14):

$$m = \cos\theta_{IW} = \frac{\gamma_I - \gamma_W}{\gamma_{IW}} \cos\theta \quad (14)$$

Where γ_{IW} is the ice- water interfacial tension which is temperature dependent and can be calculated at different temperatures according to equation (9), θ is the contact angle of water on the substrate. γ_I is the ice surface energy which is assumed to remain constant. For γ_I the value between 105-109 mJ/m^2 is considered; however, values as low as 73 mJ/m^2 have also been suggested and observed [69]. In this study, the value of γ_I is considered as 109 mJ/m^2 for the calculations. γ_W is the supercooled water surface energy which can be measured at different temperatures. Floriano and Angell, 1990, for example, calculate the surface tension and molar surface free energy and entropy of water from 67°C to -27.2°C.I In this work, this data is used for further calculations.[65].

The illustration of all components of equations (13) and (14) according to Yong's type equation is shown in Figure 1-10.

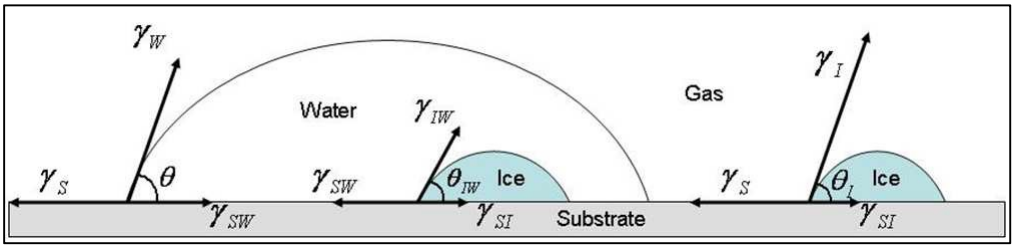

Figure 1-10: Schematic of Young's-type equations for a gas-liquid, liquid-ice and gas-ice phases [70]

Moreover, the rate of heterogeneous ice nucleation per unit time and unit surface area as shown in equation (15), which is proposed by Becker and Doring, is also related to the free energy barrier of heterogeneous nucleation of critical embryo (ΔG^*_H) [63][71].

$$I = I_0 \, exp\left(-\frac{\Delta G^*_H}{KT_k}\right) \qquad 15$$

Where I is the nucleation rate, and I_0 is the kinetic constant per unit surface. I_0, which is defined with the unit of (nucleation/m^2 s), is (10^{29} , 10^{25} and 10^{32}) orderly for condensation, desublimation and freezing. k is the Boltzmann constant (1.38066×10^{-23} J/K), and T_k is the surface temperature in Kelvin . ΔG^*_H is the free energy barrier for heterogeneous nucleation of critical embryo [43,71].

Therefore, adjusting the surface characteristics through surface modifications, changing the surface energy and roughness, affects the energy barrier for nucleation and hence the nucleation rate. These techniques can be employed to delay the onset of ice nucleation and formation [72]. It should be noted, however, that the effect of surface treatment on the ice nucleation and formation process is limited to the initial period of ice formation. There is only direct contact between humid air and the treated surface in the initial period. As soon as the ice thickness reaches a certain value, the humid air and the substrate surface will no longer be in direct contact and therefore, the surface characteristics will have no effect on ice nucleation and formation, and ice formation will only be affected by environmental conditions [18,24,73].

In time, the density of the ice layer tends to increase due to the vapor diffusion through the porous ice structure. On the other hand, ice formation on the surface of the ice layer contributes to the thickness increase [41,74]. Both ice thickness and ice density strongly affect the performance of heat exchangers [73].

1.8 FREEZING DELAY TIME

A small quantity of water does not immediately freeze when cooled under its equilibrium temperature. It has some freezing delay time which means that it remains in its metastable super cooled state for a while; this is considered freezing delay and related to the ice nucleation phenomenon and, consequently, the surface characteristics.

Freezing delay can be measured by measuring the time interval between placing the droplet on the pre-cooled substrate to when the droplet starts freezing, or from the beginning of the cooling stage until the beginning of the freezing stage. Surface characteristics, such as surface roughness and wettability, are crucial to the ice nucleation and consequently, to freezing delay [64]. As previously discussed, surface chemistry and morphology may have an effect in the initial stages of ice nucleation and may cause delay, but it cannot prevent ice formation completely [75].

Due to the small size of ice nuclei, which are just few nanometers in size, obviously, the initial stages of nucleation cannot be detected and measured by using IR or visible light cameras. It cannot be detected until the nucleus size has reached macroscopic dimensions. Another important factor to be considered in the study of freezing delay and ice nucleation is the droplet size which may affect freezing delay. In classical nucleation theory calculations, the droplet radius of 1 mm or 6 ml is considered; this is also the case for the investigations of this study [6].

Different studies and investigations have been made and have shown different results on the effects of surface characteristics on freezing delay and experimental results have been compared in different temperature ranges to the theory of nucleation. Singh and Singh, 2013, for example, studied and observed the effect of changing the surface chemistry with nanocolumnar silver surface coating of copper on the freezing delay in comparison to the conventional silver thin film. The observed delay in freezing on silver nanocolumns is explainable in terms of the reduction in effective liquid-solid interface area within the framework of the Cassie-Baxter model [76]. Wang et al., 2012, investigated and observed the effect of changing the surface chemistry of copper surface with nano-fluorocarbon coating on freezing delay [77].

Moreover, the role of surface roughness on freezing delay was also investigated recently. For instance, Jung et al., 2011, investigated supercooled (-20°C) water freezing delays on untreated and coated surfaces ranging from hydrophilic to superhydrophobic. They observed longer freezing delay times for the hydrophilic surfaces with nanoscale roughness (smaller than the size of the first stable ice nuclei) compared with typical superhydrophobic surfaces with larger hierarchical [31].

Heydari et al., 2013, measured the freezing temperature and freezing delay time of surfaces with similar chemistry but different topography, including smooth and rough surfaces, and found that water freezing delay time is not significantly affected by surface topography. They also discussed their finding within the classical theory of heterogeneous nucleation [44].

Hao et al., 2014, investigated the effect of surface roughness and wettability on the freezing delay. They conducted their study on smooth surfaces with a roughness smaller than the size of the critical ice nuclei and on superhydrophobic surfaces with hierarchical structures. They found that the freezing delay of smooth surfaces is much longer than that of superhydrophobic surfaces and [64].

In this study, the effect of surface chemistry, without significantly modifying the surface topography on the freezing delay, is investigated. The freezing delays and water contact angles are measured as a function of the substrate temperature and the results are compared to the predictions of the heterogeneous ice nucleation theory.

HAPTER 2. MATERIALS AND METHODS

2.1 MATERIALS

All solid substrates and chemical substances used in this study are mentioned in this section.

2.1.1 ALUMINUM ALLOY

Since the aluminum alloys are the materials predominantly used in heat exchanger production, the focus of this study is on aluminum alloy surface characteristics and the control of ice formation on top of their surfaces in cold working conditions. The main material used as a substrate for all the samples preparation and experiments and surface modifications of this study is aluminum alloy 8011. The aluminum alloy is used as received from the production line of air to air heat exchangers with a chemical composition according to Table 2.1. Aluminum sheets were plain, single rolled with a thickness of 0.25 mm and cut into test samples of 15× 15 mm^2 or 10 ×10 mm^2.

Samples were degreased in an ultrasound cleaner in a process consisting of 10 min in an acetone bath, then 10 min in DI-water and finally 10 min in an ethanol bath. The samples were then dried under an N_2 stream or under a clean air stream and dried in an oven overnight at 110°C.

Table 2-1 Chemical composition of Aluminum alloy 8011 according to EN 573-3.

	Si [%]	**Fe [%]**	**Cu [%]**	**Mn [%]**	**Mg [%]**	**Cr [%]**	**Zn [%]**	**Ti [%]**	**Others each [%]**	**Others total [%]**
min	0.40	0.50	-	-	-	-	-	-	-	-
max	0.8	1.0	0.10	0.10	0.10	0.10	0.10	0.05	0.05	0.05

2.1.2 ALUMINUM FOIL

The high surface roughness of bare unpolished aluminium samples renders it impossible to measure directly the thickness of the native aluminium oxide, hyperbranched PEG and perfluorooctylsilane layers formed on its top by ellipsometry. Therefore, to be able to use ellipsometry for measuring the thickness of a formed layer on top of an aluminum alloy, the smooth foil samples must be prepared as substrates and synthesized for further measurements. The aluminum foil samples were cut from a rolled aluminum foil, 0.3 mm thick and 30 mm wide produced by Merck KGaA, Darmstadt, Germany.

2.1.3 CHEMICALS

All chemical substances used during this study, such as a anhydrous methanol (99.8%), sodium methoxide, fuming nitric acid (100%), glycidol (96%), toluene (99.5%), tetrahydrofuran (99%) and (3-Aminopropyl) triethoxysilane (APTES) 99% were purchased from Sigma–Aldrich Co. 1H,1H,2H,2H- perfluorooctyltrichlorosilane was purchased from Fluorochem Ltd. and Sigma–Aldrich Co. All aforementioned chemicals were used as received.

2.2 SAMPLE PREPARATION

Aluminum alloy is the main material used in the production of heat exchangers, and in order to investigate the effect of aluminum alloy surface morphology and chemical modification on its wettability, ice nucleation, formation, growth and freezing delay, seven groups of samples were prepared and studied in this study. The seven groups of samples were bare aluminum alloy as received from the production line, polished aluminum alloy samples, samples with hyper-branched polyethylene glycol (PEG), samples with perfluorooctylsilane (PFOS) and samples with perfluorooctylsilane on top of Hyperbranched PEG (PFOS/PEG), samples with organosilane- 3-aminopropyltriethoxy silane on top (APTES)APTES and finally samples that are prepared by water plasma treatment. Moreover, four groups of samples of polished aluminum alloy and four groups of aluminum foil with the same surface modification were prepared. These samples were prepared as explained below:

2.2.1 BARE ALUMINUM ALLOY

Bare aluminum alloy samples were used for the investigation as received from the production line and after the degreasing procedure described in 2.1.1.

2.2.2 ALUMINUM FOIL

The aluminum foil samples were cut from a rolled aluminum foil and degreased using the aforementioned procedure, subsequently, the bare, hyperbranched polyethylene glycol (PEG), perfluorooctylsilane (PFOS) and perfluorooctylsilane on top of the hyperbranched PEG (PFOS/PEG) samples were papered.

2.2.3 POLISHED ALUMINUM ALLOY

Polished aluminum alloy samples were grinded with 500 grit sandpaper followed by 1200, 2400 and 4000 grit sandpaper and finally polished using colloidal silica suspension of 40 nm particles on a synthetic cloth and 3 μm diamond suspension on a wool cloth.

2.2.4 HYPERBRANCHED POLYETHYLENE GLYCOL (PEG)

The polymerization process of the surface-initiated polymerization of glycidol on the aluminum surface followed a method introduced by Khan and Huck, 2003[78]. The native oxide layer on top of the aluminum was activated by placing the washed surface samples in washed glassware under a nitrogen atmosphere in a heated (60–70°C) sodium methoxide solution in anhydrous methanol for an hour. The activated surface samples were washed with anhydrous methanol and twice with 99% ethanol and then dried under a N2 stream and placed in washed glassware under a nitrogen atmosphere.

In order to start the in situ polymerization, glycidol was added with a syringe under a nitrogen atmosphere until the samples were fully covered; they were then kept at 118◦C for an hour. The complete details of the procedure is explained in Paper I [22] and the schematic mechanism of polymerization is shown in Figure 2-1.

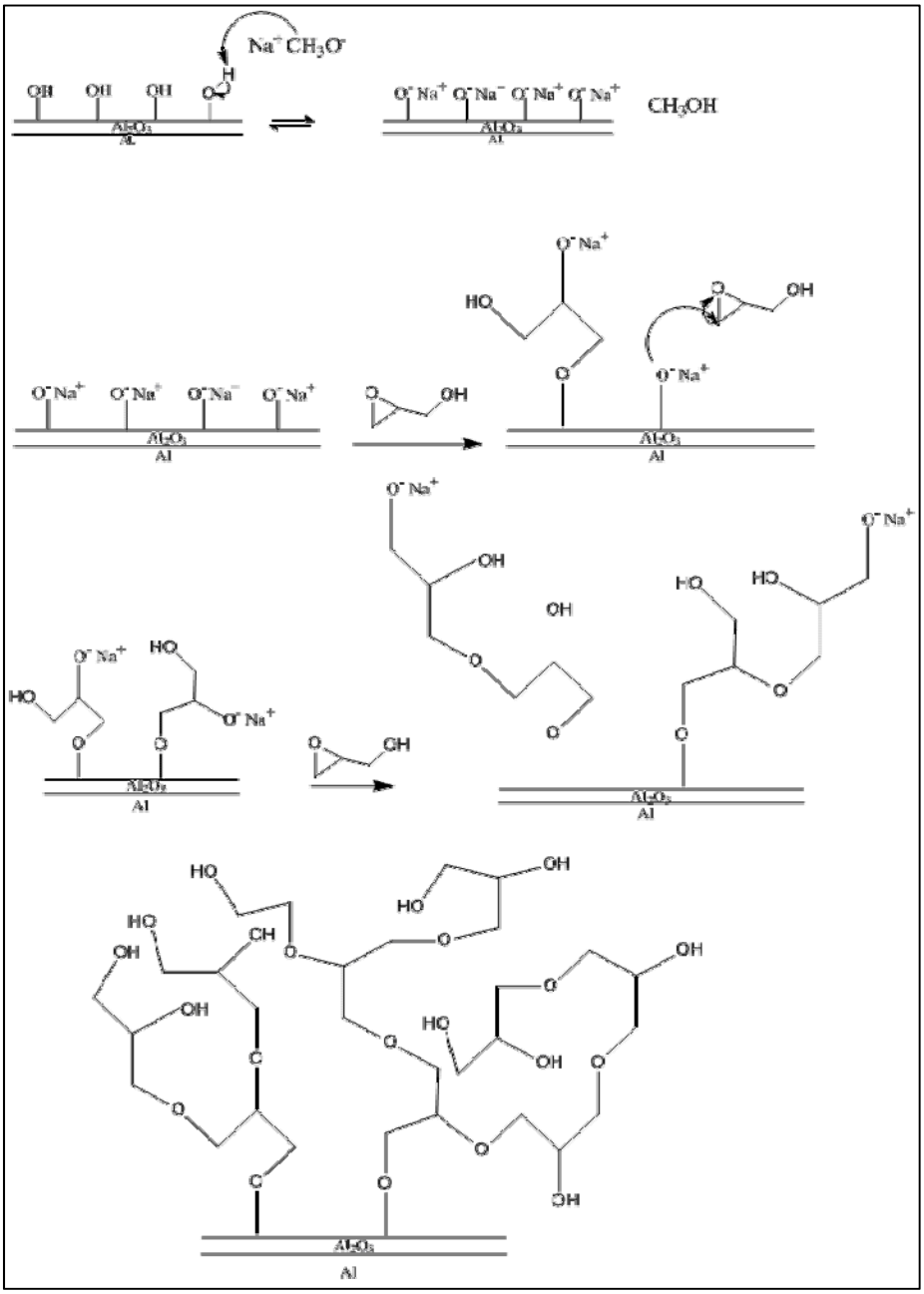

Figure 2-1 schematic of polymerization mechanism of PEG on top of the aluminum substrate [22]

2.2.5 WATER PLASMA TREATMENT

One group of samples was modified using the water plasma treatment method. Moreover, the native oxide layers on top of the aluminum substrate samples needed to be activated for further surface modification. The water plasma treatment or the chemical methods, heated sodium methoxide solution as used and explained in 2.2.4, may be applied for surface activation [22,45].

Subjecting the sample surfaces to the water plasma treatment makes a highly oxidative hydroxyl (OH) radical to oxidize chemical contaminants and creates a high concentration hydroxyl group surface [79,80]. The water plasma treatment is suggestable because of its controllability and reproducibility effects on the surface [80]. In this study, a Harrick Plasma Cleaner was used at different process times of 50, 100, 200, 300 and 400 seconds. Ionized water vapor entered the reactor from the top of the plasma source and was dissociated by the plasma electrons as it flowed through the tube [80].

The formed plasma, which is rich in -HO radicals and other strongly oxidative species generated from H_2O, oxidizes the surface and cleans it from any organic contamination that might be present on the surface after degreasing [79]. After the water plasma treatment a stable, hydrophilic, clean aluminum surface was prepared. The schematic mechanism of the water plasma treatment on the top of the aluminum substrate is shown in Figure 2-2

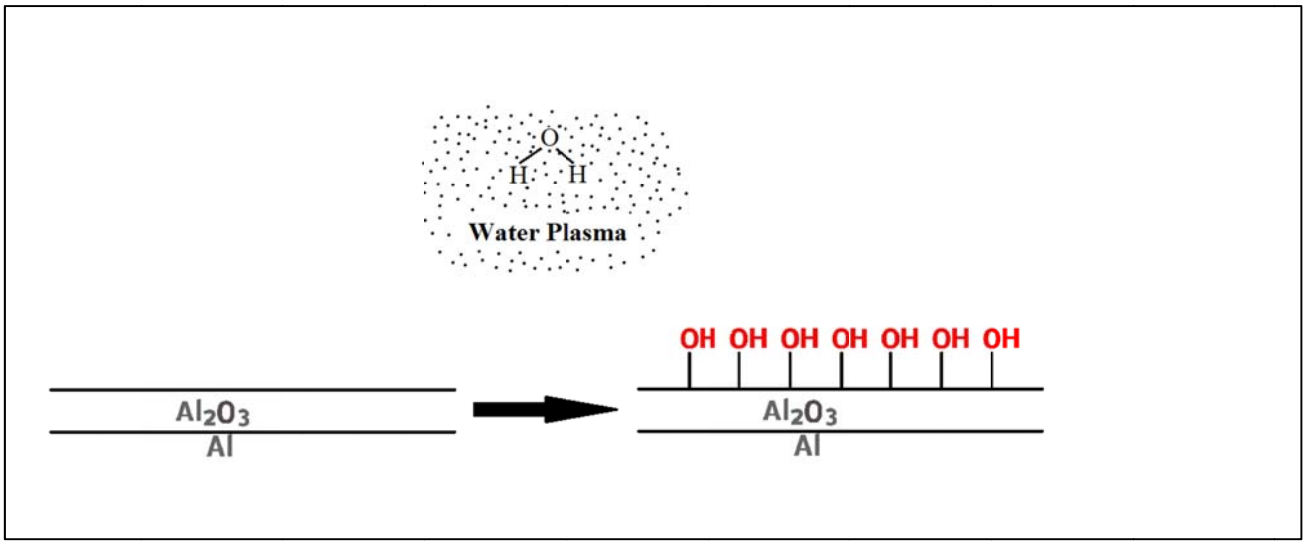

Figure 2-2 Schematic mechanism of water plasma treatment on the top of the aluminum substrate

In this study, the flow and pressure of water vapor were controlled using a mass flow controller. For optimal plasma uniformity, the plasma treatment was performed at 900 mTorr (120 Pa) pressure of water vapor and the plasma energy was set at high RF.

This relatively mild plasma treatment does not lead to significant changes in the surface roughness; however, in order to study the effect of plasma treatment time on the surface characteristics and wettability of the surface, the contact angle of surfaces were measured at different times while being exposed to the water plasma treatment. As shown in Figure 2-3, the surfaces contact angles are almost within the same range of magnification. However, the process time is set to 200 sec for optimal plasma treatment uniformity and surface activation since, as shown in Fig 2-3, this shows the lowest contact and highest degree of wettability for aluminum alloy.

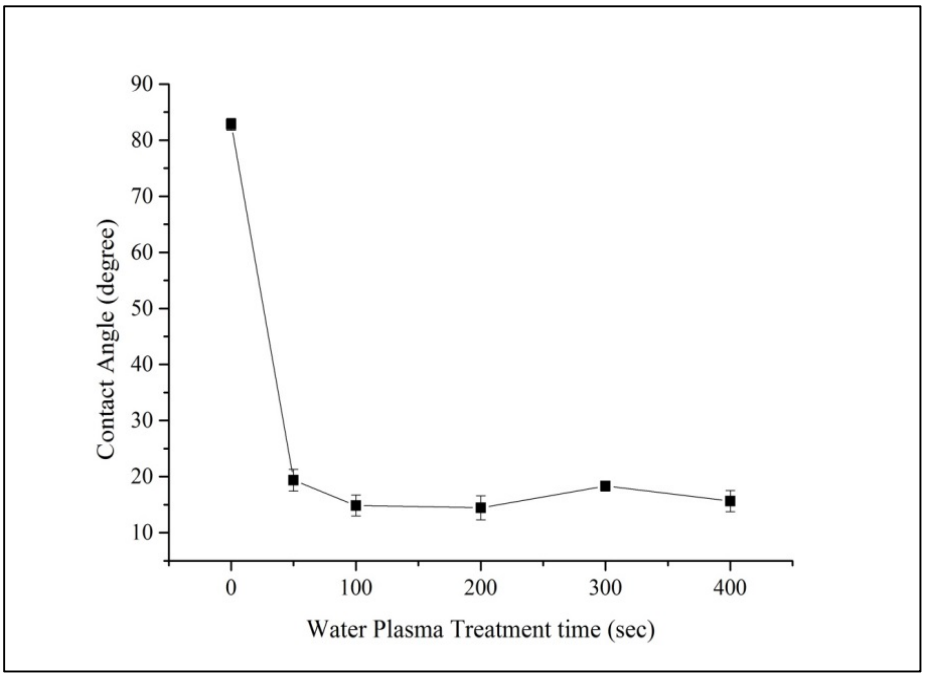

Figure 2-3. Effect of time exposure of water plasma treatment on contact angle of bare aluminum samples. Error bars show 95% confidence interval

2.2.6 GAS DEPOSITION OF PERFLUOROOCTYLSILANE (PFOS) MODIFICATION OF ALUMINUM SURFACE

The native oxide layer on top of the aluminum samples was activated either by the chemical method (heated sodium methoxide) (Sec. 2.2.4) or by the water plasma process (Sec. 2.2.5) and was then placed in an evacuated desiccator containing a solution of 250 µl 1H,1H,2H,2H-perfluorooctyltrichlorosilane in 750 µl of anhydrous, 99.8% toluene and heated to a temperature of 110◦C for 3 hours. The schematic of the reaction mechanism of the gas deposition of perflourooctylsilane by chemical and water plasma activation methods of the native aluminum oxide layer is shown in Figure. 2-4 [22].

The method was applied earlier in paper (I) and paper (V) and demonstrated the formation of continuous reproducible silane layers with high contact angles. To obtain smooth and reproducible silane layers, the deposition was performed in an evacuated chamber containing a solution of silane in toluene as was suggested and performed in previous works [22,81,82]

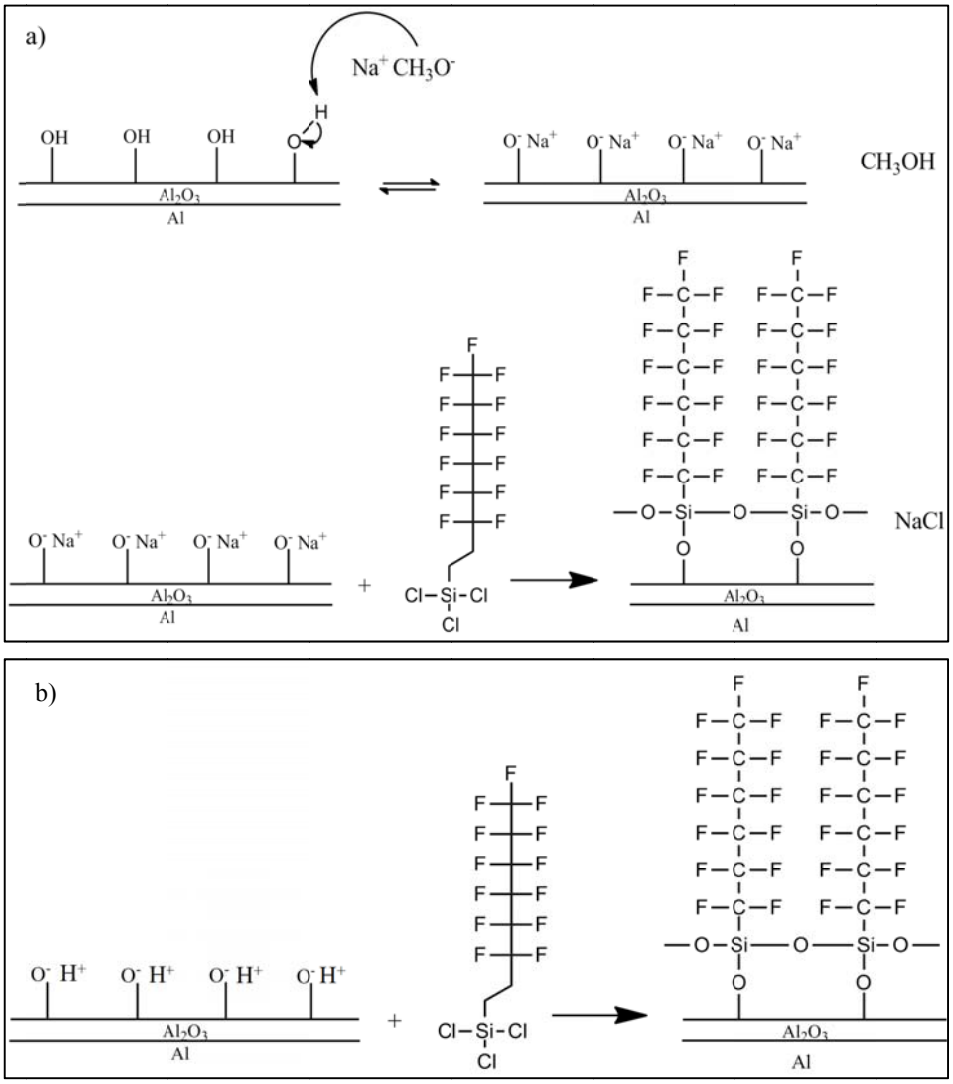

Figure 2-4 Schematic mechanism for the activation and chemical vapor deposition of perfluorooctylsilane on an aluminum surface a) by chemical surface activation, b) by water plasma surface activation

2.2.7 PERFLUOROOCTYLSILANE MODIFICATION OF THE HYPERBRANCHED PEG LAYER (PFOS/PEG)

The group of samples with a layer of PEG and a layer of perfluorooctylsilane on top are prepared by polymerization technique as mentioned in 2.2.4 and subsequently by the chemical activation of the polymer layer as explained in 2.2.4 and the vapor deposition of perfluorooctylsilane on top of the Hyperbranched PEG as explained in 2.2.6.

2.2.8 3-AMINOPROPYLTRIETHOXYSILANE (APTES) MODIFICATION OF ALUMINUM SURFACE

Organosilane reagents are commonly used to produce functionalized thin films on oxide substrates for a variety of technological applications and investigations. Among the organosilane,reagent 3-aminopropyltriethoxy- silane (APTES) is one of the most frequently used silane [45,83]. The chemical vapor deposition of APTES is an easy-to-implement deposition method which is reproducible and yields a smooth aminosilane mono layer on the surface [84,85].

In preparing the samples with the 3-aminopropyltriethoxy silane (APTES) on top, the aluminum native oxide layer is activated by water plasma treatment as explained in 2.2.5, and then the silane group is deposited on the activated surface by the vapor deposition identical to the procedure of the perfluorooctylsilane deposition by placing a chemical solution of 250 µl of (3-Aminopropyl) triethoxysilane in 750 µl of toluene in the desiccator. The schematic of the mechanism is shown in Figure 2-5.

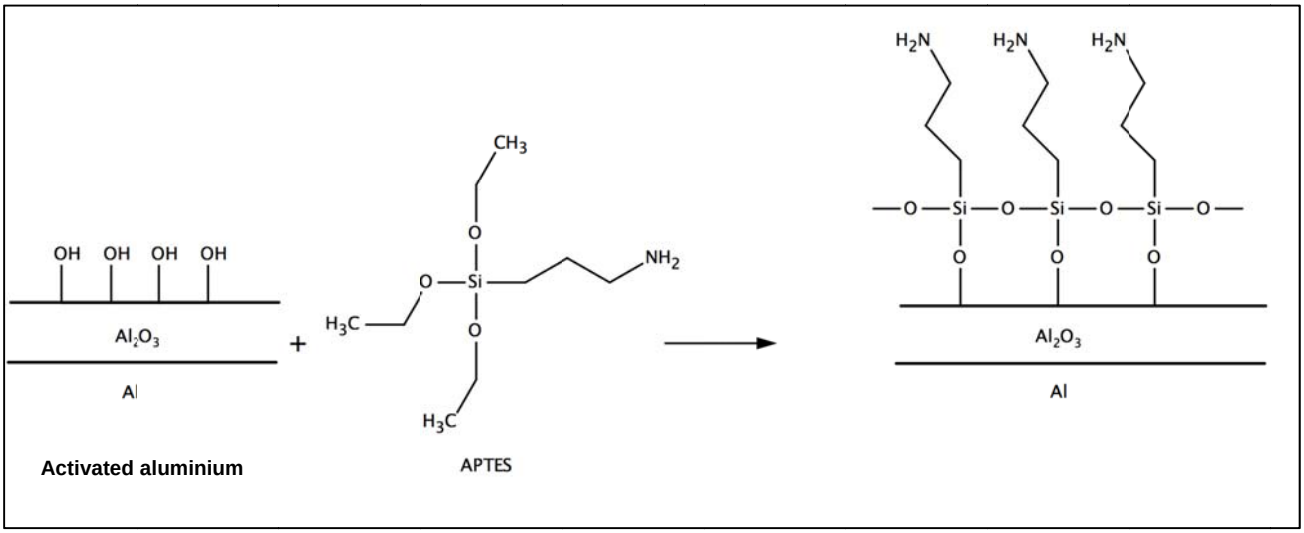

Figure 2-5 Schematic mechanism of chemical vapor deposition of APTES on water plasma activated aluminum

2.3 SURFACE CHARACTERIZATION

In order to characterize the modified surfaces in this study, surface characterization techniques, such as contact angle measurement, ellipsometry and AFM, are applied.

2.3.1 CONTACT ANGLE MEASUREMENT

In paper I, the contact angles were measured using a homemade computer-controlled evaporation of the sessile drops stage; thus was used to measure the advancing contact angle as explained in paper I [22]. In paper V, the static contact angle of a water droplet on top of the samples was measured using Attension Theta Lite Optical Tensiometer, which is a computer-controlled and user-programmable video-based instrument.

2.3.2 ELLIPSOMETRY

The ellipsometry measurement was applied for measuring the deposited and synthesized layer of PFOS and PEG on top of the smooth surface of polished aluminum and aluminum foil samples. The measurements were carried out using Sentech SE 850 Ellipsometer as explained in paper I. The ellipsometry measurements could not be completed on top of the aluminum samples due to surface roughness.

2.3.3 ATOMIC FORCE MICROSCOPY(AFM)

In paper I, the surface morphology was visualized by atomic force microscopy (NTEGRA Aura, NT-MDT Co.) in tapping mode using Olympus OMCL-160TS cantilevers for the measurement. The AFM images were analyzed using WSXM software [86]. In paper V, atomic force microscopy (NanoWizard 3, Germany) is used in tapping mode and NSC36/Cr-Au cantilever was used for the measurements. The acquired images were processed for RMS roughness calculation by JPK data processing software.

2.4 EXPERIMENTAL APPARATUS AND METHODOLOGY

In this study, two experimental apparatus are built and modified for measuring the ice thickness and density formed on top of the samples and for measuring the freezing delay.

2.4.1 ICE FORMATION AND GROWTH MEASUREMENTS

The experimental apparatus built for measuring the ice thickness and ice density formed on top of the sample surfaces are explained in details in paper III and IV[17] and its schematic is illustrated in Figure 2-6.

This experimental apparatus consisted of a climate chamber which allowed full control of the ice formation parameters, including airflow, air humidity, surrounding temperature and the cold surface temperature of the test section. Moreover, the experiments were performed in a clean room in order to ensure a low concentration of polluting gases and particles during the experiments. The air supply system in the clean room provided extensive air filtration using a F7-class filter, a charcoal filter followed by a second F7-class filter and finally, a HEPA filter.

In the presented study, the ice thickness was measured with a monochrome CCD camera (The Imaging Source, Germany) with the ability to capture up to 60 images/s at a resolution of 1280x 960 pixels. This was used for monitoring the ice formation. The camera was equipped with a video lens (Edmund Optics, UK) with 68mm WD, 3.61mm horizontal field of view and a magnification of 1.33X.

The porous structure of the ice, which creates a rather rough surface on the ice layer due to the random ice nucleation on the surface, renders measuring its thickness measurement both challenging and problematic. Since it is a crucial parameter which affects the accuracy of all other measurements, the ability to measure ice thickness is crucial; therefore, several measuring techniques have been developed and investigated. Some of these methods are mechanical methods using a micrometric screw by Lee et al., 2003 [87] and Na and Webb, 2004 [40], which require an interruption of the experiment to perform the measurement or laser method and optical measurements methods. In most cases, the laser method is not applicable due to the roughness of the ice surfaces caused by the random accumulation of water vapor on the porous structure of the ice [40,88]. The optical method is considered the most accurate method for ice thickness measurement since it involves image analysis and is independent of its morphology and have been applied by researches, such as Moallem et al. ,2012 [89] and in this study.

The optical measurement method applied in this study involved recording the side images of samples and measuring the thickness of at least 10 points on each sample and analyzing and interpreting them after each test and calculating the average thickness of the ice. For ensuring the accurate observation and control of the measurements temperature, the test chamber was equipped with a K-type thermocouple attached to the surface of the sample holder. Readings were recorded with a temperature logger at a rate of 51 samples/min (Agilent GUI data logger). During each experiment, the image video capture and the surface temperature logger simultaneously recorded the images and the temperature.

The relative humidity of the circulating air was adjusted with a cool mist ultrasonic humidifier (AIR-O-SWISS, Switzerland). The humidifier was operated with Milli-Q water to ensure the absence of mineral residues in the produced water mist. The temperature and humidity inside the chamber were measured using a humidity/temperature probe (Testo 400 Reference Meter&Logger, Testo Inc.) with an accuracy of ±1 %RH and ±0.05°C.

The mean air velocity was measured with a hotwire anemometer (DANTEC FLOWMASTER Precision Anemometer Type 54 N 60) positioned in a hole on the chamber roof, see figure 2-6 (Schematic of the test setup).

Prior to inserting a sample, the humidity and temperature in the chamber were allowed to settle to the desired parameters. The mean air velocity was kept constant at 0.57 m/s in all measurements. Table 2-1 shows a typical set of experimental conditions.

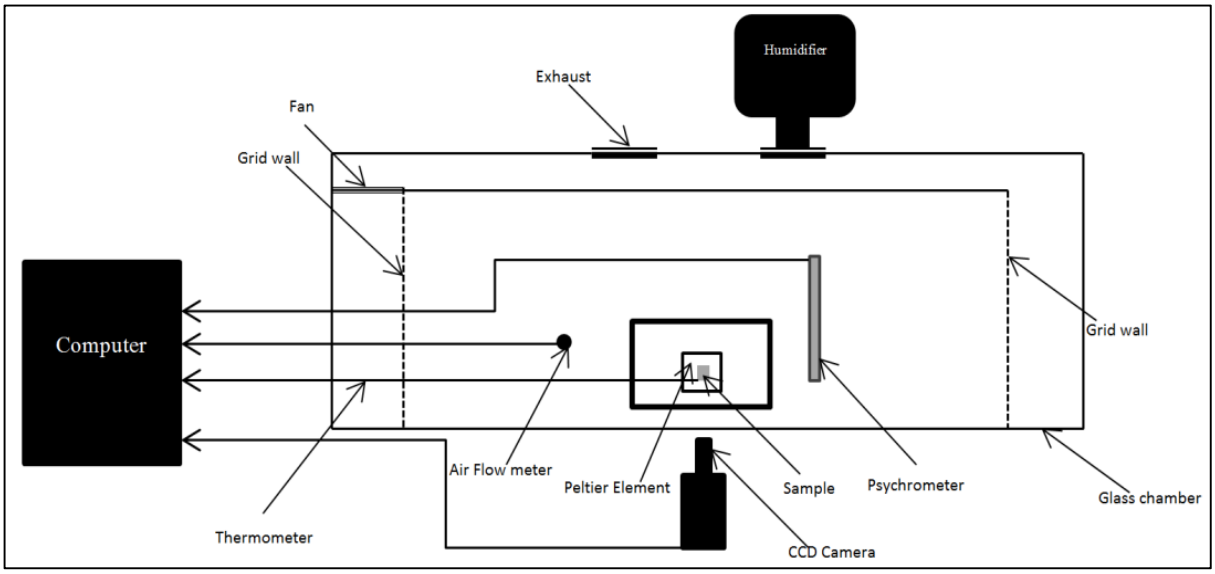

Figure 2-6 Schematic top view image of the test setup for ice formation thickness and density measurement [17]

Table 2-2 Typical experimental conditions

Typical experimental conditions	
Inlet air temperature	17 ± 0.1°C
Average inlet air velocity with confidence interval 95%	0.57 m/s
Ambient air temperature of the clean room	24°C

Moreover, in order to see the pattern of the water droplet on top of different samples, the samples were initially dried and then quickly cooled down to -10°C in order to form ice on the surface. The cooling process was then stopped and the process of de-icing was initiated and observed with the microscope STEMI 2000-C ZE 55 Microscope (Carl Zeiss, Germany) with 50x magnification, equipped with AxioCam ERc 5s 5 megapixels camera (Carl Zeiss, Germany). The patterns of water droplets acquired on top of different surfaces were visualized and quantified by converting the original microscope images to black and white using Matlab 2013, and the obtained coverage was calculated by counting black and white pixels. The results are illustrated and shown in detail in paper IV.

2.4.2 ICE DENSITY MEASUREMENTS

In order to measure mass of the accumulated ice on top of the samples for calculating the density of the formed ice, each sample was weighed on a digital balance before and after the experiment. In facilitating high-speed measurements and reducing measurement errors, the digital balance was placed next to the test chamber.

In addition to speeding up the weighing process and increasing the accuracy of the measurements, the samples needed to be detached from the cold plate and weighed as quickly as possible at the end of each measurement. Therefore, the cold plate was heated immediately before each sample was placed on the plate to prevent ice formation between the cold plate and the sample to prevent the sample from being adhere to the cold plate.

After placing the sample on the cold plate, the cooling sequence was immediately initiated. At the end of each test, the samples were quickly and carefully removed and placed on a digital balance. The accumulated ice mass on top of the sample was determined as the difference between the current and initial mass of the sample.

The density of formed ice on top of the sample was calculated as the relation of formed ice mass and its volume, as shown in equation 14.

$$\rho_{\mathrm{ice}}\left[{}^{\mathrm{gr}}/_{\mathrm{cm}^3}\right] = \frac{\mathrm{m_{ice}}}{(\mathrm{S}*\mathrm{H\ ice})} \tag{14}$$

Where ρ_{ice} is the frost density, S is the sample area in mm^2, H_{ice} is the measured height of the ice layer and m_{ice} is the mass of ice measured in grams.

2.4.3 FREEZING DELAY / ICE NUCLEATION

In this study, to investigate the effect of the surface chemistry on the freezing delay of a water droplet a homemade setup was built by modifying the Attension Theta Lite Optical Tensiometer which was used for the contact angle measurement in paper V. The water droplet was dispensed on the pre-cooled substrate in a wide range of temperatures and the freezing delay and contact angles were observed, recorded, measured and reported.

In order to cool the substrate a Circulating Bath with MX Temperature Controller (VWR®, USA) was added and installed to the sample stage of the Attension Theta Lite Optical Tensiometer. Prior to the measurement process, the sample stage, and consequently the sample, was cooled to the desired temperature by means of a cooling bath, and the surface temperature of the substrate was measured with a K-type temperature logger at a rate of 51 samples/min (Agilent GUI data logger). When the temperature had become stable the water droplet with a volume of 6 µl was placed on the substrate and the time and image recording were started simultaneously. The measured freezing delay times were defined as the time that the droplet was placed on the pre-cooled substrate and until the onset of freezing was determined by direct imaging through CCD camera. The start of the freezing process coincided with the clouding of the water volume, which was caused by the spontaneous crystallization followed by volume change conditions of air [64,90]. To simulate freezing, the experiments were conducted in low humidity. Table 2-3 shows the typical experimental conditions.

Table 2-3 Typical experimental conditions for freezing delay and contact angle measurements at subzero temperatures

Typical experimental conditions	
Ambient air humidity	30% ± 2%
Ambient air temperature	23°C ± 1°C
Inside the chamber humidity	26% ± 1%
Inside the chamber temperature	21°C ± 1°C

The discrepancy in icing behavior as reported by various authors may be caused by the lack of robustness and stability of samples surfaces, due to humidity, insufficient pressure stability during icing procedure [6]. In reducing discrepancy in the measurements performed in this study all measurements are performed on fresh synthesize samples in order to prevent any probable effects of freezing on the surface characteristics. Moreover, in order to increase the accuracy of the reported data and results of freezing delay, a minimum of seven measurements are performed for each group of samples in a specific temperature. The detailed numbers of all freezing delay and contact angle measurements are shown in Table 2-4.

For the contact angle measurement in subzero temperatures the angle is the average of a static contact angle of a droplet in the initial seconds after the droplet has been placed on the pre-cooled substrate. The schematic figure of the experimental apparatus is shown in Figure 2-7.

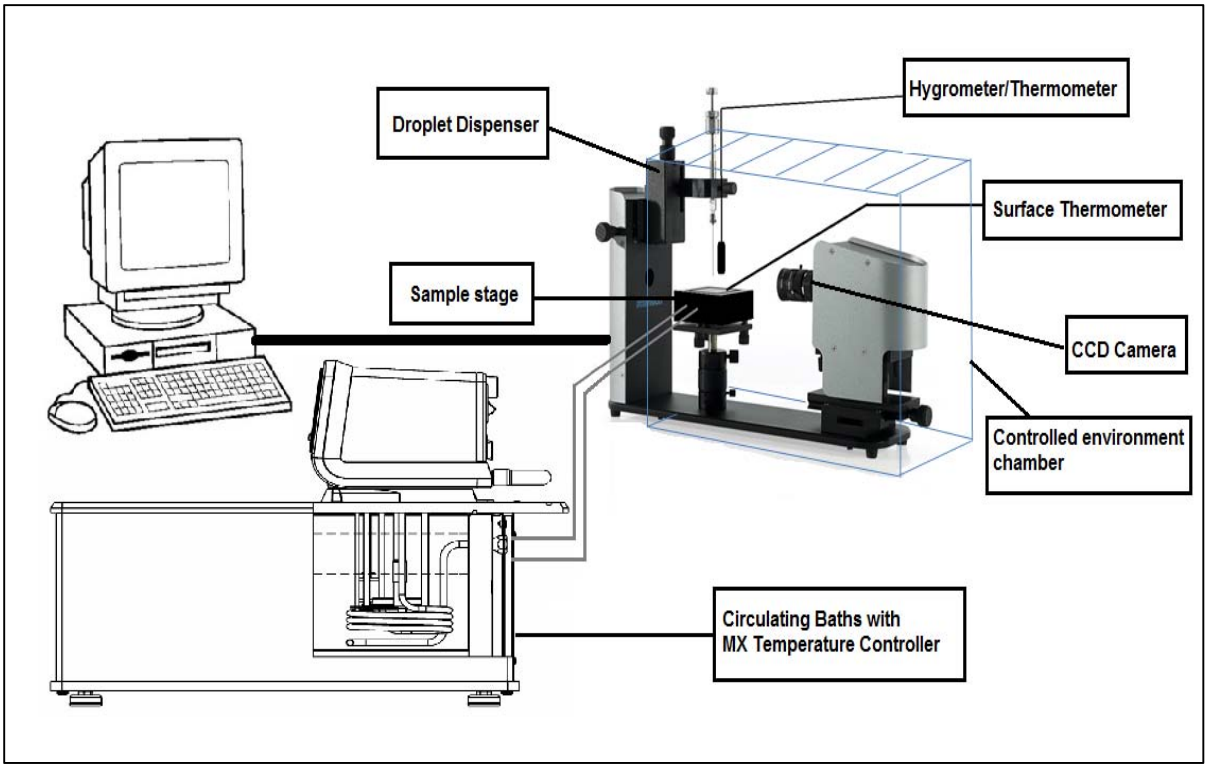

Figure 2-7 Schematic view of the test apparatus for measuring contact angle and freezing delay

Table 2-4 The detailed numbers of all measurements for measuring freezing delay and contact angle at different temperatures

		Number of Test for measurement of	
Group of Sample	**Temperature (°C)**	**Contact Angle (degree)**	**freezing Delay (sec)**
Bare Samples	23	21	
	20	8	
	15	7	
	10	7	
	5	7	
	0	14	
	-5	24	12
	-7	9	11
	-10	18	9
	-12	9	9
	-15	15	13
	-18	12	12
	-20	19	15
Samples with Water Plasma treatment	23	20	
	20	8	
	15	9	
	10	7	
	5	7	
	0	13	
	-5	28	7
	-7	18	10
	-10	11	10
	-12	8	12
	-15	17	10
	-18	11	11
	-20	24	15
Samples with a layer of APTES	23	18	
	20	11	
	15	8	
	10	9	
	5	8	
	0	8	
	-5	25	14
	-7	12	7
	-10	11	21
	-12	14	9
	-15	19	12
	-18	9	9
	-20	31	12
Samples with a layer of PFOS	20	17	
	15	7	
	10	8	
	5	8	
	0	7	
	-5	16	11
	-7	7	9
	-10	15	17
	-12	15	15
	-15	17	12
	-18	13	13
	-20	12	11

CHAPTER 3. RESULTS AND DISCUSSION

3.1 RESULTS

This PhD dissertation is based on five published articles, which are summarized in this chapter.

3.1.1 SUMMARY OF ''EFFECTS OF ALUMINUM SURFACE MORPHOLOGY AND CHEMICAL MODIFICATION ON WETTABILITY''

Aluminum alloys are among the metals predominantly used for industrial applications such as the production of heat exchangers and heat pumps. They have high heat conductivity coupled with a low specific weight. In cold working conditions, there is a risk of ice formation on the surface of aluminum in the presence of water vapour; this may lead to the deterioration of equipment performance. This work addresses the methods of surface modification of aluminium and their effect of the underlying surface morphology and wettability, which are the important parameters for ice formation. Three groups of real-life aluminium surfaces of different morphology: unpolished aluminium, polished aluminium and aluminium foil, were subjected to surface modification procedures which involved the formation of a layer of hydrophilic hyperbranched polyethyleneglycol via in situ polymerization, molecular vapour deposition of a mono- layer of fluorinated silane and a combination of these. The effects of these surface modification techniques on the roughness and wettability of the aluminium surfaces were elucidated by ellipsometry, contact angle measurements and atomic force microscopy. We demonstrated that by employing different types of surface modifications, the contact angle of water droplets on aluminium samples may be varied from 12◦ to more than 120◦. A crossover from Cassie–Baxter to Wenzel regime upon changing the surface roughness was also observed.
In this paper, the effect of changing the aluminum surface characteristics and morphology on wettability properties was investigated and the results were shown. The surface morphology was changed by different chemical surface modifications and mechanical surface modifications on the aluminum alloy 8011 (unpolished and polished) and aluminum foils as substrate.

Evidence for the layer formation on unpolished, smooth foil and polished aluminum samples surfaces was obtained by different techniques, ellipsometry, contact angle measurement and AFM.

The ellipsometry measurement carried out just on the aluminum foil and polished aluminum, however, due to the high surface roughness of the unpolished aluminum samples it was impossible to measure the thickness of the native aluminium oxide, hyperbranched PEG, and perfluorooctylsilane layers formed on their top by ellipsometry. The mean thicknesses of the formed layers on top of the samples are shown in Table 3-1.

Table 3-1 The mean thicknesses of the formed layers on top of the samples measured by ellipsometry

Layer type / Substrate	Polished Aluminium	Aluminium foil
Native Aluminium oxide layer (nm)	7 ± 0.21	11 ± 0.27
Hyperbranched PEG (nm)	3 ± 0.24	2 ± 0.12
Perfluorooctylsilane on top of Hyperbranched PEG (nm)	0.5 ± 0.05	0.5 ± 0.01
Perfluorooctylsilane (nm)	0.5 ± 0.02	0.5 ± 0.01

The contact angle measurements showed the effectiveness of chemical and mechanical surface modifications on top of the solid substrate of unpolished aluminum, polished aluminum and aluminum foils samples. Figure 3-1 shows the changes in the contact angle and wettability of the surfaces according to the surface modifications at room temperature.

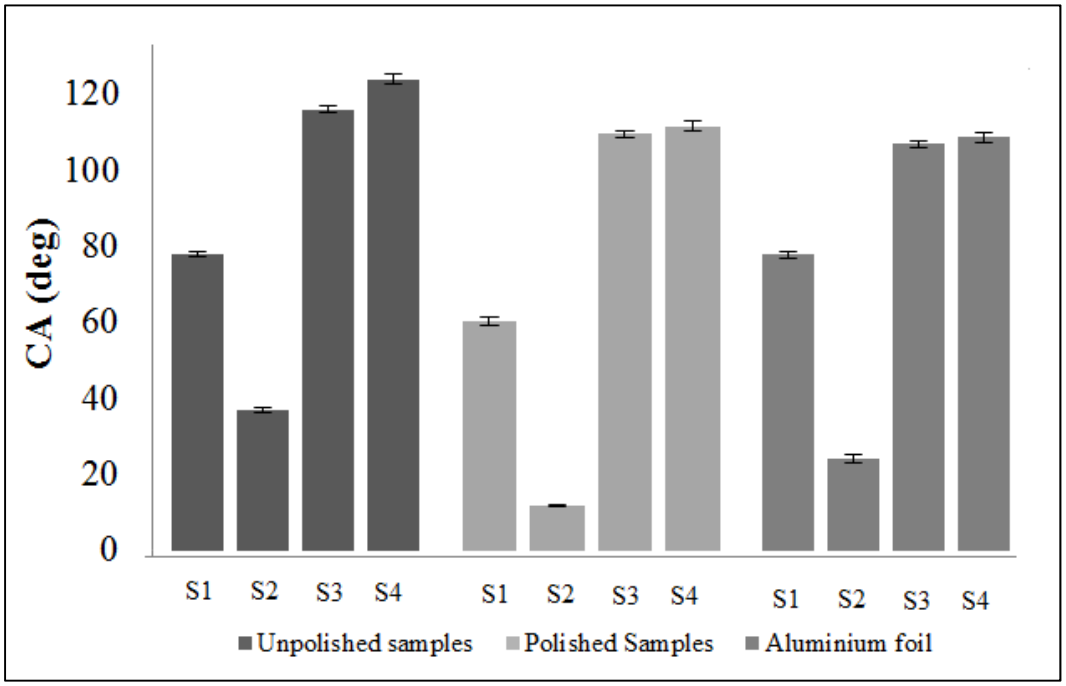

Figure 3-1 Advancing CAs for all the 3 sample groups in the study (bar shows 95% confidence interval), S1: Bare samples, S2: Samples with hyperbranched PEG, S3: Samples with hyperbranched PEG and perfluorooctylsilane and S4: Samples with perfluorooctylsilane.

As is clear from the results, the formation of a layer of hydrophilic hyperbranched polyethyleneglycol (PEG layer) via in situ polymerization can increase the hydrophilicity of the surface and consequently reduce the contact angle and increase the wettability. The lowest contact angle of 12◦ was observed on the polished aluminium surfaces with PEG layer.

Moreover, the vapor deposition of perfluorooctylsilane (PFOS) on the surface of hyperbranched PEG and on the activated aluminum substrate was completed effectively and the surfaces adopted the hydrophobic characteristics of the PFOS monolayer due to evidence of changing the surface wettability and increasing the contact angle on all surfaces. The maximum contact angle of 124◦ was observed on the unpolished aluminium surfaces with PFOS layer.

Roughness measurements were based on the AFM data. The data showed that the formation of hyperbranched PEG layer on the surface led to a significant increase in the surface roughness of all samples (bare unpolished, polished and aluminium foil); this may be caused by its brush structure.

Due to the inherent surface roughness, the chemical reaction was not uniform across the entire surface. Therefore, different growth rates at different points on a surface or different growth rates for different sample groups may be expected. Therefore, as shown in Figure 3-2, the unpolished samples with hyperbranched PEG exhibited the highest RMS roughness value compared to all other samples. Mass transportation is typically a limiting factor for chemical reactions on surfaces; this leads to the fact that chemical reactions typically proceed at faster rates on surface extremities and at slower rates in the valleys. So a bare surface with a higher initial roughness will have higher increase in roughness upon PEG brushed layer formation than the samples with lower initial roughness.

On the contrary, molecular deposition of low surface energy perfluorooctylsilane on the aluminium samples with the PEG layer reduced the surface roughness, presumably due to a higher probability of binding the perfluorooctylsilane molecules in the grooves of the hyperbranched PEG structure.
The hydrophobic group of samples, samples with perfluorooctylsilane, deposited either directly on a bare aluminium surface or on top of the hyperbranched PEG followed the Wenzel model as regards wetting. The reason for this is that increasing the surface roughness of these groups of samples will lead to an increase in their hydrophobicity, thus, the samples with a higher roughness become more hydrophobic.

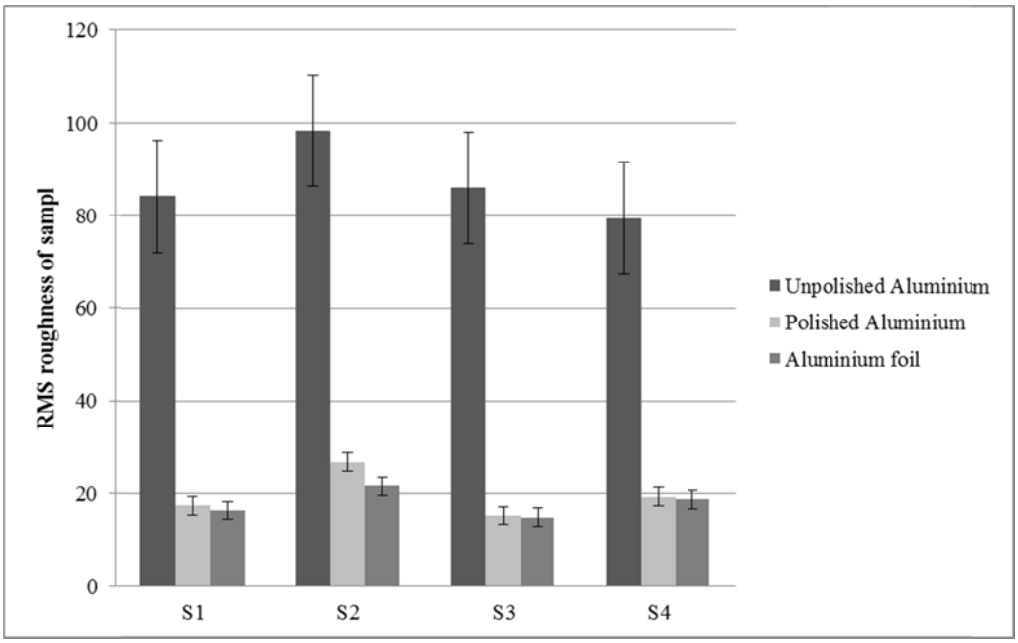

Fig.3-2 RMS roughness of samples at 95% confidence interval, S1: Bare samples, S2: Samples with hyperbranched PEG, S3: Samples with hyperbranched PEG and perfluorooctylsilane and S4: Samples with perfluorooctylsilane.

Owing to their high roughness and air pocket structure, the bare unpolished samples and unpolished samples with PEG followed the Cassie–Baxter model, since they exhibited larger contact angles and lower wettability than the polished samples. The results proved that polishing the bare aluminum alloy lead to a decrease in the surface roughness. Moreover, the advancing contact angles of bare unpolished and unpolished PEG samples were higher than those of the polished PEG samples. This means polishing may serve to reduce the hydrophilicity of bare polished aluminum and polished PEG samples. Thus, there is a transition from Cassie–Baxter's to Wenzel's regime due to changing the surface roughness upon mechanical polishing.

3.1.1.1 Actual paper I

Effects of Aluminum Surface Morphology and Chemical Modification on Wettability
M. Rahimi, P. Fojan, L. Gurevich, and A. Afshari.
Applied Surface Science Vols. 296 (2014) pp124–132

Applied Surface Science 296 (2014) 124–132

Contents lists available at ScienceDirect

Applied Surface Science

journal homepage: www.elsevier.com/locate/apsusc

Effects of aluminium surface morphology and chemical modification on wettability

M. Rahimi [a,*], P. Fojan [b], L. Gurevich [b], A. Afshari [a]

[a] Department of Energy and Environment, Danish Building Research Institute, Aalborg University, A.C. Meyers Vænge 15, 2450 København SV, Denmark
[b] Department of Physics and Nanotechnology, Aalborg University, Skjernvej 4, DK-9220 Aalborg East, Denmark

ARTICLE INFO

Article history:
Received 17 October 2013
Received in revised form 10 January 2014
Accepted 11 January 2014
Available online 22 January 2014

Keywords:
Surface modification
Contact angle
Aluminium surface
Roughness
In situ polymerization
Molecular vapour deposition

ABSTRACT

Aluminium alloys are some of the predominant metals in industrial applications such as production of heat exchangers, heat pumps. They have high heat conductivity coupled with a low specific weight. In cold working conditions, there is a risk of frost formation on the surface of aluminium in the presence of water vapour, which can lead to the deterioration of equipment performance. This work addresses the methods of surface modification of aluminium and their effect of the underlying surface morphology and wettability, which are the important parameters for frost formation. Three groups of real-life aluminium surfaces of different morphology: unpolished aluminium, polished aluminium, and aluminium foil, were subjected to surface modification procedures which involved the formation of a layer of hydrophilic hyperbranched polyethyleneglycol via *in situ* polymerization, molecular vapour deposition of a monolayer of fluorinated silane, and a combination of those. The effect of these surface modification techniques on roughness and wettability of the aluminium surfaces was elucidated by ellipsometry, contact angle measurements and atomic force microscopy. We demonstrated that by employing different types of surface modifications the contact angle of water droplets on aluminium samples can be varied from 12° to more than 120°. A crossover from Cassie–Baxter to Wenzel regime upon changing the surface roughness was also observed.

1. Introduction

Aluminium alloys play an important role in modern industry, for instance in the production of aircrafts, vehicles, different types of heat exchangers and heat pumps [1,2]. This is due to their particular characteristics such as its high heat conductivity, low specific weight, and high specific strength. Moreover aluminium has self-passivation properties due to the formation of a stable native oxide layer, hence protecting the bulk material from further oxidation and corrosion [3–5]. In cold working conditions in the presence of water vapour, condensation of water vapour or frost formation can occur when the temperature of aluminium surface drops below the dew point. The condensation of water vapour or accretion of frost is mostly undesirable, for example frost accretion on aircraft wings can pose a serious problem. In addition, this can lead to the deterioration of equipment performance. For example, frost formation can clog or narrow the air passages of heat exchangers hence increasing the pressure difference. Moreover, it increases thermal and flow resistance and consequently lowers heat performance of heat exchangers and overall reduces the system performance [6,7]. Alongside with the importance of psychrometric parameters such as air temperature, velocity, humidity and surface temperature on the frost formation process, surface conditions such as surface temperature, roughness, drop adhesion to the surface and consequently contact angle are also important parameters for frost formation [8–10]. Therefore surface characteristics and surface modifications of aluminium strongly affect the performance characteristics of a whole range of different machinery involving aluminium and its alloys.

Different strategies and methods need to be applied in order to delay or prevent the frost formation on the surface of aluminium. One of the key factors of frost formation on solid surfaces is adhesion of a droplet to the surface and its wettability. The drop adhesion can be measured by dedicated experimental techniques such as centrifugal adhesion balance (CAB). This technique allows the study of the relation between lateral adhesion forces at a solid–liquid interface and the resting time of a droplet prior to sliding off the surface [10]. The wettability can be controlled by varying the surface chemistry, e.g., by chemical modification of the surface, or by changing the surface morphology, e.g., by forming micro/nanostructures on the surface [11]. The relation between the surface morphology and contact angle is generally described by two models, which address the wettability of rough surfaces: the Wenzel and the Cassie–Baxter model [12–14]. Both models

* Corresponding author. Tel.: +45 50123969.
E-mail addresses: mar@sbi.aau.dk, maral.rahimi1@gmail.com (M. Rahimi).

0169-4332/$ – see front matter © 2014 Elsevier B.V. All rights reserved.
http://dx.doi.org/10.1016/j.apsusc.2014.01.059

denote the wettability in terms of the angle that a liquid droplet forms on a solid surface (contact angle) [15–17]. Although these models are commonly used for the interpretation of data related to the wettability of surfaces, it should be mentioned that there is some ongoing discussion about the validity of these models in recent scientific literature. We can refer the reader to a recent comprehensive review by Gao and McCarthy summarizing this issue [18]. They claim that the contact angle is not only related to the contact area and the interfacial free energies, which the Wenzel and the Cassie–Baxter models are based upon, but also to other parameters such as the activation energies that the contact line has to overcome to move from one metastable state to another one and demonstrated that the Wenzel and the Cassie–Baxter model are unsuitable for interpreting certain experimental results [19]. On the other hand, as has been pointed out by Marmur and Bittoun, the contact angle predicted by the Wenzel and Cassie–Baxter models matches the experimental results in the case where the droplet is sufficiently large compared to the wavelength of the surface roughness or chemical inhomogeneity, i.e. within the limits of applicability of the models [20].

The Wenzel model is based on the assumption that the liquid has the ability to penetrate into the surface roughness and is always in contact with the substrate surface. According to this model the contact angle of liquid droplets on solid substrate is described by Wenzel's equation [13]:

$$\cos\theta_r = R\cos\theta_s \quad (1)$$

where θ_s and θ_r are the contact angles on perfectly smooth and rough surfaces of the same composition, respectively. R is the roughness factor defined as the ratio of actual (wetted) surface area to that of flat material (geometrical area). By increasing roughness of a hydrophilic surface, it should become more hydrophilic and a hydrophobic surface should become more hydrophobic according to the Wenzel model [21].

The Cassie–Baxter model treats the solid surface as microscopically mosaic composed of several components, each of which possesses their specific wetting properties. If, for instance, a surface is composed of two materials, where material 1 and 2 occupy the surface area fractions f_1 and f_2 and exhibit the contact angles θ_1 and θ_2, respectively, the contact angle of a liquid on such a surface is [14]:

$$\cos\theta = f_1\cos\theta_1 + f_2\cos\theta_2 \quad (2)$$

In the case when component 2 is air and, as the contact angle of air θ_2 is 180°, the contact angle of liquid on such a substrate is:

$$\cos\theta = f_1\cos\theta_1 - f_2 \quad (3)$$

The aforementioned phenomenon commonly occurs on rough surfaces, in particular hydrophobic ones, where air remains entrapped in the surface depressions. The entrapped air below the liquid reduces the interfacial contact area between the solid surface and the liquid and, therefore, causes an increase in contact angle [22].

Another phenomenon that should be taken into account when dealing with contact angle measurements is the contact angle hysteresis. On a real surface, which contains imperfections, the actual contact angle is not equal to the equilibrium contact angle (θ_{eq}) as defined by the Young equation [23]. The observed contact angle is different for a liquid droplet advancing on a dry surface (advancing contact angle, θ_{adv}) or receding on a previously wetted surface (receding contact angle, θ_{rec}) [24–26]. The difference between the advancing and receding contact angles is the contact angle hysteresis. Any deviation from the ideal surface condition can cause the contact angle hysteresis, for instance, chemical heterogeneities of the surface or surface roughness or local defects [27]. Therefore, measurement of both advancing and receding angles is necessary to characterize a surface [23]. In many cases, due to small size of droplets commonly used in experiments, evaporation of a sessile droplet on the surface provides a convenient receding rate to perform the measurements (see, for instance [28]) and was also employed in the present paper. During the initial stages of evaporation of a sessile drop, the wetting diameter stays constant, and the contact angle and height of the droplet decrease constantly. It means that the three-phase contact line is pinned to the surface. At a certain point, the three-phase contact line is de-pinned and the wetting diameter and drop height start to decrease with a more-or-less constant contact angle. This constant contact angle is commonly taken as the receding contact angle (θ_{rec}). Finally, in the last stage, the contact angle, drop height and the wetting diameter are decreased until the droplet disappears [29–31].

Shanahan and Bourgès-Monnier observed that on rough surfaces the three-phase contact line remains pinned after the initial stage [30]. This means that the subsequent stage, where the contact angle of a sessile droplet is constant, does not exist on rough surfaces. They have also found that it is not possible to introduce a specific value of a receding contact angle due to the constant decrease of the contact angle and height of droplet till the moment of total evaporation of the droplet. This phenomenon has been also observed on aluminium and steel surfaces by Bormashenko et al. [28]. Besides the surface roughness and its effect on the contact angle and wettability, the other effective parameter of wettability is surface chemistry. Solid surface properties can be tailored by coating the surfaces with a material with a different surface energy. For instance, to make a surface hydrophobic, it can be covered by low surface-energy materials in order to decrease water attraction toward the surface [4,32,33]. Even coating with a monolayer of molecules can be sufficient to obtain the required hydrophobic or hydrophilic characteristics [34]. A relatively recent approach, so called molecular vapour deposition, relies on gas-phase deposition of a self-assembled monolayer of surface-modifying molecules. Using this method, extremely thin and uniform layers of, e.g., silane molecules can be created on glass, aluminium oxide as well as many other oxide surfaces. The process is commonly carried out in vacuum to prevent contamination of the surface and minimise unwanted reactions between the surface-modifying molecules [35]. There are also other methods reported in literature to obtain superhydrophobic surfaces on aluminium using silane chemistry. For example, Saleema et al. have introduced a one-step process to make a superhyrdrophobic aluminium alloy surface by immersing aluminium alloy substrates in a solution containing fluoroalkyl-silane (FAS-17) molecules as well as NaOH as an etchant to induce micro roughness of the surface [36].

Another approach to modifying solid surface properties involves grafting of a dense polymer brush layer covalently attached to the surface. For example, a surface can be made more hydrophilic by forming a layer of hyperbranched polyethylene glycol (PEG) on the surface. This can be done by *in situ* polymerization (synthesis of the polymer directly on the surface—"grafting from") of glycidol on the surface of aluminium with a native aluminium oxide layer. One method of *in situ* polymerization is a surface initiated, anionic, ring-opening polymerization proposed by Khan and Huck, 2003 for modification of glass surfaces [37,38]. In this method the polymerization is initiated on the surface and then continues forming a polymer brush on the surface until the monomer is used up [35]. In the present paper we adapted this method to form a dense hyperbranched PEG layer on aluminium surfaces. Moreover, we demonstrated that the surface of hyperbranched PEG can be further modified (e.g., rendered hydrophobic) using molecular vapour deposition of silanes, which, to our knowledge, has not been demonstrated elsewhere.

In the present work, we applied the aforementioned techniques of surface modification to three different real-life aluminium

surfaces: unpolished aluminium, polished aluminium, and aluminium foil. The effect of different surface treatments on the wettability and morphology of the different aluminium surfaces is studied by using contact angle measurements, ellipsometry and AFM.

2. Experimental details

2.1. Materials

Three groups of aluminium samples were studied: unpolished aluminium samples, polished aluminium samples and aluminium foil samples. A 0.25 mm thick aluminium alloy sheet (8011A) was cut into test samples measuring $15 \times 15\,mm^2$. The aluminium foil samples were cut from a rolled aluminium foil, 0.3 mm thick and 30 mm wide produced by Merck KGaA, Darmstadt, Germany. Anhydrous methanol (99.8%), sodium methoxide, fuming nitric acid (100%), glycidol (96%), toluene (99.5%), tetrahydrofuran (99%) were purchased from Sigma–Aldrich Co. 1H,1H,2H,2H-perfluorooctyltrichlorosilane was purchased from Fluorochem Ltd. All the aforementioned chemicals were used as received.

2.2. Sample preparation

2.2.1. Polishing

Twelve samples of aluminium were mounted by using resin on the substrate for polishing. The samples were first grinded with 500 grit sandpaper followed by 1200, 2400 and 4000 grit sandpaper. After the grinding, the samples were washed with cold water prior to final polishing. The polishing was carried out using colloidal silica suspension of 40 nm particles on a synthetic cloth followed by 3 μm diamond suspension on a wool cloth.

2.2.2. Degreasing

All the bare aluminium samples, polished samples and aluminium foil samples were degreased in an ultrasonic cleaner first in an acetone bath for 10 min followed by a 10 min DI-water bath and a 10 min ethanol bath. The samples were then dried under a N_2 stream and put in an oven at 110 °C for 12 h for further drying.

2.3. Experimental methods

2.3.1. Synthesis of hyperbranched polyglycidol on aluminium surface

In order to surface-initiate polymerization of glycidol on aluminium surface, the native oxide layer on top of the aluminium samples should be activated. The polymerization process followed a method introduced by Khan and Huck, 2003. For activation, a heated sodium methoxide solution in anhydrous methanol was used. The samples of each group (unpolished aluminium, polished aluminium and aluminium foil) were placed in glassware under N_2 atmosphere in an *in situ* formed solution of 0.18 M sodium methoxide at 60–70 °C for an hour. Afterwards, the solution was removed and the samples were washed once with anhydrous methanol and twice with 99% ethanol and then dried under a N_2 stream. The glassware to be used in the polymerization step was washed intensively with 10% nitric acid for one hour at 100 °C followed by rinsing with ethanol and Milli-Q water and extensive drying in order to prevent initiation and consequent polymerization of glycidol on the surface of the glassware. The initiated aluminium samples of each group were placed in the washed glassware under nitrogen atmosphere. Glycidol was added with a syringe under nitrogen atmosphere until the samples were fully covered. The polymerization was carried out at 118 °C for an hour. The polymerization mechanism is schematically shown in Fig. 1. After one hour, the

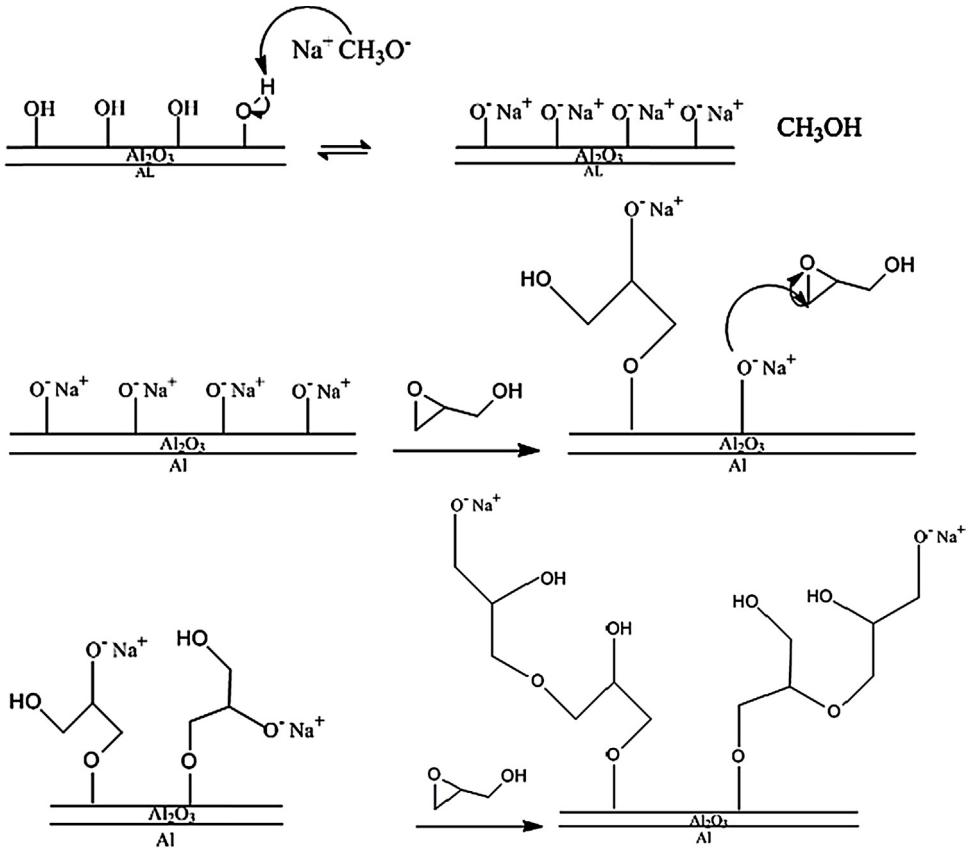

Fig. 1. Schematic mechanism for the activation and chemical vapour deposition of perfluorooctylsilane on aluminium surface, adapted and modified from Ref. [33].

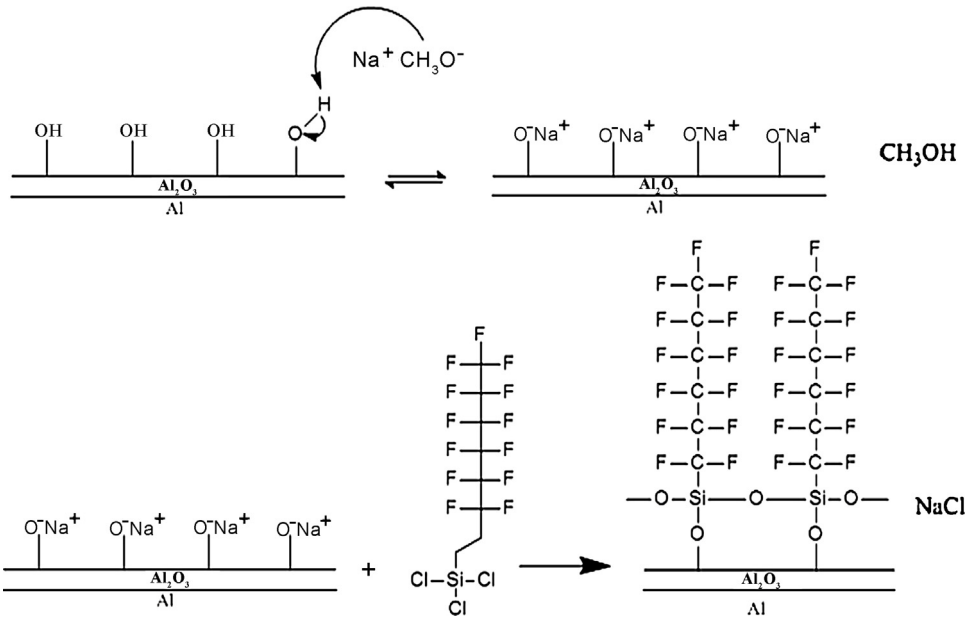

Fig. 2. Schematic mechanism for the activation and chemical vapour deposition of perfluorooctylsilane on aluminium surface, adapted and modified from Ref. [33].

reaction was stopped by removing the samples from the reaction solution. The samples were then washed, first in an acetone bath for 2 min in the ultrasonic cleaner, followed by a 2 min ethanol bath in the ultrasonic cleaner. The samples were then dried under a N_2 stream.

In order to check that the polymer layer was only formed on the sample surface and no polymerization took place in the bulk of the solution, the following test was performed as described in Ref. [37]. Four droplets of each reaction solution (bare aluminium, polished aluminium and aluminium foil) were poured into the 10 ml THF. Since no precipitation or turbidity change was observed, we can conclude that the polymerization occurred on the samples surface only.

2.3.2. Sample surface modification with fluorinated silane

Both bare samples of all types (unpolished, aluminium, polished aluminium and aluminium foil) and the samples with hyperbranched PEG grafted on the surface (unpolished, polished aluminium and aluminium foil samples) were subjected to this treatment. First, the sample surfaces were activated by heated methoxide following the aforementioned method. After activation, the samples (both with bare surface and coated with hyperbranched PEG) were placed in an evacuated desiccator containing a solution of 250 μl 1H,1H,2H,2H-perfluorooctyltrichlorosilane in 750 μl of toluene and heated up to 110 °C. The proposed reaction mechanism is shown in Fig. 2.

2.4. Surface characterisation

2.4.1. Contact angle measurement

Contact angle measurements were performed by using a home-made computer-controlled evaporation of the sessile drops stage. Advancing (θ_{adv}) angles were measured as Milli-Q water was supplied via a micro tube on the surface at a room temperature of 24 °C with the fluid rate of 6 μL/min. The reported contact angle data were determined by averaging values measured at 3 different points on each sample's surface and at least 3 samples in each group. Changes in the shapes of droplets during dynamic contact angle measurements were recorded by CCD camera. The recorded images were interpreted and analysed by DropSnake software, which is based on a plugin for ImageJ software [39–41].

2.4.2. Ellipsometry

The measurements were carried out using Sentech SE 850 Ellipsometer. During the measurement, light with a wavelength ranging from 300 nm to 800 nm at 60° incidence was used. The refractive indices of aluminium oxide layer, polymer layer and perfluorooctylsilane layer were taken as 1.77, 1.64 (equal to poly (ethylene glycol)) and 1.352, respectively [37,42,43].

2.4.3. AFM

The surface morphology was visualized by atomic force microscopy (NTEGRA Aura, NT-MDT Co.) in intermittent contact mode using Olympus OMCL-160TS cantilevers (Asylum Research). The RMS roughness for each group of samples was calculated as an average value of the measurements carried out over 3 areas on each sample using 3 samples in each group. The AFM images were analysed using WSXM software [44].

3. Results and discussions

The key surface functionalization method employed in this paper involves initiation of the native oxide layer of aluminium by heated sodium methoxide solution. The produced initiator (O—Na bonds) attacks the epoxy ring of glycidol monomer and opens it. The opened ring has two alkoxide terminations, so each initiator has two options for binding and the reaction can run in two directions per monomer, hence leading to a branched polymerization process. The released sodium ions of bonding can substitute to a new O—H termination and can make a new alkoxide. The new alkoxide termination can continue the reaction until all monomers are used or until all the (O—Na bonds) become inaccessible to the monomers.

Evidence for the layer formation on smooth foil and polished aluminum sample surfaces was obtained by ellipsometry measurements. The measurements were performed on aluminium oxide, brushed hyperbranched PEG polymer and perfluorooctylsilane layers formed on polished aluminium and aluminium foil samples. For estimation and measurement of layer thickness, point estimation was chosen (at least 3 samples for each group and at least

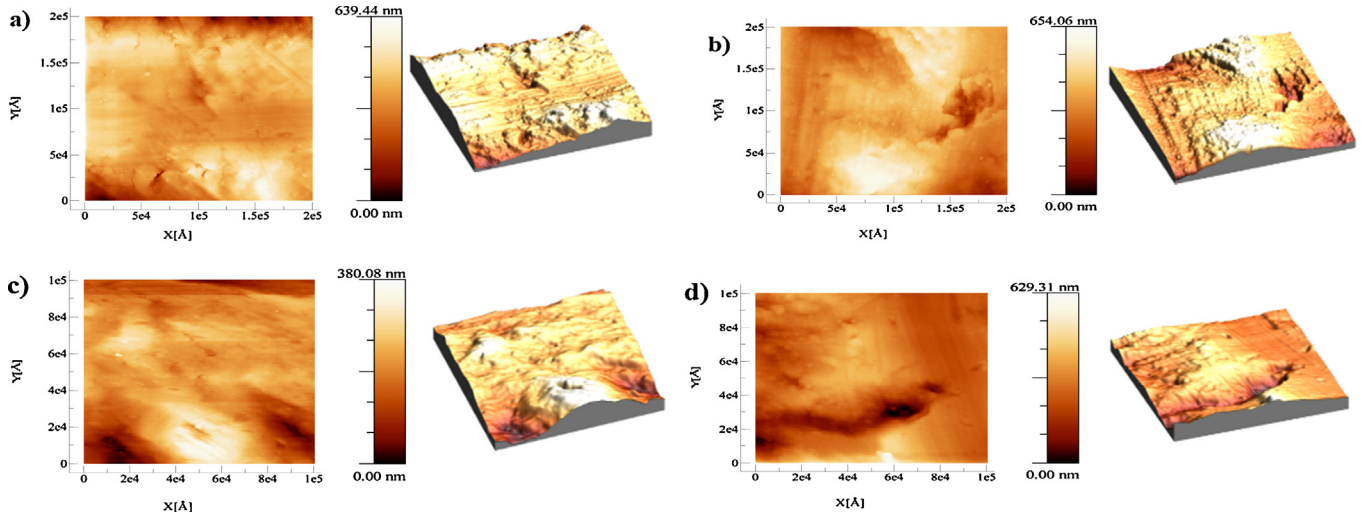

Fig. 3. AFM images of unpolished aluminium: (a) bare, (b) with PEG, (c) with PEG and perfluorooctylsilane and (d) with perfluorooctylsilane.

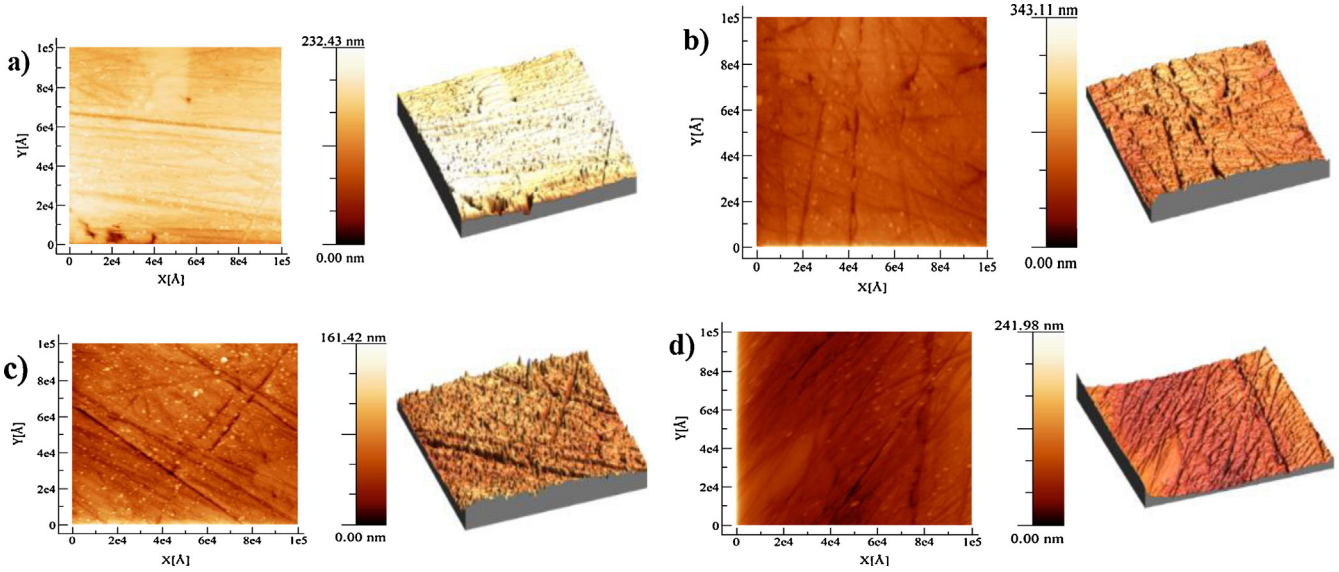

Fig. 4. AFM images of polished aluminum: (a) bare, (b) with PEG, (c) with PEG and perfluorooctylsilane and (d) with perfluorooctylsilane.

3 points in each sample). At 95% confidence interval, the mean thicknesses of the formed layers on top of the samples are shown in Table 1. However, high surface roughness of bare unpolished aluminium samples makes it impossible to measure directly the thickness of the native aluminium oxide, hyperbranched PEG and perfluorooctylsilane layers formed on its top by ellipsometry.

It should be noted that the thickness of synthesised hyperbranched PEG on top of the polished samples is higher than the hyperbranched PEG on top of the aluminium foil samples in the same condition of polymerization, shown in Table 1. We attribute this to a higher RMS surface roughness of polished aluminium samples compared with aluminium foil, as shown by AFM images discussed below.

For imaging and analysing the surface topography of thin rough layer with nanometre size AFM is particularly suitable since it can provide true topography information [45,46]. All roughness calculations in the paper were based on the AFM data and the typical AFM height images of all 12 different samples are shown

Table 1
Mean thickness of different layers on top of the samples at 95% confidence interval.

Layer type / Substrate	Polished Aluminium	Aluminium foil
Native Aluminium oxide layer (nm)	7± 0.21	11 ± 0.27
Hyperbranched PEG (nm)	3 ± 0.24	2 ± 0.12
Perfluorooctylsilane on top of Hyperbranched PEG (nm)	0.5 ± 0.05	0.5 ± 0.01
Perfluorooctylsilane (nm)	0.5 ± 0.02	0.5 ± 0.01

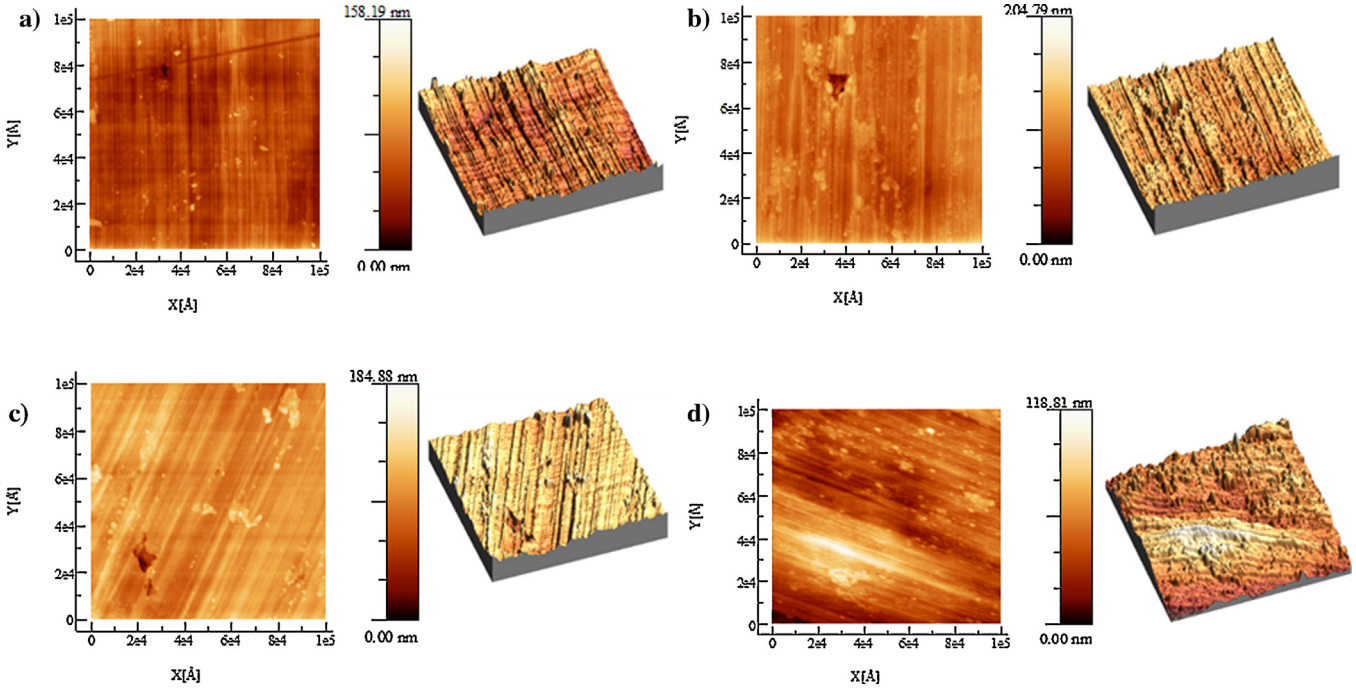

Fig. 5. AFM images of aluminum foil: (a) bare, (b) with PEG, (c) with PEG and perfluorooctylsilane and (d) with perfluorooctylsilane.

in Figs. 3–5. These images provide an overview of the surface topographies and their evolution upon different surface treatments employed in the paper.

Generally, the formation of hyperbranched PEG layer on the surface leads to a significant increase in the surface roughness for all the samples (bare unpolished, polished and aluminium foil), as illustrated in Fig. 6. This can be attributed to the hyperbranched character of the PEG layer and its brush structure as illustrated in Fig. 1. Due to the inherent surface roughness, the chemical reaction does not proceed uniformly across the entire surface. Therefore differences in the growth rate at different points on the surface can be expected. Moreover, Fig. 6 shows that the unpolished samples with hyperbranched PEG exhibit an RMS roughness of 98 nm, which is the highest value compared to all other samples. The roughness of bare unpolished aluminium samples is almost 5 times higher than the roughness of bare polished and aluminium foil samples. The observed increase in roughness of unpolished samples after polymerization of hyperbranched PEG monolayers is approximately 1.5 times higher than that on polished samples and approximately 2.5 times higher than that on aluminium foil samples. This can be explained, presumably due to a higher probability of growing hyperbranched PEG chains on extreme points of the surface due to characteristics of chemical reaction. Typically for chemical reactions on surfaces, mass transport is a limiting factor, which leads to the fact that chemical reactions typically proceed at a faster rate on surface extremities and at a slower rate in the valleys. This is illustrated by the fact that the roughness increase upon PEG brushed layer formation on polished aluminium samples with higher initial roughness is higher than on the aluminium foil samples with lower initial roughness.

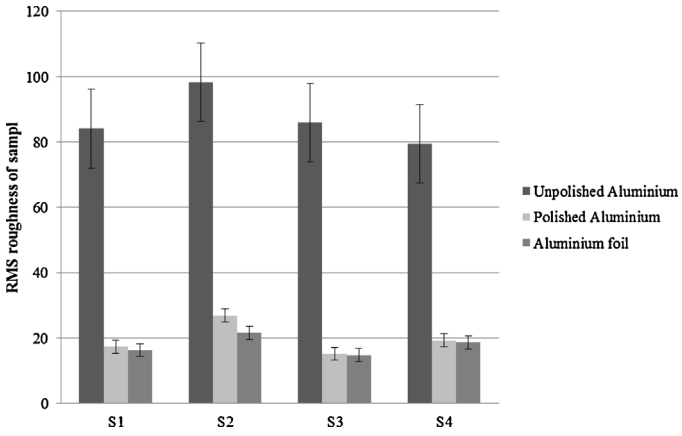

Fig. 6. RMS roughness of samples at 95% confidence interval, S1: bare samples, S2: samples with hyperbranched PEG, S3: samples with hyperbranched PEG and perfluorooctylsilane and S4: samples with perfluorooctylsilane.

We expect that the perfluorooctylsilane forms a monolayer on the surface of the substrates studied, so the layer thickness is expected to be comparable with a single molecule size. This was indeed confirmed by the ellipsometry measurements, which showed the thickness of perfluorooctylsilane monolayer on top of the polished aluminium and foil to be 0.5 nm (Table 1). On the other hand, it reduced the roughness of aluminium samples with hyperbranched PEG. We suggest that this can be explained by a higher probability of binding the perfluorooctylsilane molecules in the grooves of a hyperbranched PEG structure. This is because the three reactive group of the silane molecule prefer to react with three initiator groups forming Si—O bonds. Since, the probability of finding three closely located reactive groups is higher in the grooves as compared to extremities; perfluorosilane molecules will preferably bind to the hyperbranched PEG molecules located in the grooves hence lowering the overall surface roughness as illustrated in Fig. 6.Additionally, Fig. 6 shows that the roughness of polished samples is dramatically lower compared to the unpolished samples. This confirms the efficiency of the polishing procedure.

As can be seen in Fig. 6, the surface roughness of polished bare aluminium samples and polished aluminium samples with a hyperbranched PEG layer is higher than that of bare samples of aluminium foil and aluminium foil samples with a hyperbranched PEG layer. Moreover, Fig. 7(a and b) show that the contact angles of bare polished aluminium and polished aluminium with a hyperbranched PEG layer are lower than that of bare aluminium foil and

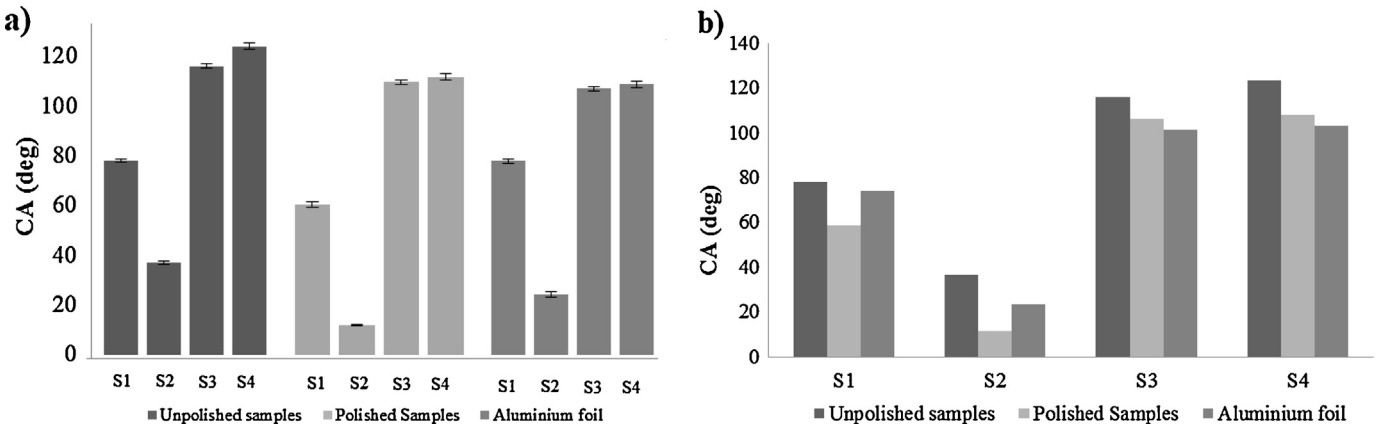

Fig. 7. Advancing CAs for all sample groups in the study: (a) grouped by the treatment applied (bar shows 95% confidence interval), (b) grouped by the sample type. S1: bare samples, S2: samples with hyperbranched PEG, S3: samples with hyperbranched PEG and perfluorooctylsilane and S4: samples with perfluorooctylsilane.

aluminium foil with a hyperbranched PEG layer. This is in line with the observed increase in the RMS surface roughness. Since these surfaces are hydrophilic in nature, according to the Wenzel model, the roughness increase (*R*-factor in Eq. (1)) should lead to a decrease in the contact angle. In other words, this means that the hydrophilic surface of polished bare aluminium and polished aluminium with a hyperbranched PEG layer becomes more hydrophilic than the bare aluminium foil samples [46] (Fig. 8).

Therefore we can conclude that the polished aluminium and aluminium foil samples follow the Wenzel model, stating that increasing the roughness of a hydrophilic surface (bare aluminium) makes it more hydrophilic, while a hydrophobic surface (aluminium with PEG) becomes more hydrophobic [13,21]. It should be mentioned that all three groups of samples (unpolished, polished aluminium and aluminium foil) with hydrophobic characteristics (samples with perfluorooctylsilane on top of hyperbranched PEG and samples with perfluorooctylsilane) followed the Wenzel model, i.e. hydrophobicity of hydrophobic samples is increased with the increase in surface roughness as shown in Fig. 7(b).

It should be noted that the samples of bare unpolished aluminium alloy exhibit a large contact angle of 78°. A priory, aluminium alloys are expected to be high surface-energy materials as any other clean surfaces of minerals, including oxides and sulphides. These materials are expected to be completely wetted and exhibit zero or small contact angles. However, research showed that even short term exposure of a clean hydrophilic solid surface to any atmosphere except a very pure gas will cause hydrophobic organic contamination and consequently will lead to an increase in the water contact angle on the surface up to ~90° [47]. The value of the contact angle observed in the present study on aluminium is roughly in line with the other observations, see, for instance, Bormashenko, Musin, and Zinigrad [28].

The bare unpolished samples exhibit the highest advancing contact angle compared with that of bare polished aluminium and aluminium foil despite their higher roughness. As mentioned earlier, the bare unpolished samples due to their high roughness and air pocket structure follow the Cassie–Baxter model and have a large contact angle. The rough surface of bare unpolished aluminium entraps air in the gaps hence forming a composite surface of air and solid material. The entrapped air under the liquid reduces the interfacial contact area between the solid surface and the liquid leading to a higher water contact angle. We therefore observe a transition from Cassie–Baxter's to Wenzel's regime due to changing the surface roughness upon mechanical polishing. This transition is also observed on the aluminium samples with PEG layer since the unpolished samples with PEG exhibit larger contact angles and lower wettability than the polished samples although their roughness are higher than that of polished aluminium samples with PEG. It should be noted that Cassie–Baxter

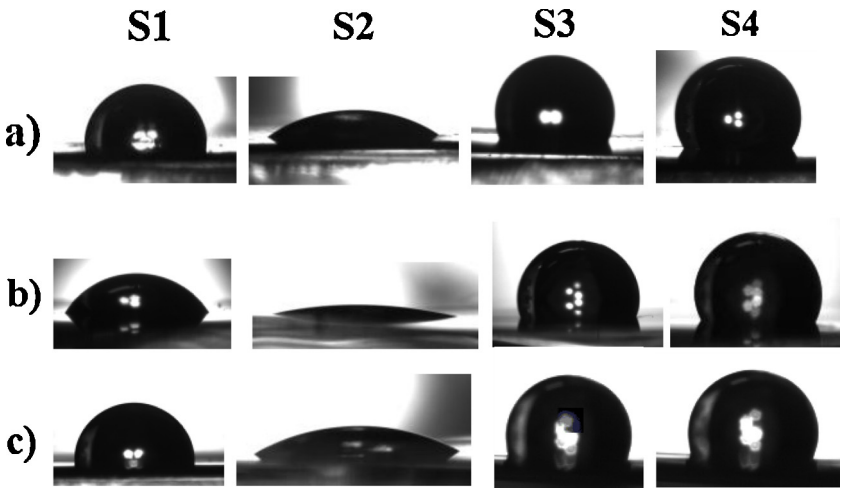

Fig. 8. Shape of a water droplet on the surface of different sample groups after different surface modifications.

and Wenzel models have their limitations inherent to the fact that they are only valid in the long-wavelength approximation. In other words, the typical scale of the sample inhomogeneity should be much smaller than the size of the droplet. As has been shown in a recent study by Gao and McCarthy (2007) the wettability and contact angle are not related to the contact area and the interfacial energy in the case of a surface morphology comparable to the droplet dimensions. In this case, the contact line energy should be considered and the contact angle is only related to the contact line structure and activation energy [18,19]. In the present study, due to the rather small roughness scale and uniformity of the studied surfaces, the obtained data are at least qualitatively consistent with the models and a transition from Cassie–Baxter's to Wenzel's regime due to a change in surface roughness is observed.

Hydrophilic or hydrophobic properties of a surface can be tailored by changing the chemical composition of the surface. Since surface will adopt the properties of the coated material, coating is an effective method for forming a hydrophilic or hydrophobic surface. In this work, a hydrophilic polymer of glycidol is formed on the surface of all three sample groups: unpolished, polished aluminium, and aluminium foil. The modified surface adopted the surface characteristics of the polymer and the advancing contact angle reduced for the unpolished, polished and aluminium foil samples from 78°, 59° and 74° to 37°, 12° and 24°, respectively (Fig. 7(a)). This confirms successful polymerization on the surface of aluminium samples with the native aluminium oxide layer.

In order to increase the contact angle of the surface through formation of a hydrophobic layer on the surface, all three groups of sample surfaces were coated by a monolayer of perfluorooctylsilane. Moreover, the same monolayer was also successfully deposited on the surface of hyperbranched PEG by vapour deposition which, to our knowledge, has not been reported earlier. The deposition of perfluorooctylsilane on top of the bare aluminium samples and samples coated with hyperbranched PEG, the contact angle on all the surfaces increased and the surfaces adopted the hydrophobic characteristics of the perfluorooctylsilane monolayer; see Fig. 7(a). The maximum contact angle of 124° was observed on the unpolished aluminium surfaces, presumably due to a higher surface roughness of the unpolished samples. Fig. 7(b) shows the comparative diagram of advancing contact angle for groups of samples after different surface modifications, the surface chemistry of samples in each group is the same.

Due to high surface roughness, the three-phase contact line remains pinned to the surface during the evaporation of sessile drops and the contact angle and the drop height decreases constantly up to the final stage of evaporation. This phenomenon makes it impossible to measure the receding contact angles and is consistent with the result of Shanahan and Bourgès-Monnier (1994) [30]

4. Conclusion

(1) Formation of the hydrophilic PEG layer on aluminium samples by surface-initiated polymerization increased the surface roughness and hydrophilicity of the samples. Consequently, it led to the lower contact angles and increased wettability of aluminium samples. The higher the initial surface roughness, the larger the increase observed upon forming PEG. On the contrary, molecular deposition of low surface energy perfluorooctylsilane on aluminium samples increased their hydrophobicity and contact angle. It should be noted that the deposition of perfluorooctylsilane on the aluminium samples with the PEG layer caused the surface roughness to reduce, which is presumably due to a higher probability of binding the perfluorooctylsilane molecules in the grooves of the hyperbranched PEG structure.

(2) The groups of surfaces with hydrophobic characteristics (the samples with perfluorooctylsilane deposited either directly on bare aluminium surface or on top of the hyperbranched PEG) followed the Wenzel model, i.e. upon increasing the surface roughness, their hydrophobicity increased and the samples with a higher roughness were more hydrophobic.

(3) The bare unpolished and unpolished PEG samples followed the Cassie–Baxter model due to their high roughness and the presence of air pocket in their structure. So there is a transition from Cassie–Baxter's to Wenzel's regime due to changing the surface roughness upon mechanical polishing in aluminium samples.

Acknowledgments

We acknowledge with thanks the financial support provided by the Greenland government and COWIfonden in this work. We would also like to acknowledge the support of EXHAUSTO A/S which contributed with components and materials.

References

[1] E. Moallem, L. Cremaschi, D.E. Fisher, S. Padhmanabhan, Experimental measurements of the surface coating and water retention effects on frosting performance of microchannel heat exchangers for heat pump systems, Exp. Therm. Fluid Sci. 39 (2012) 176–188.
[2] E.A. Starke, J.T. Staleyt, Application of modern alluminum alloys to aircraft, Prog. Aerosp. Sci. 32 (1996) 131–172.
[3] W. Zhang, D. Zhang, Y. Le, L. Li, B. Ou, Fabrication of surface self-lubricating composites of aluminum alloy, Appl. Surf. Sci. 255 (2008) 2671–2674.
[4] W. Liu, Y. Luo, L. Sun, R. Wu, H. Jiang, Y. Liu, Fabrication of the superhydrophobic surface on aluminum alloy by anodizing and polymeric coating, Appl. Surf. Sci. 264 (2013) 872–878.
[5] H. Wang, D. Dai, X. Wu, Fabrication of superhydrophobic surfaces on aluminum, Appl. Surf. Sci. 254 (2008) 5599–5601.
[6] S. Jhee, K. Lee, W. Kim, Effect of surface treatments on the frosting/defrosting behavior of a fin-tube heat exchanger, Int. J. Refrig. 25 (2002) 1047–1053.
[7] K.S. Lee, W.S. Kim, T.H. Lee, A one-dimensional model for frost formation on a cold flat surface, Int. J. Heat Mass Transf. 40 (1997) 4359–4365.
[8] C.J.L. Hermes, An analytical solution to the problem of frost growth and densification on flat surfaces, Int. J. Heat Mass Transf. 55 (2012) 7346–7351.
[9] C.J.L. Hermes, R.O. Piucco, J.R. Barbosa, C. Melo, A study of frost growth and densification on flat surfaces, Exp. Therm. Fluid Sci. 33 (2009) 371–379.
[10] R. Tadmor, P. Bahadur, A. Leh, H.E. N'guessan, R. Jaini, L. Dang, Measurement of lateral adhesion forces at the interface between a liquid drop and a substrate, Phys. Rev. Lett. 103 (2009) 266101.
[11] M.K. Kwak, H.-E. Jeong, T. Kim, H. Yoon, K.Y. Suh, Bio-inspired slanted polymer nanohairs for anisotropic wetting and directional dry adhesion, Soft Matter 6 (2010) 1849.
[12] K.L. Cho, A.H.-F. Wu, I.I. Liaw, D. Cookson, R.N. Lamb, Wetting transitions on hierarchical surfaces, J. Phys. Chem. C 116 (2012) 26810–26815.
[13] R.N. Wenzel, Resistance of solid surfaces, Ind. Eng. Chem. 28 (1936) 988–994.
[14] A.B.D. Cassie, S. Baxter, Wettability of porous surfaces, Trans. Faraday Soc. 40 (1944) 546–551.
[15] A. Sarkar, A.-M. Kietzig, General equation of wettability: a tool to calculate the contact angle for a rough surface, Chem. Phys. Lett. 574 (2013) 106–111.
[16] B. Qian, Z. Shen, Fabrication of superhydrophobic surfaces by dislocation-selective chemical etching on aluminum, copper, and zinc substrates, Langmuir 21 (2005) 9007–9009.
[17] Y. Chen, H. Kim, Preparation of superhydrophobic membranes by electrospinning of fluorinated silane functionalized poly(vinylidene fluoride), Appl. Surf. Sci. 255 (2009) 7073–7077.
[18] L. Gao, T.J. McCarthy, Wetting 101 degrees, Langmuir 25 (2009) 14105–14115.
[19] L. Gao, T.J. McCarthy, How Wenzel and Cassie were wrong, Langmuir 23 (2007) 3762–3765.
[20] A. Marmur, E. Bittoun, When Wenzel and Cassie are right: reconciling local and global considerations, Langmuir 25 (2009) 1277–1281.
[21] C. Dorrer, J. Rühe, Drops on microstructured surfaces coated with hydrophilic polymers: Wenzel's model and beyond, Langmuir 24 (2008) 1959–1964.
[22] N.J. Shirtcliffe, G. McHale, M.I. Newton, The superhydrophobicity of polymer surfaces: recent developments, J. Polym. Sci. B Polym. Phys. 49 (2011) 1203–1217.
[23] E. Bormashenko, Wetting transitions on biomimetic surfaces, Philos. Trans. A Math. Phys. Eng. Sci. 368 (2010) 4695–4711.
[24] A.G. Bayer, D. Krefeuuerdingen, J.J. Schrijder, The wettability of industrial surfaces: contact angle measurements and thermodynamic analysis*, Chem Eng. Process. 19 (1985) 277–285.
[25] R. Tadmor, Line energy and the relation between advancing, receding, and young contact angles, Langmuir 20 (2004) 7659–7664.

[26] T. Young, An essay on the cohesion of fluids, Philos. Trans. R Soc. Lond. 95 (1805) 65–87.
[27] S. Schwartz, L.W. Garoff, Contact angle hysteresis and the shape of the three-phase line, J.Colloid Interface Sci. 106 (1985) 422–437.
[28] E. Bormashenko, A. Musin, M. Zinigrad, Evaporation of droplets on strongly and weakly pinning surfaces and dynamics of the triple line, Colloids Surf. A Physicochem. Eng. Asp. 385 (2011) 235–240.
[29] P.G. Pittoni, C.-C. Chang, T.-S. Yu, S.-Y. Lin, Evaporation of water drops on polymer surfaces: pinning, depinning and dynamics of the triple line, Colloids Surf. A Physicochem. Eng. Asp. 432 (2013) 89–98.
[30] M.E.R. Shanahan, C. Bourg, Effects of evaporation on contact angles on polymer surfaces, Int. J. Adhes. Adhes. 14 (3) (1994) 201–205.
[31] C. Bourg, M.E.R. Shanahan, Influence of evaporation on contact angle, Int. J. Adhes. Adhes. 14 (1995) 2820–2829.
[32] N. Saleema, M. Farzaneh, R.W. Paynter, Prevention of ice accretion on aluminum surfaces by enhancing their hydrophobic properties, J. Adhes. Sci. Technol. 25 (1–3) (2011) 27–40.
[33] N. Saleema, D.K. Sarkar, D. Gallant, R.W. Paynter, X.-G. Chen, Chemical nature of superhydrophobic aluminum alloy surfaces produced via a one-step process using fluoroalkyl-silane in a base medium, ACS Appl. Mater. Interfaces 3 (2011) 4775–4781.
[34] C.K. Luscombe, H. Li, W.T.S. Huck, A.B. Holmes, Fluorinated silane self-assembled monolayers as resists for patterning indium tin oxide, Langmuir 19 (2003) 5273–5278.
[35] H. Butt, K. Graf, M. Kappl, Physics and Chemistry of Interfaces, WILEY-VCH GmbH & Co. KGaA, 2003.
[36] N. Saleema, D.K. Sarkar, R.W. Paynter, X.-G. Chen, Superhydrophobic aluminum alloy surfaces by a novel one-step process, ACS Appl. Mater. Interfaces 2 (2010) 2500–2502.
[37] M. Khan, W.T.S. Huck, Hyperbranched polyglycidol on Si/SiO_2 surfaces via surface-initiated polymerization, Macromolecules 46 (2003) 5088–5093.
[38] O. Prucker, J. Ru, Synthesis of poly(styrene) monolayers attached to high surface area silica gels through self-assembled monolayers of azo initiators, Macromolecules 9297 (1998) 592–601.
[39] a.F. Stalder, G. Kulik, D. Sage, L. Barbieri, P. Hoffmann, A snake-based approach to accurate determination of both contact points and contact angles, Colloids Surf. A Physicochem. Eng. Asp. 286 (2006) 92–103.
[40] A.F. Stalder, T. Melchior, M. Müller, D. Sage, T. Blu, M. Unser, Low-bond axisymmetric drop shape analysis for surface tension and contact angle measurements of sessile drops, Colloids Surf. A Physicochem. Eng. Asp. 364 (2010) 72–81.
[41] M.D. Abràmoff, P.J. Magalhães, S. Ram, Image processing with imageJ, Biophoton. Int. 11 (2004) 36–42.
[42] Al2O3 reflective index. (n.d.). http://www.ioffe.ru/SVA/NSM/nk/index.html, (accessed 01.01.14).
[43] Sigma–Aldrich, Trichloro(1H,1H,2H,2H-perfluorooctyl)silane properties. http://www.sigmaaldrich.com/catalog/product/aldrich/448931?lang=en & region=DK, (accessed 01.01.14).
[44] I. Horcas, R. Fernández, J.M. Gómez-Rodríguez, J. Colchero, J. Gómez-Herrero, A.M. Baro, WSXM: a software for scanning probe microscopy and a tool for nanotechnology, Rev. Sci. Instrum. 78 (2007) 013705.
[45] J.D. Miller, S. Veeramasuneni, J. Drelich, M.R. Yalamanchili, G. Yamauchi, Effect of roughness as determined by atomic force microscopy on the wetting properties of PTFE thin films, Polym. Eng. Sci. 36 (1996) 1849–1855.
[46] W. Possart, H. Kamusewitz, Wetting and scanning force microscopy on rough polymer surfaces: Wenzel's roughness factor and the thermodynamic contact angle, Appl. Phys. A Mater. Sci. Process. 76 (2003) 899–902.
[47] W.A. Zisman, K.W. Bewig, The wetting of gold and platinum by water, J. Phys. Chem. 1097 (1966) 4238–4242.

3.1.2 SUMMARY OF ‘‘CONTROL AND PREVENTION OF ICE FORMATION AND ACCRETION ON HEAT EXCHANGERS FOR VENTILATION SYSTEMS’’

In cold climates, mechanical ventilation systems with heat recovery, such as air-to-air exchangers, are commonly applied for reducing the energy consumption used for heating buildings; the systems transfer the heat of the exhaust air to the supply air. However, the increased efficiency of heat exchanger results in lower exhaust air temperatures and ice formation on heat exchanger fins which may cause problems. Therefore, the prevention and control of ice formation on heat exchangers is necessary. The existing methods are divided into two different methods: active and passive ice control methods. The active methods include bypass, recirculation and preheating. The passive methods relate to the surface characteristics of the heat exchanger fins as they have an effect on the initial phase of the ice formation. These methods all have varying levels of success, cost and effectiveness, all of which depend on the operating condition and construction of heat exchangers. Since, the active methods reduce the efficiency of the heat exchanger and the passive methods are not permanent solutions, it may be suggested that the optimum ice protection method could constitute a combination of both methods. The aim of this paper is to review and evaluate the current methods to provide new insights on the ice formation problem.

In this paper, the different existing methods of ice formation control and prevention on air to air heat exchangers are reviewed systematically and investigated in order to discuss and detect the strengths and weaknesses of each method. Moreover, the limitation and lacks of knowledge in this field and suggestions for further investigation are discussed.

The active methods seek to prevent ice formation on heat exchanger fins by preheating the cold supply air or by de-icing the formed ice layer on heat exchanger fins through bypassing the warm exhaust air, periodic de-icing or through a variation of the mass flow ratio techniques.

The active method require energy or use the energy content of the supply air for preventing ice formation; the activation of these methods for preventing ice formation cause for a significant reduction in the efficiency of heat exchangers which is not desirable. Furthermore, some of these methods, such as bypassing and the variation of the mass flow ratio methods based on reducing the supply air flow, may reduce the air quality of system.

The passive methods present other options for controlling and preventing ice formation. These methods are based on the modification of the surface characteristics of heat exchanger fins. The surface characteristics have crucial roles on ice nucleation and formation. The advantage of these methods is that their operation does not require extra energy, and consequently, their operation does not reduce the air quality. By applying the passive method, ice nucleation can be delayed and the formed ice may have a structure and density that allows it to be removed easily. Moreover, the passive methods may decrease the ice growth rate and it may take longer for the heat exchanger air passage to be clogged and blocked by the formed ice as compared to the ice formed on a normal heat exchanger fin surface.

In spite of the advantages of the passive methods and their effect on heat exchanger efficiency in cold working days, these methods also have disadvantages. They can be effective in the initial stage of ice nucleation and formation. Due to nucleation and formation of ice after the initial stage of ice formation the direct contact of the humid exhaust air with the heat exchanger fin will disappear. The surface effects will then disappear and the humid air will come into contact with the ice layer.

3.1.2.1 Actual paper II

Control and Prevention of Ice Formation and Accretion on Heat Exchangers for Ventilation Systems
M. Rahimi, and A. Afshari.
Conference: Healthy Building Conference Europe 2015, May, Eindhoven.

D. Energy & sustainability
D.1 Energy and IEQ

Control and prevention of ice formation and accretion on heat exchangers for ventilation systems

Maral Rahimi[1*], Alireza Afshari [2]

[1&2] Department of Energy and Environment, Danish Building Research Institute, Aalborg University, A.C. Meyers Vænge 15, 2450 Copenhagen SV, Denmark

[*]Corresponding email: mar@sbi.aau.dk

Keywords: Ice formation, Heat exchangers, Passive and active prevention methods

SUMMARY

In cold climates, the application of mechanical ventilation systems with heat recovery like are air-to-air exchangers is used for reducing energy consumption for heating buildings by transferring heat exhausted air to supply air. However, increase efficiency of heat exchanger results in lower exhaust air temperatures and Ice formation on heat exchanger fins, which can cause problem and is not favourable. Therefore, prevention and control of ice formation on heat exchangers is necessary. The existing methods are divided into two different methods: active and passive ice control methods. The active methods are e.g. bypass, recirculation, preheating. The passive methods relate to the surface characteristics of the heat exchanger fins as they have effect on ice formation in initial phase. All these methods have varying levels of success, cost, and effectiveness, which are depending on the heat exchangers operating condition and construction. Since, the active method are reducing efficiency of heat exchanger and the passive methods are not permanent solution it can be suggested that the optimum ice protection method may be a combination of both methods. The aim of this paper is to review and evaluate the current methods to provide new insight of concern for the ice formation problem.

INTRODUCTION

Ice formation and accretion on heat exchanger fins are common problems for air-to-air heat recovery systems under cold working conditions. The ice formation can occur on the surface of heat exchangers when the heat is transferred from the warm, humid exhaust air to the cold supply air (Kragh, Rose, Nielsen, & Svendsen, 2007)(Rose, Nielsen, Kragh, & Svendsen, 2008). Moreover, by increasing the efficiency of heat exchangers and consequently lower exhaust air temperature the risk of ice formation on cold working days is increased. Ice formation and growth may clog and block the air passage of heat exchangers fully or partially and may affect the thermal performance of

heat exchangers in several ways (Ahmed & Appelhoff, 2013)(Rose et al., 2008)(Jhee, Lee, & Kim, 2002). The risk of ice formation on the heat exchanger's plates decreases with increasing humidity of exhaust air and by higher exhaust air temperature. The risk also increases by increasing the efficiency of the heat exchanger and by increasing the mass flow ratio of supply air to the exhaust air ($m_{supply\ air}/m_{exhustair}$). Beyond the thermodynamically and psychrometric parameters such as airflow temperature, velocity, humidity, some other parameters related to the installation position and air path of the plate heat exchanger and some related to the surface characteristics of the heat exchanger fins are also causal factors in the ice formation process. These surface characteristics include surface material, roughness, drop adhesion to the surface , wettability of surface and consequently the angle that the droplet is making on the surface (contact angle) (Moallem, Cremaschi, Fisher, & Padhmanabhan, 2012) (Hermes, 2012) (Hermes, Piucco, Barbosa, & Melo, 2009) (Tadmor et al., 2009). The focus of this literature review is on the control, prevention and de-icing methods of ice accretion on heat exchanger fins. The journal article related to this problem were reviewed and categorised into two main categories: passive methods and active methods of control and prevention of ice formation and accretion on heat exchangers for ventilation systems. The objective of this paper was to provide a comprehensive comparison of these methods and analyse their pros and cons.

ICE ACCRETION EFFECTS ON HEAT EXCHANGERS

The formation of ice layer is a general physical phenomenon that occurs under cold weather conditions in air-to-air heat exchangers. As illustrated in Mollier diagram, Figure 1, condensation occurs on heat exchanger fins when airflow containing water vapour in the room temperature point 1 is cooled to saturation point.2. this is because of transferring the heat to the cold supply air flow from exhaust air. As soon as the temperature reaches to the 0° degree the ice formation starts on the heat exchanger surface. The by time passing moisture molecules migrating to the frosted surface leads to ice growth and densification of the ice layer. The formed ice layer reduce the heat exchanger performance in two ways: first by acting as an insulation layer between the heat exchangers' fins surface and the passing airflow it reduces the heat transfer rates and consequently reduces the heat exchanger efficiency. Second, the formed ice layers can partially or completely decrease the airflow and can cause a higher-pressure drop and consequently reduce the amount of thermal energy available for recovery. It can also affect negatively the function of the heat exchanger (Phillips, Chant, Fisher, & Bradley, 1989)(Ahmed & Appelhoff, 2013)(Phillips, Chant, Bradley, & Fisher, 1989). Therefore, there is a need of control, prevention and de-icing methods of ice accretion on heat exchangers fins in order to maintain the efficiency and working condition of heat exchangers.

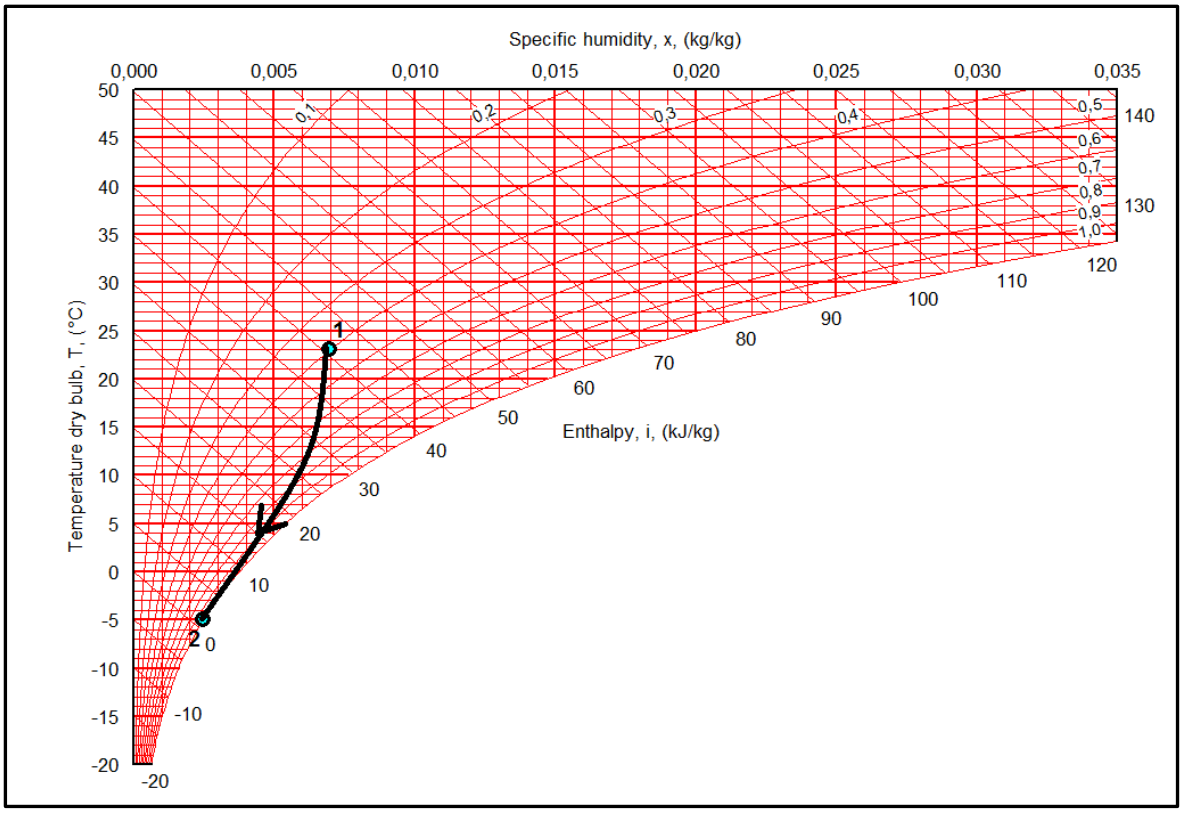

Figure 1: Mollier diagram that shows condensation that occurs on heat exchanger fins when airflow containing water vapour is cooled to saturation point.

METHODOLOGY

In this systematic review, various pre-reviewed articles related to the ice formation problem on heat exchangers are identified, appraised, combined, studied, and reviewed. This is done as a methodology in order to summarize, introduce and compare different existing control and prevention methods for ice formation problem and discuss the strength and weakness of each. The limitation of this study was the amount of articles that were precisely investigates this problem on heat exchanger since the research within the exact focus on this subject is limited.

CONTROL, PREVENTION AND DE-ICING METHODS OF ICE ACCRETION

In this review, the existing methods are categorised into two different groups according to their energy usage for control, prevention and de-icing of ice accretion. The two groups of methods are passive methods and active methods. Ice control methods mean methods that prevent ice from forming in the heat exchanger, while de-icing methods mean methods that routinely remove formed ice from heat exchanger surfaces.

Active methods

Ice formation on heat exchanger‘ fins can be sensed in three common techniques, i.e., sensing the supply air temperature, sensing the exhaust air temperature located in the cold corner of the heat exchanger and by sensing the pressure drop across the heat exchange for further control of ice formation by using active methods. After sensing the ice formation condition the controller of the heat exchanger system can decide to activate the de-icing methods.
The existing active methods according to literature review are periodic de-icing, by passing, pre heating and variation of the mass flow ratio ($m_{\text{supply air}}/m_{\text{exhaust air}}$). All these methods reduce the efficiency of heat exchangers.

Periodic de-icing of the ice accumulation on the surface of heat exchanger fins: This can be achieved by using two different techniques: whole exchanger de-icing or partial de-icing.
The whole exchanger de-icing can be carried out by stopping the supply airflow as soon as the supply air temperature fall below the set point temperature, which means the ice formed on top of the heat exchanger. Stopping the supply air means only warm exhaust air passes through the exchanger and consequently the heat exchanger can be de-iced. This method is done at fixed interval and fixed de-icing cycle in a freezing condition and takes few minutes (Phillips, Chant, Fisher, et al., 1989).
For using partial de-icing technique, some dampers are been installed in the cold supply air inlet. These dampers operate individually and are open under normal conditions but in the case a risk of ice formation, individual dampers are alternately closed for a certain period of time and preventing cold supply air from entering into the respective part of the exchanger. The warm exhaust air de-ices the respective part of the heat exchanger.

By passing method: In this method a set point for the exhaust air temperature or supply air is given to the controller of heat exchanger system for activating the de-icing methods. The set point temperature is determined by a temperature sensor where located in the cold corner of heat exchanger or by temperature sensor in the supply air. An ice prevention switch can be continuously regulated and ensuring optimum energy use by changing the set point. If there is no risk of condensation or ice formation in the exhaust air, ice protection action remains out of the operation, otherwise by bypassing the supply air the system will be ice-free. This means that the bypass dampers will be opened to reduce the airflow of the cold supply air through the heat exchanger system (Ahmed & Appelhoff, 2013).

Preheating method: Preheating of the supply air, or exhaust air in order to prevent reaching the temperature of ice formation condition is another common active method of de-icing. The other method can be done by mixing supply air with exhaust air or by hydraulic or electrical preheating of them. This method significantly reduces energy efficiency of heat exchangers (Ahmed & Appelhoff, 2013)(Phillips, Chant, Fisher, et al., 1989)(Phillips, Chant, Bradley, et al., 1989).

Variation of the mass flow ratio method: This method reduces the ratio of mass flow of the cold supply air. This is due to the fact that the low amount of cold supply air cannot cool much warm exhaust air. Then the thermal energy of the warm exhaust air can prevent ice formation on the surface of heat exchanger (Phillips, Chant, Bradley, et al., 1989).

Passive methods

The other methods of ice formation control on heat exchanger fins are passive methods that require extra energy like the active methods. Therefore, the energy efficiency of heat exchangers is not diminished by implementing these methods and they can improve the cold working condition of heat exchangers. These methods are able to control and prevent the ice formation partially by changing the surface characteristics of the heat exchanger fins. This is due to the important roles of surface characteristics such as surface wettability, roughness and surface energy on ice nucleation and formation. Some researchers are focused on the effect of surface characteristics in the real heat exchanger application such as Qi (Qi, 2013) and Rahman and Jacobi (Rahman & Jacobi, 2012) (Jhee et al., 2002). Some other studies are focused on the effect of surface characteristics on plate samples representing the surfaces of heat exchanger fins in order to investigate the effect of surface characteristics on wettability and ice formation (Rahimi, Fojan, Gurevich, & Afshari, 2014) (Lee, Shin, Ha, Choi, & Lee, 2004). The wettability is an important factor on ice formation and therefore many studies focus on changing it by tailoring the surface roughness or tailoring surface chemistry and making the surface more hydrophobic or more hydrophilic (Kwak, Jeong, Kim, Yoon, & Suh, 2010) (Rahimi et al., 2014).

The results of He et al. showed that tailoring a surface to a super hydrophobic surface could retard the ice formation. On the other hand, it showed that by changing the surface to become more hydrophilic, the wettability is increased (He et al., 2010). Many other researches are done and showed the preference of more hydrophobic surfaces such as (Cao, Jones, Sikka, Wu, & Gao, 2009) (Farhadi, Farzaneh, & Kulinich, 2011) (Kulinich & Farzaneh, 2011).

Moreover, the results of a study by Rahimi et al, 2015 also show that any surface modification on the surface of bare aluminium, which is the main material for production of heat exchanger' fins, can improve the anti-ice characteristics of the surface. As the Fig.2 shows by modifying the aluminium surface and gaining, different surface characteristics with different contact angle the ice thickness at 100 % RH after 10 min on modified surface aluminium samples are lower than the bare aluminium samples.

It should be mentioned that although the surface characteristics played crucial a role in ice formation but it should be mention that its effect is restricted to the initial stage of ice formation and it became weaker as ice grew and the direct contact of humid air with the modified surface disappeared (Rahimi et al, 2015) and (Kim & Lee, 2011).

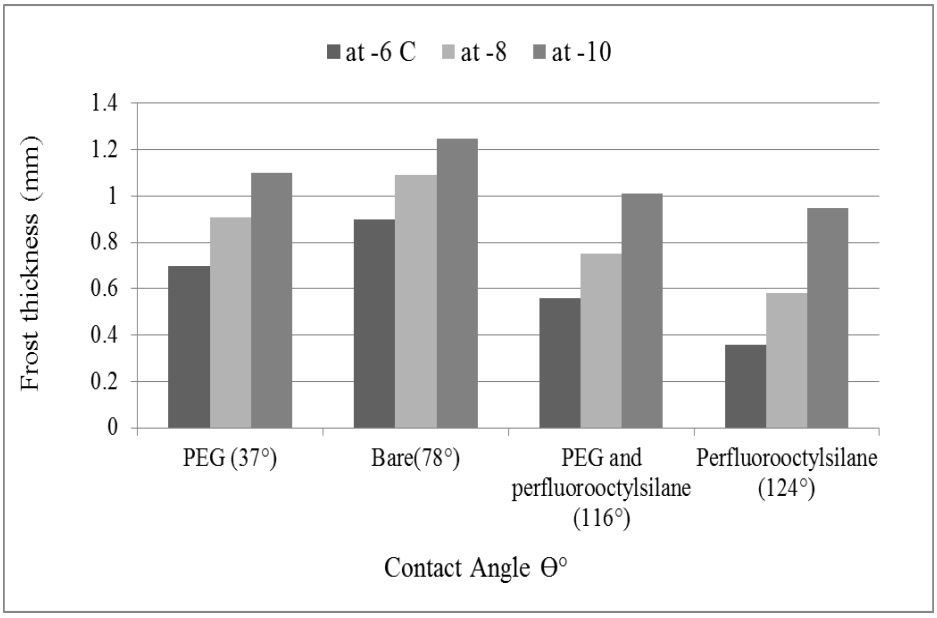

Figure 2: Ice thickness and contact angle at 100 % RH after 10 min on aluminium samples with different surface characteristics with an uncertainty of ±0.014mm.

Although the effect of the passive methods is not permanent it should be mentioned that according to previous research the passive methods with focus on the surface characteristics are cheaper and easier to implement in compare with the active methods (Menini, Ghalmi, & Farzaneh, 2011). There is a need of more research and investigation in order to find a permanent passive method for ice formation control.

The problem of ice formation on heat exchangers' fin is a problem in cold winter times in Nordic countries in Europa. The mentioned active methods are applied in heat exchangers and tested in the cold working condition in wintertime. All of them prevent the ice formation problem by decreasing the efficiency and increasing the energy costs comparing to an ideal ice-free heat exchanger. But according to the knowledge of authors the passive method are still in the research stage and are not implement in the real working condition in order to see its effect and efficiency.

CONCLUSION

In spite of several years of research and investigation to find the most efficient solution for control or prevention of ice formation on heat exchangers and increase the efficiency of heat exchangers under cold working conditions, there is still not a reliable and permanent solution to this problem.

The active methods use electrical energy for control of ice formation and consequently they reduce the efficiency of ventilation systems, which is not desirable. Also choosing the most suitable active method solution is depends on the operating condition and heat exchangers construction. On the other hand, although all the existing passive methods are cheaper and do not use electrical energy, they are not a permanent solution for ice

control since after ice formation by ice growth on the surface, the direct contact between the air flow and the heat exchanger fins surface will be disappear.

It is clear that even though there is many research and studies available about passive methods, there is a need of more research and investigation in order to find a permanent passive method for ice formation control. In addition, it is suggested that based on the existing knowledge in this area, the optimum ice protection method may be a combination of active and passive methods. Therefore, more research into these methods is needed in order to deepen the understanding of the advantages and application of these methods in heat exchanger fins.

REFERENCES

Ahmed, R., & Appelhoff, J. (2013). Frost-protection measures in energy recuperation with multiple counterflow heat exchangers. *Rehva*, *05*, 37–40.

Cao, L., Jones, A. K., Sikka, V. K., Wu, J., & Gao, D. (2009). Anti-icing superhydrophobic coatings. *Langmuir : The ACS Journal of Surfaces and Colloids*, *25*(21), 12444–8. doi:10.1021/la902882b

Farhadi, S., Farzaneh, M., & Kulinich, S. a. (2011). Anti-icing performance of superhydrophobic surfaces. *Applied Surface Science*, *257*(14), 6264–6269. doi:10.1016/j.apsusc.2011.02.057

He, M., Wang, J., Li, H., Jin, X., Wang, J., Liu, B., & Song, Y. (2010). Super-hydrophobic film retards frost formation. *Soft Matter*, *6*(11), 2396. doi:10.1039/c0sm00024h

Hermes, C. J. L. (2012). An analytical solution to the problem of frost growth and densification on flat surfaces. *International Journal of Heat and Mass Transfer*, *55*(23-24), 7346–7351. doi:10.1016/j.ijheatmasstransfer.2012.06.070

Hermes, C. J. L., Piucco, R. O., Barbosa, J. R., & Melo, C. (2009). A study of frost growth and densification on flat surfaces. *Experimental Thermal and Fluid Science*, *33*(2), 371–379. doi:10.1016/j.expthermflusci.2008.10.006

Jhee, S., Lee, K., & Kim, W. (2002). Effect of surface treatments on the frosting / defrosting behavior of a fin-tube heat exchanger. *International Journal of Refrigeration*, *25*, 1047–1053.

Kim, K., & Lee, K.-S. (2011). Frosting and defrosting characteristics of a fin according to surface contact angle. *International Journal of Heat and Mass Transfer*, *54*(13-14), 2758–2764. doi:10.1016/j.ijheatmasstransfer.2011.02.065

Kragh, J., Rose, J., Nielsen, T. R., & Svendsen, S. (2007). New counter flow heat exchanger designed for ventilation systems in cold climates. *Energy and Buildings*, *39*(11), 1151–1158. doi:10.1016/j.enbuild.2006.12.008

Kulinich, S. a., & Farzaneh, M. (2011). On ice-releasing properties of rough hydrophobic coatings. *Cold Regions Science and Technology*, *65*(1), 60–64. doi:10.1016/j.coldregions.2010.01.001

Kwak, M. K., Jeong, H.-E., Kim, T., Yoon, H., & Suh, K. Y. (2010). Bio-inspired slanted polymer nanohairs for anisotropic wetting and directional dry adhesion. *Soft Matter*, *6*(9), 1849. doi:10.1039/b924056j

Lee, H., Shin, J., Ha, S., Choi, B., & Lee, J. (2004). Frost formation on a plate with different surface hydrophilicity. *International Journal of Heat and Mass Transfer*, *47*(22), 4881–4893. doi:10.1016/j.ijheatmasstransfer.2004.05.021

Menini, R., Ghalmi, Z., & Farzaneh, M. (2011). Highly resistant icephobic coatings on aluminum alloys. *Cold Regions Science and Technology*, *65*(1), 65–69. doi:10.1016/j.coldregions.2010.03.004

Moallem, E., Cremaschi, L., Fisher, D. E., & Padhmanabhan, S. (2012). Experimental measurements of the surface coating and water retention effects on frosting performance of microchannel heat exchangers for heat pump systems. *Experimental Thermal and Fluid Science*, *39*, 176–188. doi:10.1016/j.expthermflusci.2012.01.022

Phillips, E. G., Chant, R. E., Bradley, B. C., & Fisher, D. R. (1989). A Model to Compare Freezing Control Strategies for Residential Air-to-Air Heat Recovery Ventilators. *Ashrae Trans, 95*(2).

Phillips, E. G., Chant, R. E., Fisher, D. R., & Bradley, B. C. (1989). Comparison of Freezing Control Strategies for Residential Air-to-Air Heat Recovery Ventilators. *ASHRAE Transactions 95*, *95*(2).

Qi, Z. (2013). Water retention and drainage on air side of heat exchangers—A review. *Renewable and Sustainable Energy Reviews*, *28*, 1–10. doi:10.1016/j.rser.2013.07.014

Rahimi, M., Fojan, P., Gurevich, L., & Afshari, A. (2014). Effects of aluminium surface morphology and chemical modification on wettability. *Applied Surface Science*, *296*, 124–132. doi:10.1016/j.apsusc.2014.01.059

Rahimi, M., Gurevich, L., Fojan, P., & Afshari, A. (2015). The effect of aluminium surface morphology on incipient ice formation. Submitted to journal of *Applied Surface Science*

Rahman, M. A., & Jacobi, A. M. (2012). Drainage of frost melt water from vertical brass surfaces with parallel microgrooves. *International Journal of Heat and Mass Transfer*, *55*(5-6), 1596–1605. doi:10.1016/j.ijheatmasstransfer.2011.11.015

Rose, J., Nielsen, T. R., Kragh, J., & Svendsen, S. (2008). Quasi-steady-state model of a counter-flow air-to-air heat-exchanger with phase change. *Applied Energy*, *85*(5), 312–325. doi:10.1016/j.apenergy.2007.07.009

Tadmor, R., Bahadur, P., Leh, A., N'guessan, H. E., Jaini, R., & Dang, L. (2009). Measurement of Lateral Adhesion Forces at the Interface between a Liquid Drop and a Substrate. *Physical Review Letters*, *103*(26), 266101. doi:10.1103/PhysRevLett.103.266101

3.1.3 SUMMARY OF ‘‘ALUMINUM ALLOY 8011: SURFACE CHARACTERISTICS’’

Aluminum alloys are the predominant materials used in modern industries. Increased knowledge about the surface characteristics of bare aluminium may enhance the understanding of how to optimize the working conditions of equipment involving aluminium parts. This work focuses on the properties of the native surface of aluminium alloy 8011, which is the main construction material for the production of air-to-air heat exchanger fins. In this study, we address its water wettability, surface roughness and frost formation in different psychometric parameters. The contact angle measurements revealed that this aluminium alloy exhibits a relatively high contact angle of about 78 degrees, i.e. it is not wetted completely. AFM measurements revealed significant surface roughness of typical heat exchanger fins. The thickness of formed ice was studied in relation to the wettability, humidity and the cold surface temperature.

The focus of this paper was the investigation and in depth study of the aluminum alloy 8011 as the main material of air to air heat exchanger fins and the main substrate for the investigation of this study.

In order to better understand the surface structure and roughness of aluminum alloy 8011 the AFM scanning is conducted and the images are processed. The AFM roughness measurements reveal the rough surface of this aluminum as it is shown in Figure 3-3.

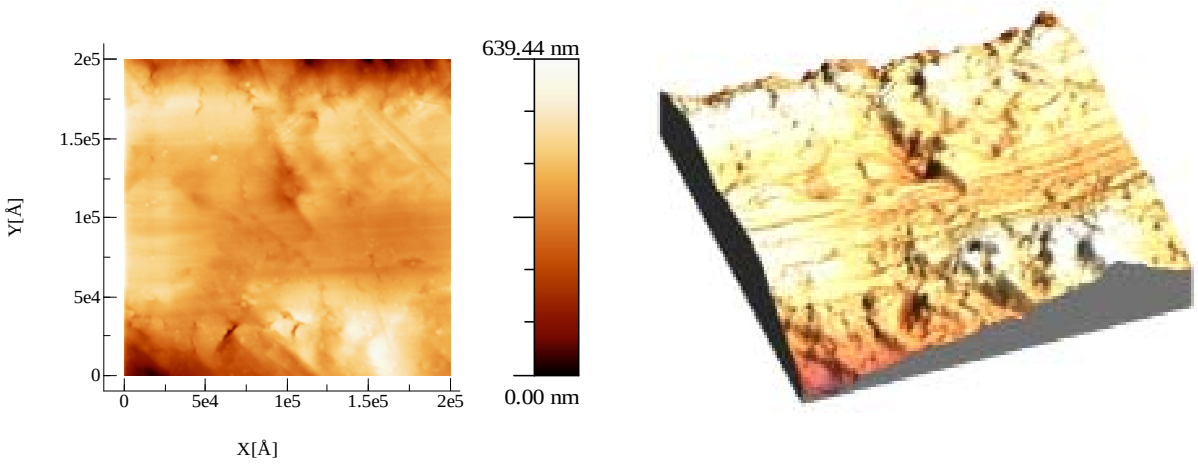

Figure 3-3 A typical topography of native aluminum alloy 8011 imaged with an AFM ((a) and (b) show 2D and 3D representations of the same image).

The results show that the high surface roughness and inhomogeneous surface of aluminum alloy renders it almost impossible to measure the receding contact angle on its surface; this is due to the pinning phenomenon and the continuous reduction of the contact angle caused by evaporation. Figure 3-4 illustrates the evolution of an evaporating sessile drop of an initial contact angle of 78° on the surface of aluminium alloy 8011. As is clear in Figure 3-4, the contact angle does not remain constant, and thus, cannot be considered as the receding contact angle.

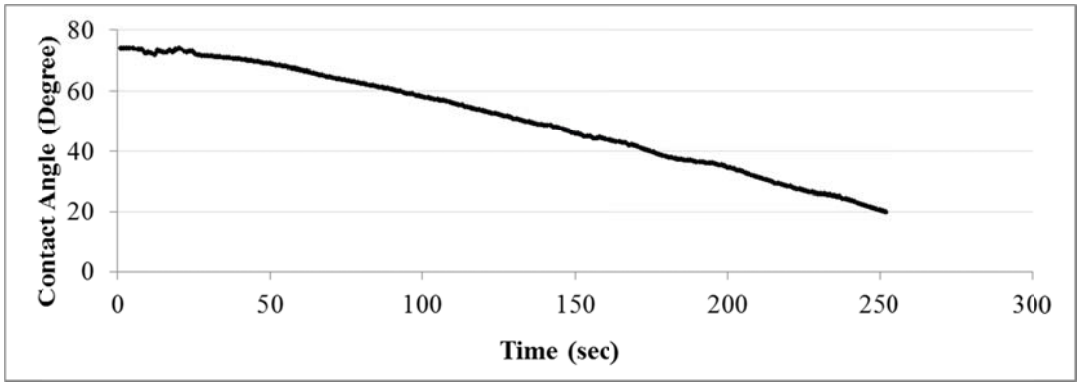

Figure 3-4 Evolution of an evaporating sessile drop of initial contact angle contact angle of 78° on the surface of aluminium alloy 8011

Moreover, in order to investigate and study of the ice nucleation and formation on the bare surface of aluminum alloy 8011 and study the effect of psychrometric factors on the formed ice, an experimental setup is designed and modified; the schematic illustration of this is shown in Figure 3-5. The designed chamber had the ability of controlling and measuring the environmental conditions, such as humidity, air flow and temperature, and monitoring them online.

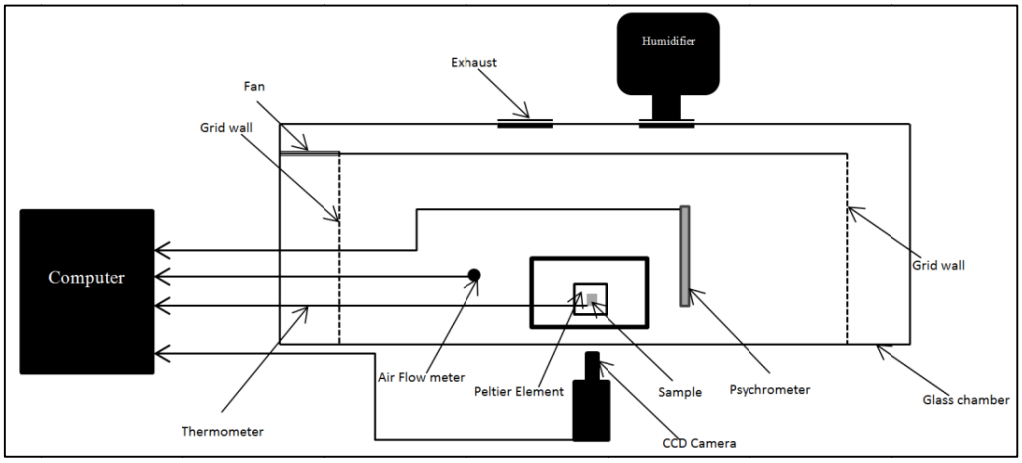

Figure 3-5 Schematic picture of the test setup for ice formation

The results of the observation of the effect of ice structure and growth rate to the relative humidity revealed that both ice thickness and density directly relates to the relative humidity; and a higher relative humidity in the environment causes an increased ice thickness and density.

3.1.3.1 Actual paper III

Aluminum Alloy 8011: Surface Characteristics
M. Rahimi, P. Fojan, L. Gurevich, and A. Afshari.
Applied Mechanics and Materials Vols. 719-720 (2015) pp 29-37

Applied Mechanics and Materials Vols. 719-720 (2015) pp 29-37
© (2015) Trans Tech Publications, Switzerland
doi:10.4028/www.scientific.net/AMM.719-720.29

Submitted: 2014-05-09
Revised: 2014-09-26
Accepted: 2014-09-26
Online: 2015-01-13

Aluminium alloy 8011:Surface characteristics

M.Rahimi[1, a], P.Fojan[2,b], L.Gurevich[3,c] and A.Afshari[4,d]

[1,4] Department of Energy and Environment, Danish Building Research Institute, Aalborg University, A.C. Meyers Vænge 15, DK-2450 Copenhagen SV, Denmark

[2,3] Department of Physics and Nanotechnology, Aalborg University, Skjernvej 4, DK-9220, Aalborg East, Denmark

[a]mar@sbi.aau.dk, [b] fp@nano.aau.dk, [c] lg@nano.aau.dk, [d] ala@sbi.aau.dk

Keywords: Aluminium alloy 8011, wettability, contact angle, roughness, frost

Abstract. Aluminium alloys are the predominant materials in modern industries. Increased knowledge about the surface characteristics of bare aluminium can enhance the understanding about how to optimize the working conditions for the equipment involving aluminium parts. This work focusses on the properties of native surface of aluminium alloy 8011, which is the main construction material for the production of air-to-air heat exchanger fins. In this study, we address its water wettability, surface roughness and frost formation in different psychometric parameters. The contact angle measurements revealed that this aluminium alloy exhibits a relatively high contact angle of about 78 degree, i.e. is not wetted completely. AFM measurements revealed significant surface roughness of typical heat exchanger fins. The thickness of formed frost was studied in relation to the wettability, humidity and the cold surface temperature.

Introduction

Aluminium alloys are the predominant materials in outdoor structures like electrical cabling, in aircraft industries and in ventilation system such as in heat exchanger production. It is widely used because of its relatively low cost, light weight, high heat conductivity and proper corrosion resistance. Aluminium alloys can be heat treated and loaded to relatively high stress levels [1][2][3].In cold conditions at temperatures below the dew point of water, formation of frost is inevitable and can cause serious malfunctions of the equipment. [4]. Aluminium alloy surface characteristics such as its roughness, contact angle and wettability play an important role for applications in cold working conditions. Frost formation and frost accretion is related to the wettability of a surface, which can be described by the contact angle that a liquid droplet form on the solid surface, is related to the surface morphology and surface chemistry[5][6][7][8].

There are two models for describing the relation between the surface morphology and the contact angle the Wenzel and Cassie-Baxter models[9][10][11].

If the liquid penetrates through the surface roughness and is in full contact with the solid surface, the contact angle is described by Wenzel's equation. On the other hand, if the water remains suspended on top of the rough surface and air is entrapped below the liquid, the contact angle is described by Cassie's state of wetting. It means that the effect of surface morphology on the contact angle is described by the Cassie-Baxter model[12].

Frost formation on the surface of aluminium alloy is an important topic of research and much significant prior research has been carried out to understand frost growth on a flat plate. In this paper, the frost formation on top of the aluminium samples in different psychrometric parameters

such as air temperature, humidity and surface temperature is investigated in addition to the surface characteristics of aluminium plate samples.

Frost growth is divided into three main steps which are: crystal growth period, frost layer growth, and frost layer full-growth period. During the first stage, the ice crystals grow away from the cold surface and they are far apart and show little interaction. In the second stage, as the process continues, the crystals grow, branch out and meet together to form a layer and frost is characterised as "frost layer growth". In the "full-layer frost growth", the surface temperature of the frost reaches 0^{o}C and continuous cycles of melting and refreezing occur at this temperature which is the reason for increasing the frost layer density. These categories for frost growth are introduced first by Hayashi et al 1997 and then also observed by other researchers [13][14][15].

In frost formation and deposition on a surface psychrometric parameters such as air temperature, velocity, humidity and surface temperature have an important impact on the frost formation process, its nucleation and growth, and also on frost properties such as density and thickness[6][16][17].

Besides these psychrometric parameters, surface conditions such as surface temperature, roughness, drop adhesion to the surface and consequently the contact angle are also important parameters for frost formation [18]. It has been shown that frost formation is a heterogeneous nucleation process that is mainly influenced by the contact angle[19].Frost thickness which can block the air passage and increase the thermal resistance between air and the cold surface is the most important parameter in this frost formation study. The research results showed that the frost layer thickness increases during the frost formation process while the growing speed decreases gradually. However, it should be noted, that by increasing the air humidity or decreasing the temperatures of the cold surface and air, the frost growth can be increased[15].

Increased knowledge about the bare aluminium surface characteristics can enhance understanding how to improve working conditions for aluminium equipment and decrease manufacturing and maintenance costs. In this paper, we address surface wettability of untreated aluminium alloy 8011, which is one of the most common materials for air-to-air heat exchanger fins. To the authors' knowledge, the surface characteristics of this aluminium alloy have never been addressed in connection with its application in heat exchangers

Material

Aluminium alloy 8011 with chemical composition according to Table.1, which is used for the production of heat exchangers, was used in this study. Aluminium sheets were plain, single rolled with a thickness of 0.25 mm were cut into test samples of 15× 15 mm^2. Samples were degreased in an ultrasound cleaner in a process consisting of 10 min in an acetone bath, then 10 min in DI-water and finally 10 min in an ethanol bath. The samples were then dried under an N2 stream and put in an oven at 110 C° over night for drying.

Table 1: Chemical composition of Aluminium alloy 8011 according to EN 573-3.

Grade 8011A – content [%]										
	Si [%]	Fe [%]	Cu [%]	Mn [%]	Mg [%]	Cr [%]	Zn [%]	Ti [%]	Others each [%]	Others total [%]
min	0.40	0.50	-	-	-	-	-	-	-	-
max	0.8	1.0	0.10	0.10	0.10	0.10	0.10	0.05	0.05	0.15

Methodology

Contact angle measurement. Contact angle measurements were made by means of homemade computer-controlled sessile drops stage. Milli-Q water was supplied via a micro tube on the surface at room temperature of 24 C° with the fluid rate of 6 µL/min. The shape of contact angles were recorded by CCD camera over time and the images were interpreted and analysed by Drop Snake software (plugin for Image J software)[20]. The reported contact angle data were determined by averaging values measured at 3 different points on 4 samples.

AFM. The surface roughness morphology was measured and visualised by atomic force microscopy (NTEGRA Aura, NT-MDT Co.) in intermittent contact mode using Olympus OMCL-160TS cantilevers (Asylum Research). The RMS roughness for each group of samples was calculated as an average value of the measurements carried out over 3 areas on 3 samples. The AFM images were analysed using WSXM software [21].

Observation of the frost formation. A dedicated chamber was assembled to allow full control of the frost formation parameters, including airflow, air humidity, surrounding temperature and cold surface temperature of the test section. The experiments were performed in a clean room to ensure low concentration of polluting gases and particles. Air supply system in the clean room involved extensive air filtration using a F7-class filter, a charcoal filter followed by a second F7-class filter and finally a HEPA filter. Frost formation on the sample was monitored by a CCD camera. The recorded images were interpreted and analysed after each test and the thickness of the frost was calculated for each sample. Fig. 1shows a schematic picture of the test setup. It should be noted that due to the random nucleation on the surface, the frost layer is not flat. To account for this, several measuring techniques have been developed [22]. In the presented data, the frost thickness was measuring in at least 10 points on each sample using side images acquired with a CCD camera.

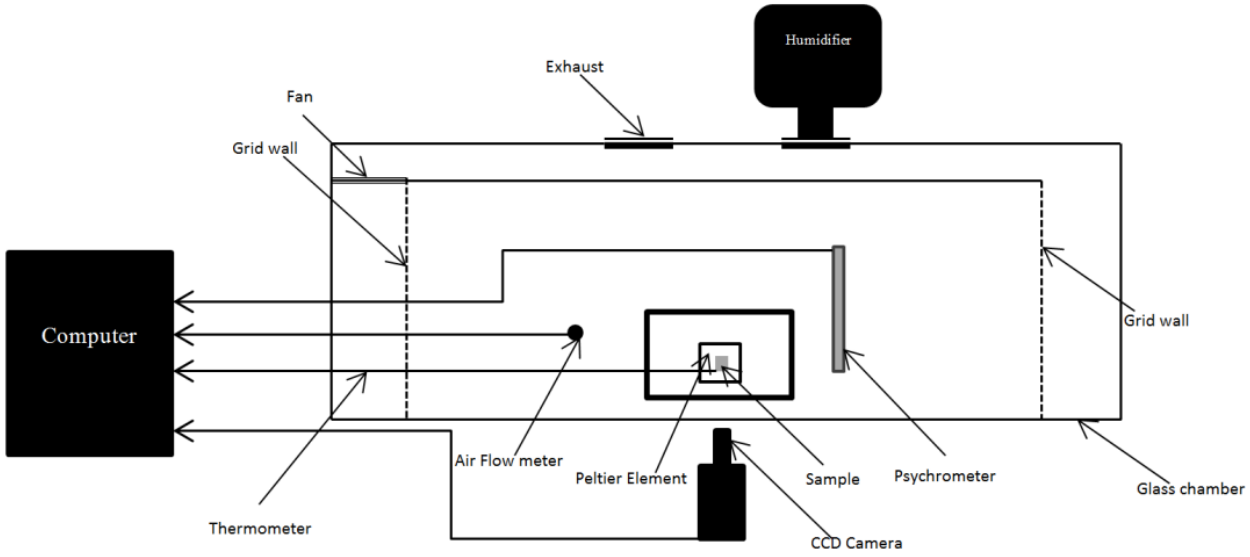

Fig.1: Schematic picture of the test setup for frost formation

Result and discussion

The measured RMS roughness of aluminium alloy samples by AFM was 84.05 nm with a 95 % confidence interval of 16.65A typical example of the observed surface morphology is shown in in Fig.2..

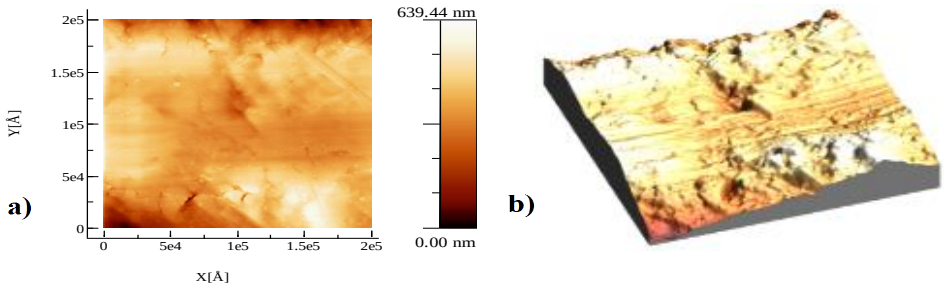

Fig.2: A typical topography of native aluminum alloy 8011 imaged with an AFM ((a) and (b) show 2D and 3D representations of the same image).

The contact angle measurement on the surface of the samples showed that the water drop forms a contact angle of 78° on the untreated surface of aluminium alloy 8011.The measured amount is a significantly high contact angel since aluminium alloys are considered to be high surface-energy materials and they were expected to be hydrophilic with a low contact angle and be completely wetted. This can be explained by the fact that the exposure of aluminium surface to the atmosphere causes hydrophobic organic contamination and hence the water contact angle on its surface is increased. This observation was in line with the other observations and also in line with other clean metal surfaces,[23][24].Due to its high roughness and the air pocket structure in its surface, it

follows the Cassie-Baxtermodel and has a large contact angle. The rough surface of aluminium entraps air in the gaps and forms a composite surface of air and solid material. The entrapped air under the liquid reduces the interfacial contact area between the solid surface and the liquid which leads to a higher water contact angle[5][25][23][24].

On the other hand, such a rough and inhomogeneous surface also leads to the pinning of the contact line during evaporation of the droplet. Fig.3shows that the three-phase contact line remained pinned and that the contact angle decreased constantly after the initial stage of evaporation with a constant advancing contact angle. A similar phenomenon has been observed by Shanahan and Bourgès-Monnier who noted that the surface roughness makes it impossible to introduce a specific value of the receding contact angle due to the constant decrease of the contact angle and the height of droplet till the moment of total evaporation of the droplet[26]. Bormashenko et al. also observed this phenomenon on aluminium and steel surfaces [24].

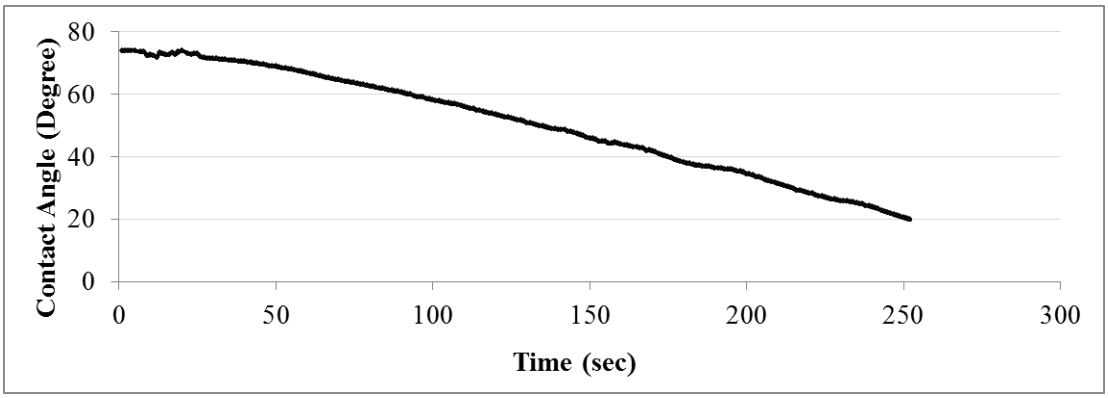

Fig.3: Receding contact angle of an evaporating sessile drop on the surface of aluminium alloy 8011

The thickness of the frost formed on top of the aluminium alloy samples after 5 and 10 min is shown in Fig.4 for three different values of relative humidity. As, it can be seen at a constant humidity, the frost thickness increases over time.

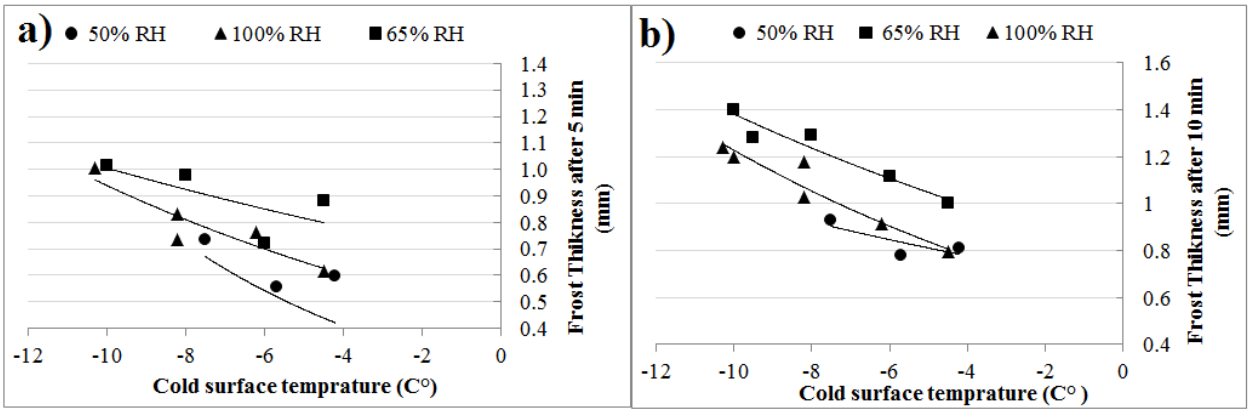

Fig.4: Thickness of the frost formed on top of the samples after a) 5 min and b)10 min at different humidity

The density of the formed frost at relative humidity of 50%, 65% and 100% is shown in Fig.5.It can be seen that the frost density decreased upon decrease in cold surface temperature. This observation is in line with previous works and researches [27][13][22].

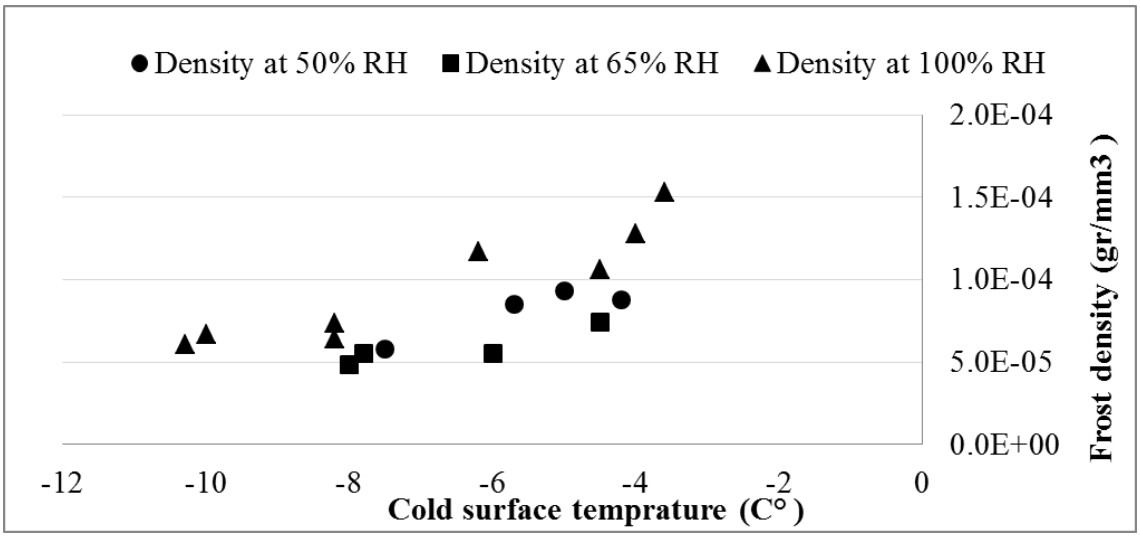

Fig.5: The density of formed frost on top of the samples at different humidity

Fig.6 shows that the frost formation can indeed be divided into three main stages. In the beginning of process, individual ice crystals nucleate on the cold surface(see Fig.6.a),then these crystalsgrow, with approximately the same rate, in a direction perpendicular to the surface, see Fig.6.b. Over time, the crystals branched out, collide and grew in a direction parallel to the surface direction forming a layer of frost, seeFig.6.c. This observation was in line with the steps that reported by Hayashi et al. (1977).

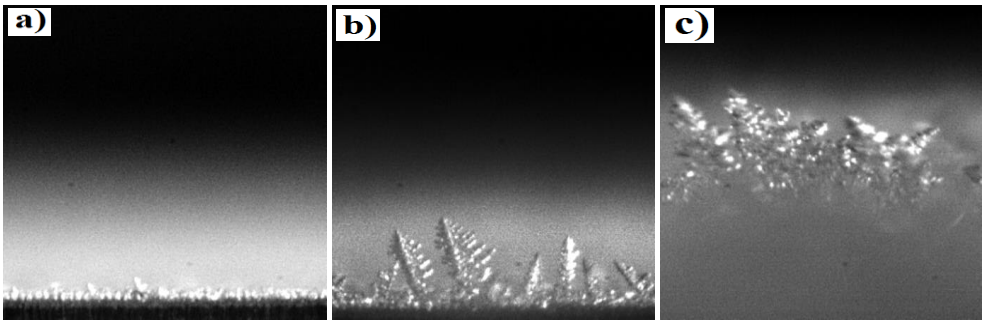

Fig.6: Frost formation images at a humidity of 65% and at -8 C° a) in the beginning nucleation, b) after 5 min, and c) after 10 min viewed from the edge of aluminum plate

Fig.7 shows that increasing the humidity of the air stream clearly increased the frost deposition rate Since by increasing the humidity the mass transfer rate will be increased and the mass of deposited frost will be increased.

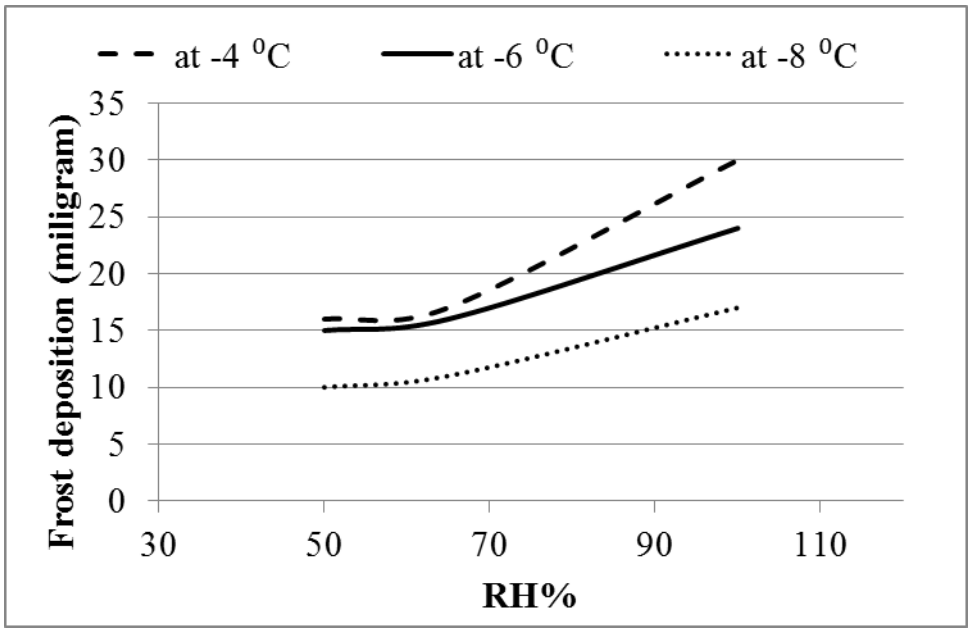

Fig.7: Frost deposition (milligram) at different humidity and cold surface temperatures

Conclusion

The studies of wetting characteristics of the native surface of aluminium alloy 8011 revealed that this surface exhibit a relatively high contact angle of 78 °C. This result can be explained by a significant roughness of the native surface of the alloy (shown by AFM measurements) in combination with inevitable surface contaminations common for high-energy metal surfaces. As we found in our previous publication [5].Such a combination of parameters should lead to Cassie-Baxter behaviour, where the interface between the water droplet and aluminium includes patches of trapped air. In this case a simple further roughening of the surface can make it stably hydrophobic which may be essential for alloy application in heat exchangers and outdoor equipment. Our measurements also provide an insight into the receding behaviour of water droplet on the alloy. It was observed that upon drying of a droplet the three-phase contact line remained pinned and the contact angle decreased constantly. Further, this paper experimentally studied the local frost formation process on a cold surface of aluminium alloy 8011 at different air humidityand cold surface temperatures.

References

[1] E.A. Starke, J.T. Staleyt, Application of modern alluminum alloys to aircraft, Prog. Aerosp. Sci. 32 (1996) 131–172.

[2] T. Dursun, C. Soutis, Recent developments in advanced aircraft aluminium alloys, Mater. Des. 56 (2014) 862–871.

[3] W. Zhang, D. Zhang, Y. Le, L. Li, B. Ou, Fabrication of surface self-lubricating composites of aluminum alloy, Appl. Surf. Sci. 255 (2008) 2671–2674.

[4] R. Menini, Z. Ghalmi, M. Farzaneh, Highly resistant icephobic coatings on aluminum alloys, Cold Reg. Sci. Technol. 65 (2011) 65–69.

[5] M. Rahimi, P. Fojan, L. Gurevich, A. Afshari, Effects of aluminium surface morphology on wettability and roughness, Appl. Surf. Sci. 2014, http//dx.doi.org/doi10.1016/j.apsusc.2014.01.059.

[6] C.J.L. Hermes, An analytical solution to the problem of frost growth and densification on flat surfaces, Int. J. Heat Mass Transf. 55 (2012) 7346–7351.

[7] A. Bayer, J.J. Schrijder, The Wettability of Industrial Surfaces : Contact Angle Measurements and Thermodynamic Analysis, 19 (1985) 277–285.

[8] M.K. Kwak, H.-E. Jeong, T. Kim, H. Yoon, K.Y. Suh, Bio-inspired slanted polymer nanohairs for anisotropic wetting and directional dry adhesion, Soft Matter. 6 (2010) 1849.

[9] R.N. Wenzel, Resistance of solid surfaces, Ind. Eng. Chem. 28 (1936) 988–994.

[10] A.B.D. Cassie, S. Baxter, Wettability of porous surfaces, Trans. Faraday Soc. 40 (1944) 546–551., Trans. Faraday Soc. 40 (1944) 546–551.

[11] a J.B. Milne, a Amirfazli, The Cassie equation: how it is meant to be used., Adv. Colloid Interface Sci. 170 (2012) 48–55.

[12] C. Dorrer, J. Rühe, Drops on microstructured surfaces coated with hydrophilic polymers: Wenzel's model and beyond, Langmuir. 24 (2008) 1959–64.

[13] Y. Hayashi, A. Aoki, S. Adashi, K. Hori, Study of frost properties correlating with frost formation types, ASME J. Heat Transf. 99 (1977) 239–245.

[14] K.S. Lee, W.S. Kim, T.H. Lee, A one-dimensional model for frost formation on a cold flat surface, Int. J. Heat Mass Transf. 40 (1997) 4359–4365.

[15] K. Qu, S. Komori, Y. Jiang, Local variation of frost layer thickness and morphology, Int. J. Therm. Sci. 45 (2006) 116–123.

[16] K.S. Lee, S. Jhee, D.-K. Yang, Prediction of the frost formation on a cold flat surface, Int. J. Heat Mass Transf. 46 (2003) 3789–3796.

[17] W. Wang, Q.C. Guo, W.P. Lu, Y.C. Feng, W. Na, A generalized simple model for predicting frost growth on cold flat plate, Int. J. Refrig. 35 (2012) 475–486.

[18] R. Tadmor, P. Bahadur, A. Leh, H.E. N'guessan, R. Jaini, L. Dang, Measurement of Lateral Adhesion Forces at the Interface between a Liquid Drop and a Substrate, Phys. Rev. Lett. 103 (2009) 26610-1–26610-4.

[19] B. Na, R.L. Webb, A fundamental understanding of factors affecting frost nucleation, Int. J. Heat Mass Transf. 46 (2003) 3797–3808.

[20] M.D. Abràmoff, P.J. Magalhães, S.. Ram, Image Processing with ImageJ, Biophotonics Int. 11 (2004) 36–42.

[21] I. Horcas, R. Fernández, J.M. Gómez-Rodríguez, J. Colchero, J. Gómez-Herrero, a M. Baro, WSXM: a software for scanning probe microscopy and a tool for nanotechnology., Rev. Sci. Instrum. 78 (2007) 013705-1–013705-9.

[22] I. Tokura, H. Saito, K. Kishinami, Study on properties and growth rate of frost layers on cold surface.pdf, Trans. ASME,J. Heat Transf. 105 (1983) 895–901.

[23] W.A. Zisman, K.W. Bewig, The Wetting of Gold and Platinum by Water, J. Phys. Chem. 1097 (1966) 4238–4242.

[24] E. Bormashenko, A. Musin, M. Zinigrad, Evaporation of droplets on strongly and weakly pinning surfaces and dynamics of the triple line, Colloids Surfaces A Physicochem. Eng. Asp. 385 (2011) 235–240.

[25] S.H. Kim, Fabrication of Superhydrophobic Surfaces, J. Adhes. Sci. Technol. 22 (2008) 235–250.

[26] M.E.R. Shanahan, C. Bourg, Effects of evaporation on contact angles on polymer surfaces, Int. J. Adhes. Adhes. 14 (3) (1994) 201–205.

[27] C.-H. Cheng, Y.-C. Cheng, Prediction of frost groeth on a cold plate in atmospheric air, Int. Comm. Heat Mass Transf. 28 (2001) 953–962.

Materials and Engineering Technology
10.4028/www.scientific.net/AMM.719-720

Aluminium Alloy 8011: Surface Characteristics
10.4028/www.scientific.net/AMM.719-720.29

DOI References
[1] E.A. Starke, J.T. Staleyt, Application of modern alluminum alloys to aircraft, Prog. Aerosp. Sci. 32 (1996) 131-172.
http://dx.doi.org/10.1016/0376-0421(95)00004-6
[2] T. Dursun, C. Soutis, Recent developments in advanced aircraft aluminium alloys, Mater. Des. 56 (2014) 862-871.
http://dx.doi.org/10.1016/j.matdes.2013.12.002
[3] W. Zhang, D. Zhang, Y. Le, L. Li, B. Ou, Fabrication of surface self-lubricating composites of aluminum alloy, Appl. Surf. Sci. 255 (2008) 2671-2674.
http://dx.doi.org/10.1016/j.apsusc.2008.07.209
[4] R. Menini, Z. Ghalmi, M. Farzaneh, Highly resistant icephobic coatings on aluminum alloys, Cold Reg. Sci. Technol. 65 (2011) 65-69.
http://dx.doi.org/10.1016/j.coldregions.2010.03.004
[6] C.J.L. Hermes, An analytical solution to the problem of frost growth and densification on flat surfaces, Int. J. Heat Mass Transf. 55 (2012) 7346-7351.
http://dx.doi.org/10.1016/j.ijheatmasstransfer.2012.06.070
[8] M.K. Kwak, H. -E. Jeong, T. Kim, H. Yoon, K.Y. Suh, Bio-inspired slanted polymer nanohairs for anisotropic wetting and directional dry adhesion, Soft Matter. 6 (2010) 1849.
http://dx.doi.org/10.1039/b924056j
[9] R.N. Wenzel, Resistance of solid surfaces, Ind. Eng. Chem. 28 (1936) 988-994.
http://dx.doi.org/10.1021/ie50320a024
[10] A.B.D. Cassie, S. Baxter, Wettability of porous surfaces, Trans. Faraday Soc. 40 (1944) 546- 551., Trans. Faraday Soc. 40 (1944) 546-551.
http://dx.doi.org/10.1039/tf9444000546
[11] a J.B. Milne, a Amirfazli, The Cassie equation: how it is meant to be used., Adv. Colloid Interface Sci. 170 (2012) 48-55.
http://dx.doi.org/10.1016/j.cis.2011.12.001
[12] C. Dorrer, J. Rühe, Drops on microstructured surfaces coated with hydrophilic polymers: Wenzel's model and beyond, Langmuir. 24 (2008) 1959-64.
http://dx.doi.org/10.1021/la7029938
[13] Y. Hayashi, A. Aoki, S. Adashi, K. Hori, Study of frost properties correlating with frost formation types, ASME J. Heat Transf. 99 (1977) 239-245.
http://dx.doi.org/10.1115/1.3450675
[14] K.S. Lee, W.S. Kim, T.H. Lee, A one-dimensional model for frost formation on a cold flat surface, Int. J. Heat Mass Transf. 40 (1997) 4359-4365.
http://dx.doi.org/10.1016/S0017-9310(97)00074-4
[15] K. Qu, S. Komori, Y. Jiang, Local variation of frost layer thickness and morphology, Int. J. Therm. Sci. 45 (2006) 116-123.
http://dx.doi.org/10.1016/j.ijthermalsci.2005.05.004

[16] K.S. Lee, S. Jhee, D. -K. Yang, Prediction of the frost formation on a cold flat surface, Int. J. Heat Mass Transf. 46 (2003) 3789-3796.
http://dx.doi.org/10.1016/S0017-9310(03)00195-9
[17] W. Wang, Q.C. Guo, W.P. Lu, Y.C. Feng, W. Na, A generalized simple model for predicting frost growth on cold flat plate, Int. J. Refrig. 35 (2012) 475-486.
http://dx.doi.org/10.1016/j.ijrefrig.2011.10.011
[18] R. Tadmor, P. Bahadur, A. Leh, H.E. N'guessan, R. Jaini, L. Dang, Measurement of Lateral Adhesion Forces at the Interface between a Liquid Drop and a Substrate, Phys. Rev. Lett. 103 (2009) 26610-1-26610-4.
http://dx.doi.org/10.1103/PhysRevLett.103.266101
[19] B. Na, R.L. Webb, A fundamental understanding of factors affecting frost nucleation, Int. J. Heat Mass Transf. 46 (2003) 3797-3808.
http://dx.doi.org/10.1016/S0017-9310(03)00194-7
[21] I. Horcas, R. Fernández, J.M. Gómez-Rodríguez, J. Colchero, J. Gómez-Herrero, a M. Baro, WSXM: a software for scanning probe microscopy and a tool for nanotechnology., Rev. Sci. Instrum. 78 (2007) 013705-1-013705-9.
http://dx.doi.org/10.1063/1.2432410
[22] I. Tokura, H. Saito, K. Kishinami, Study on properties and growth rate of frost layers on cold surface. pdf, Trans. ASME,J. Heat Transf. 105 (1983) 895-901.
http://dx.doi.org/10.1115/1.3245679
[24] E. Bormashenko, A. Musin, M. Zinigrad, Evaporation of droplets on strongly and weakly pinning surfaces and dynamics of the triple line, Colloids Surfaces A Physicochem. Eng. Asp. 385 (2011) 235-240.
http://dx.doi.org/10.1016/j.colsurfa.2011.06.016
[25] S.H. Kim, Fabrication of Superhydrophobic Surfaces, J. Adhes. Sci. Technol. 22 (2008) 235- 250.
http://dx.doi.org/10.1163/156856108X305156
[26] M.E.R. Shanahan, C. Bourg, Effects of evaporation on contact angles on polymer surfaces, Int. J. Adhes. Adhes. 14 (3) (1994) 201-205.
http://dx.doi.org/10.1016/0143-7496(94)90031-0
[27] C. -H. Cheng, Y. -C. Cheng, Prediction of frost groeth on a cold plate in atmospheric air, Int. Comm. Heat Mass Transf. 28 (2001) 953-962.
http://dx.doi.org/10.1016/S0735-1933(01)00299-8

3.1.4 SUMMARY OF ‘‘THE EFFECT OF SURFACE MODIFICATION ON INITIAL ICE FORMATION ON ALUMINUM SURFACES’’

One of the most promising energy saving methods in cold climate areas is using air-to-air heat exchangers for the heat recovery of ventilation systems. However, the high humidity of the exhaust air causes the risk of ice formation on the heat exchanger fins at subzero temperatures. Since the main material of heat exchanger fins is aluminum, this paper focuses on the effect of aluminum wettability on the initial stages of ice formation. We studied ice growth on bare as well as hydrophilically and hydrophobically modified surfaces of aluminum (8011A) sheets, commonly used in heat exchangers, at different psychrometric parameters. Moreover, we investigated how surface modification and changing the wettability of aluminum surface affected ice formation, its thickness, density and structure and we present the results of this investigation. The investigations and experiments are performed on samples of bare aluminum group, aluminium with hyperbranched polyethylene glycol (PEG) coating group, aluminium with Perfluorooctylsilane (PFOS) coating group and aluminium with PEG-PFOS coating group.

The obtained results show that the surface modification of aluminum plays a crucial role in ice formation. We demonstrated that flat hydrophobic surfaces exhibit slower ice growth and denser ice layers, hence this type of treatment is preferable for aluminum heat exchangers. Furthermore, we provided an explanation for a commonly observed phenomenon that bare aluminum surfaces are characterized by faster ice growth and less dense ice layers as compared to both hydrophilically and hydrophobically modified surfaces.

The distribution of water droplets observed upon melting of the incipient ice layer was studied in order to study the effect of chemical surface modification on the uniformity of the wetting properties. The results of imaging showed that the non-uniformity of the size distribution of the droplets formed on the samples was caused by the heterogeneous nature of nucleation on the surfaces which is dependent on the surface functionalization procedure (Figure 3-6).

As is clear in Figure 3-6 c and d, the hydrophobic surfaces with a layer of PFOS exhibit lower surface coverage, smaller size and more uniformly distributed droplets. These wetting characteristics correlate with a lower ice growth rate and lower ice thickness. In addition due to smaller area of water–substrate interface and reduction in heat transfer from the cold surface to the droplets and consequently slower growth kinetics, as is clear in Figure 3-7.

On the other hand, hydrophilic samples with a PEG layer on the surface have higher surface coverage, larger droplet size and lower energy barriers for nucleation. This will cause a higher ice nucleation rate and growth rate. As Figure 3-7 shows, the PEG samples have a higher ice thickness.

As illustrated in figure 3-8, there is a reverse relation between ice density and ice thickness, thus, the samples with a thicker ice layer exhibit lower density and vice versa. It can be concluded that the deposited mass is roughly the same for all samples and the mass transfer coefficient is not a function of contact angle; thus, these results are in line with the results of Brian et al.,1970 and Shin et al., 2003 [73,91]

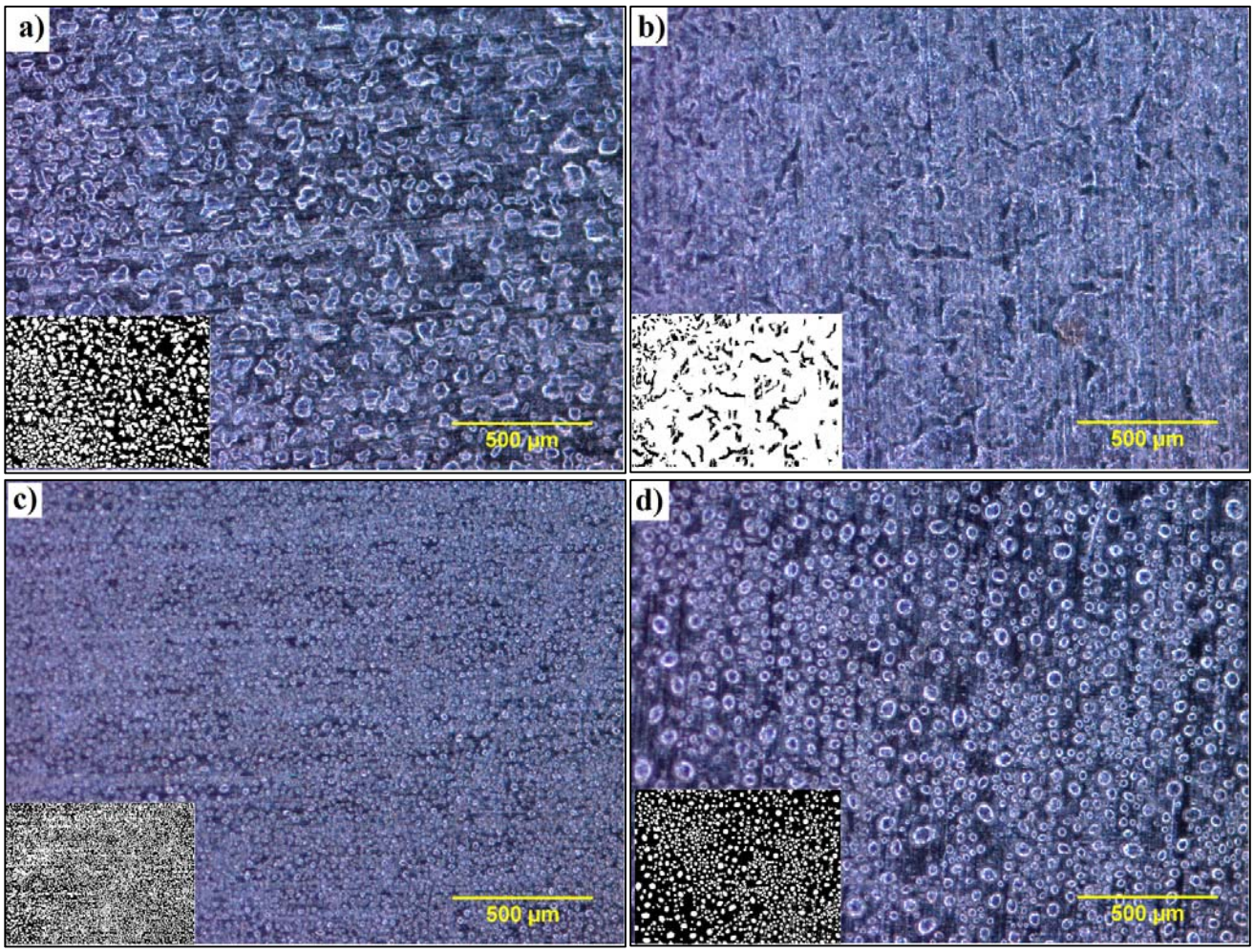

Figure 3-6 Pattern of water droplets observed on aluminum samples with different surface modifications after melting the ice formed during one minute of exposure to ambient air of 43% RH at surface temperature −10◦C: (a) bare aluminum (73% ± 4% coverage), (b) PEG-modified aluminum (86% ± 5% coverage), (c) PEG–PFOS-modified aluminum (76% ± 7 coverage), and (d) PFOS-modified aluminum (73% ± 4 coverage). The insets show binary images obtained using Matlab 2013. Black represents the aluminum surface and white is the droplets pattern. The coverage was calculated by counting black and white pixels.

The general tendency is that a lower contact angle corresponds to a thicker ice layer, however, the bare aluminum sample falls off the general trend, as can be seen in Figure 3-7. Moreover, as illustrated in Figure 3-8, the general trend for the formed ice density is the higher contact angle the higher ice density; again the bare aluminum sample falls off the general trend. These results for the bare aluminum are in line with the obsrevations of Shin et al., 2003 and Seki et al.,1985 [73,74]. In order to explain the observed results on the bare aluminum alloy, the formed ice morphology in the the same psychrometric parameters need to be further studied and investigated.

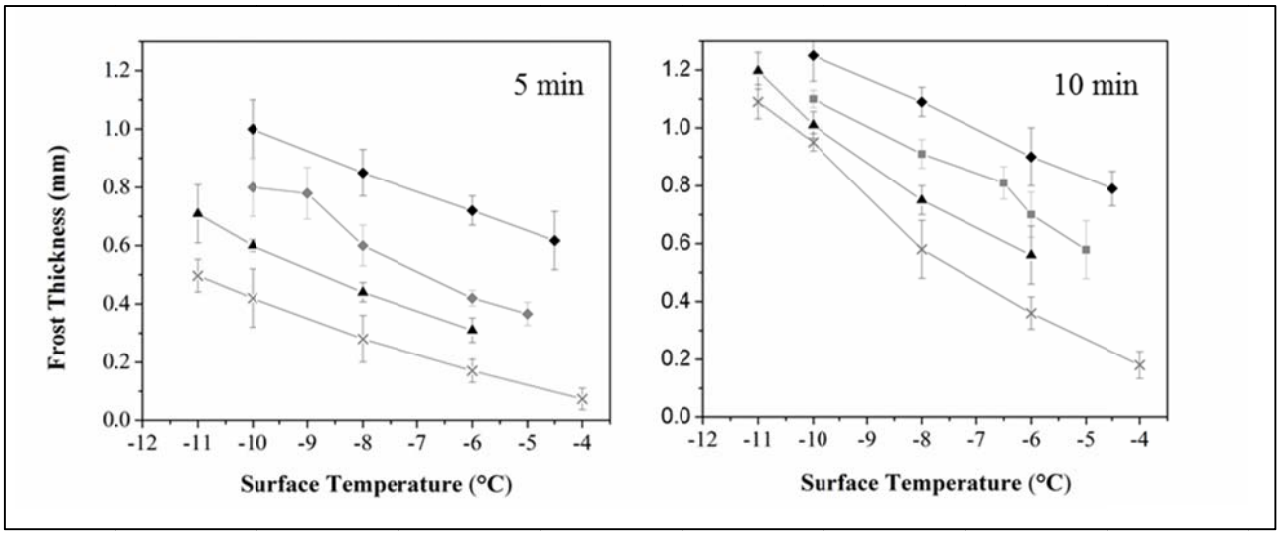

Figure 3-7 Frost thickness on aluminium samples with different surface modifications after 5 and 10 minutes exposure to air of 100% RH at 17°C plotted as a function of the cold surface temperature. ◆—bare, ■—PEG, ▲—PEG-PFOS, and ✕—PFOS-modified aluminium. Error bars show 95% confidence interval.

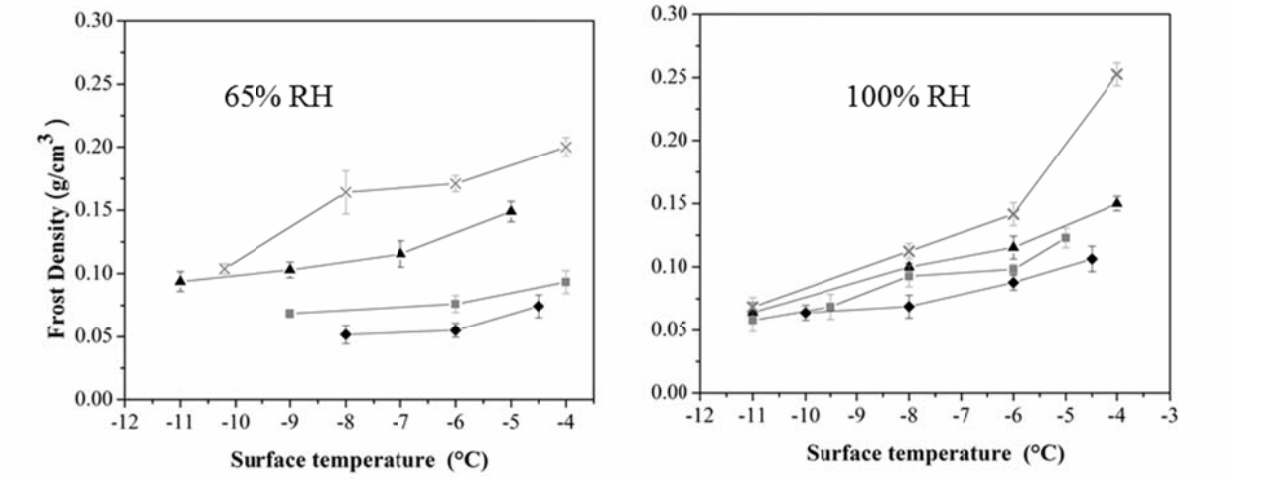

Figure 3-8 Density of ice on top of different aluminium samples plotted as a function of the surface temperature for different surface treatment at 65% RH and 100% RH: ◆—bare, ■—PEG, ▲—PEG-PFOS, and ✕—PFOS-coated aluminium. Error bars show 95% confidence interval.

The results of the study of ice morphology on top of all sample groups are shown in Figure 3-9. As it can be observe in Figure 3-9, the ice morphology on bare aluminum is rather different from both hydrophobically and hydrophilically modified samples.

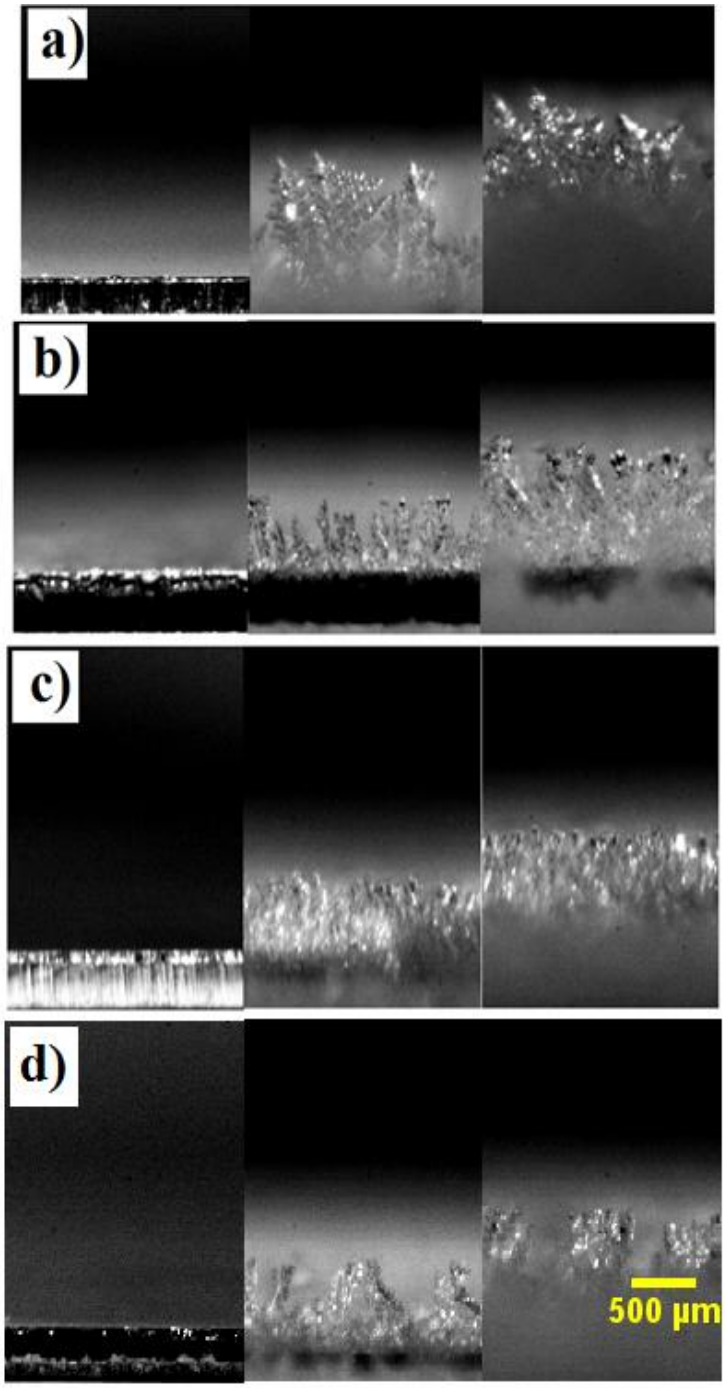

Figure 3-9 Side view of the ice morphology formed on differently treated surfaces in three stages (starting the measurement, after 5 min and after 10 min) 0020at -8°C a) bare aluminium, b) aluminium with PEG layer, c) aluminium with perfluorooctylsilane

The ice morphology on top of the bare aluminum in all the psychrometric conditions used in this study exhibited a feather-like structure which was maintained during the entire experiment. The ice morphology on top of the modified surfaces (hydrophobic and hyrophilic ones) exhibited a grass-like ice structure during the expriments, according to the classification of Lee et al., 2007 [24].

The presence of a feather-like ice layer structure explains the lower density of the ice layer observed on bare aluminum. Moreover, the results of the observation of the distribution of droplets on the surface aluminum alloy showed the insignificantly non-uniform chemistry of bare aluminum alloy.

This is caused by the fact that alluminum alloy 8011 is composed of Al, Fe and Si, which leads to the formation of various intermetallic inclusions. Consequently, the bare aluminum surface is composed of the surface structure of the aluminium grains and different intermetallic compounds with different surface energies which create a microscopic, heterogeneous surface. As a results of this microscopic heterogeneous surface, all nucleation will not be activated and will not start freezing at a certain degree of supercooling. However, on top of the modified allumium surface with a uniform surface energy, both macroscopically and microscopically, the nucleation centers are activated at a certain degree of supercooling, leading to the formation of a denser grass-like structure

In conclusion, on such a heterogeneous surface structure a wetting angle does not provide a complete picture, but only corresponds to average (in the Cassie-Baxter sense) surface properties.

3.1.4.1 Actual paper IV

The Effect of Surface Modification on Initial Ice Formation on Aluminum Surfaces
M. Rahimi, A. Afshari, P. Fojan, L. Gurevich.
Applied Surface Science Vols.355 (2015) PP 327–333

Applied Surface Science 355 (2015) 327–333

Contents lists available at ScienceDirect

Applied Surface Science

journal homepage: www.elsevier.com/locate/apsusc

The effect of surface modification on initial ice formation on aluminum surfaces

M. Rahimi [a], A. Afshari [a], P. Fojan [b], L. Gurevich [b,*]

[a] Department of Energy and Environment, Danish Building Research Institute, Aalborg University, A.C. Meyers Vænge 15, 2450 København SV, Denmark
[b] Department of Physics and Nanotechnology, Aalborg University, Skjernvej 4, DK-9220 Aalborg East, Denmark

ARTICLE INFO

Article history:
Received 21 April 2015
Received in revised form 27 June 2015
Accepted 30 June 2015
Available online 11 July 2015

Keywords:
Aluminum
Surface modification
Ice formation
Hydrophobicity
Hydrophilicity

ABSTRACT

One of the most promising energy saving methods in cold climate areas is heat recovery in ventilation system by using air-to-air heat exchangers. However, due to a higher humidity in the exhaust air, there is a risk of ice formation on the heat exchanger fins at subzero temperatures. Since the main material of heat exchanger fins is aluminum, this paper focuses on the effect of aluminum wettability on the initial stages of ice formation. The ice growth was studied on bare as well as hydrophilically and hydrophobically modified surfaces of aluminum (8011A) sheets, commonly used in heat exchangers, at different psychrometric parameters. The obtained results show that the surface modification of aluminum plays a crucial role in the ice formation. We demonstrated that flat hydrophobic surfaces exhibit slower ice growth and denser ice layers, hence making this type of treatment preferable for aluminum heat exchangers. Furthermore we provide an explanation for a commonly observed phenomenon that bare aluminum surfaces are characterized by a faster ice growth and less dense ice layer as compared to both hydrophilically and hydrophobically modified surfaces.

1. Introduction

Heat recovery in ventilation systems with an air-to-air heat exchanger is one of the most promising energy saving methods, which can reduce energy demand in a cold climate. On the other hand, in the case of subzero inlet air temperature, the surface temperature of the heat exchanger fins drops below the freezing point of water. Increasing the heat exchanger efficiency causes the exhaust humid air to be cooled almost to the outside temperature. As a result, condensation and ablimation (direct vapor to ice deposition) of the water vapor in airflows and consequent ice formation is a common problem [1]. Ice formation and accumulation on the cold surface of heat exchanger fins has attracted interest of many scientists for decades [2,3]. The growth and accumulation of ice is inevitable and undesirable, unless some strategies and methods are applied to postpone or alleviate it [4]. Ice formation on the surface of heat exchanger fins leads to a drop in the heat exchanger efficacy and lowers the overall system performance due to an insulating effect of the ice layer. Moreover, the ice layer increases the pressure drop due to clogging or narrowing the air passages of the heat exchanger [1,5,6]. Despite the ongoing efforts there are no reliable methods to reduce or alleviate ice deposition problem and maintain the performance of a heat exchanger in a cold climate.

Generally, there are two general approaches to tackle this problem: active and passive ice control methods. The active ice control methods require heat generation or mechanical action to remove existing ice or prevent ice formation. Such methods include, for instance, bypass of the cold supply air, preheating of the cold supply air, preheating of the exhaust air and recirculation of the supply air for preheating [7]. All these active methods lead to a reduction of the overall efficiency [8]. On the other hand, passive methods do not require additional energy and address the surface characteristics of the heat exchanger fins. Generally, surface characteristics such as roughness and surface energy play a crucial role in ice formation [4,9]. Knowledge about ice formation process and its relation to the psychrometric parameters and surface characteristics could help designers, engineers, and manufacturers of heat exchangers to improve their overall performance.

Ice formation process on flat solid surfaces has been addressed in the vast amount of studies. Here, I would specifically mention modeling of ice formation process in [1,6,10,11]. The studies showed the importance of the psychrometric parameters such as air temperature, velocity, humidity, and surface temperature as well as the surface conditions such as surface temperature, contact angle, and roughness for the ice formation. The effects of surface chemistry and surface structure on ice nucleation and formation have

* Corresponding author. Tel.: +45 99407487.
E-mail address: lg@nano.aau.dk (L. Gurevich).

http://dx.doi.org/10.1016/j.apsusc.2015.06.201
0169-4332/

been addressed in [12,13]. In the present experimental paper, the effect of surface modification on incipient ice formation is investigated by considering the psychrometric parameters together with the different surface conditions.

According to Hayashi et al., 1977, the initial stage of ice formation can be divided into three sub-stages. (i) The so-called "crystal growth period", in which the ice crystals nucleate and grow away from the cold surface. At this stage, ice crystals are relatively far apart and have little interaction. (ii) The "frost layer growth," in which the crystals continue to grow and fuse together to form a layer. (iii) The "frost layer full growth period", in which the surface temperature of the ice layer reaches 0 °C resulting in an equilibrium between the condensed liquid water film and underlying ice layer, leading to an increase in ice layer density [14].

Ice nucleation on a solid surface (substrate) is controlled by the substrate temperature, roughness, and wettability, where the latter is commonly characterized by the contact angle of a water droplet on a solid substrate [10,15,16]. Specifically, it has been shown that a change in wettability has a significant effect on ice formation [17]. Wettability can be changed by surface treatment such as altering the surface roughness or surface chemistry [18]. For a droplet on a solid surface, according to the Young equation (Eq. (1)), its shape is determined by the interfacial tension (γ) between the phases (gas, liquid, and solid) in contact see, e.g., [19]. The contact angle θ for a water drop on an aluminum substrate is related to the surface tensions between the air, aluminum, and the liquid phases:

$$\cos\theta = \frac{\gamma_{\mathrm{Al,air}} - \gamma_{\mathrm{W,Al}}}{\gamma_{\mathrm{W,air}}}. \quad (1)$$

For such a droplet to form it is necessary to overcome the Gibbs energy barrier which is also a function of the interfacial energy (γ) and the contact area (A). Fletcher has shown that a change in the free energy upon heterogeneous nucleation of ice on a solid surface can be written as Eq. (2) [20].

$$\Delta G = V_{\mathrm{ice}}\Delta G_{\mathrm{V}} + A_{\mathrm{ice,air}}\gamma_{\mathrm{ice,air}} + A_{\mathrm{ice,Al}}(\gamma_{\mathrm{ice,Al}} - \gamma_{\mathrm{Al,air}}) \quad (2)$$

where V_{ice} is the volume of the formed nucleus of ice, ΔG_{V} is the Gibbs energy change between the vapor and the formed ice per unit volume. This Gibbs energy change depends on temperature and vapor pressure. Accordingly, $\gamma_{\mathrm{ice,air}}$ is the interfacial tension between the ice and air, $\gamma_{\mathrm{Al,air}}$ is the interfacial tension between the air and the substrate, and $\gamma_{\mathrm{ice,Al}}$ is the interfacial tension between ice and the substrate. $A_{\mathrm{ice,air}}$ and $A_{\mathrm{ice,Al}}$ are the contact areas between ice and air and ice and substrate, respectively.

The nucleation rate per unit surface area is related to the Gibbs energy and consequently the interfacial energy γ [11,21]. Equation (3) shows the nucleation rate for heterogeneous nucleation as proposed by Becker and Doring see, e.g., [22]:

$$I = I_0 \exp\left(-\frac{\Delta G_{\mathrm{c}}}{k_{\mathrm{B}}T_{\mathrm{S}}}\right), \quad (3)$$

where I is the nucleation rate, I_0 is the kinetic constant of desublimation per unit surface (1025 nucleation/cm^2 s), k_{B} is the Boltzmann constant and T_{S} is the surface temperature. Thus, changing the surface energy or the surface area (by, e.g., changing the surface roughness) affects the energy barrier for nucleation and hence the nucleation rate [23].

Therefore, adjusting the surface characteristics through surface modifications, changing the surface energy and roughness, can be employed to delay the onset of ice formation. It should be however noted that the effect of surface treatment on the ice nucleation and formation process is limited to the initial period of ice formation, since, only in the initial period there is a direct contact between humid air and the treated surface. As soon as the ice thickness reaches a certain value, ice formation will only be affected by environmental conditions [4,24,25].

With time, the density of the ice layer tends to increase due to the vapor diffusion through the porous ice structure. On the other hand, ice formation on the surface of the layer contributes to the thickness increase [3,8]. Both ice thickness and ice density strongly affect the performance of heat exchangers [4].

In the present study an aluminum alloy, the most common metal used for manufacturing of heat exchanger fins, is chosen for investigation. Ice thickness and density on differently modified aluminum samples were investigated as a function of both psychrometric parameters and the surface characteristics. Gaining knowledge regarding the effect of the surface modification on incipient ice formation on aluminum surfaces is essential for improving the design and efficacy of heat exchangers [4,26,27]

2. Methodology

2.1. Materials

An aluminum sheet (8011A, 0.25 mm thick), which is commonly used in the production of heat exchangers, was cut into test samples measuring 15 × 15 mm^2, which were subjected to different surface treatments and surface modifications. Four groups of samples were selected for ice formation tests. The first group consisted of bare aluminum samples; aluminum was used "as received" after degreasing in an ultrasonic bath. The second group contained aluminum samples with the surface functionalized by in situ ring-opening polymerization of glycidol resulting in the formation of a layer consisting of hyper-branched polyethylene glycol (PEG) as described in Ref. [28]. Briefly, the sample surface was first activated by hot sodium methoxide in anhydrous methanol at 60–70 °C for an hour. The activated samples were placed in clean glassware under nitrogen atmosphere. After glycidol addition the polymerization reaction was carried out at 118 °C for 1 h. The samples were washed in an ultrasonic bath, first in acetone for 2 min, followed by a 2 min ethanol wash.

The third group of samples was activated in the same way as the second one, followed by vapor deposition of perfluorooctylsilane carried out in an evacuated desiccator containing a solution of 250 μl 1H,1H,2H,2H-perfluorooctyltrichlorosilane in 750 μl of toluene at 110 °C for 4 h.

The fourth group contained samples with the surface coated first by a layer of PEG and further functionalized with PFOS, rendering the top layer hydrophobic [28]. It should be noted that the PEG–PFOS modified surfaces inherit the roughness of the underlying PEG layer, which is, due to the structure of the hyper-branched PEG, is higher than that of the bare aluminum. In this way both rough and smooth hydrophobic and hydrophilic surfaces were formed. Further details of surface modification and surface morphologies obtained have been described earlier [28].

2.2. Observation of ice formation

For the study of ice formation, a dedicated custom-designed chamber with optical access for real-time observation of ice formation was constructed. The chamber allowed control of the ice formation parameters, including airflow, air temperature and humidity, as well as the surface temperature of the sample. Fig. 1 shows a schematic picture of the test setup as it is described in the previous work [29]. The experiments were carried out in a clean room environment to ensure low concentration of airborne contaminants.

It should be noted that due to the random nucleation on the surface and the porous structure of ice, the ice layer is rather rough, which makes accurate measurements of the thickness problematic. Since the thickness of ice is a critical parameter affecting the

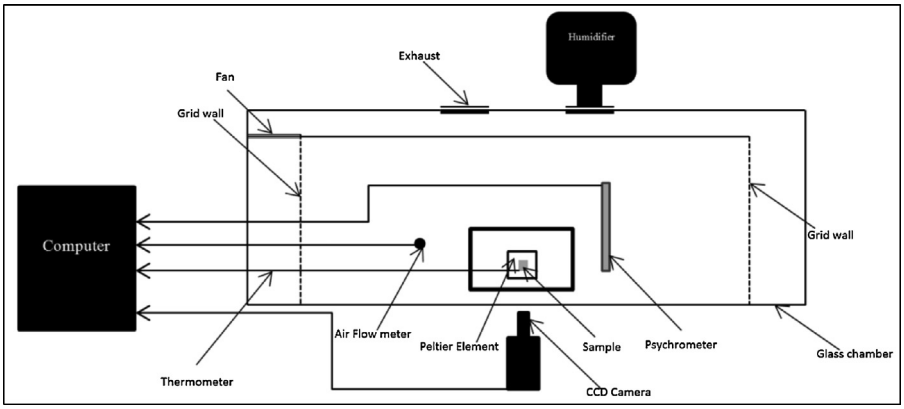

Fig. 1. Schematics of the measurement setup [29].

accuracy of all other measurements, several measuring techniques have been developed such as mechanical methods using a micrometric screw by Lee et al. [30] and Na and Webb [31]. However, these methods require an interruption of the experiment to perform the measurement. Other methods include laser and optical measurements. The laser method is not applicable in most cases due to high roughness of ice surfaces caused by the random accumulation of water vapor on the porous structure of ice [31,32]. The optical method involving image analysis provides an accurate way to measure the parameters of the ice surface independently of its morphology. Such a method has been used by Moallem et al. [33] and was also applied in the present work. In the presented data the reported ice thickness is the average of thickness measurements in at least 10 points for each sample using side images acquired with a fast CCD camera.

A monochrome CCD camera with the ability of capturing up to 60 images/s at a resolution of 1280 × 960 pixels (The Imaging Source, Germany) was used for monitoring the ice formation. The camera was equipped with a video lens (Edmund Optics, UK) with 68 mm WD, 3.61 mm horizontal field of view and a magnification of 1.33×. The recorded side images of the samples were analyzed and interpreted after each test and the thickness of the ice was calculated from the images. Each data point was an average of at least 10 thickness measurements at different points of a sample.

For temperature-controlled measurements, the test chamber was equipped with a K-type thermocouple attached to the surface of the sample holder. Readings were recorded with a temperature logger at a rate of 51 samples/min (Agilent GUI data logger). Image video capture and the surface temperature logger were started simultaneously to record the images and the temperature.

The relative humidity of the circulating air was adjusted with a cool mist ultrasonic humidifier (AIR-O-SWISS, Switzerland). The humidifier was operated with Milli-Q water to ensure the absence of mineral residues in the produced water mist. Temperature and humidity inside the chamber were measured by a humidity/temperature probe (Testo 400 Reference Meter&Logger, Testo Inc.) with an accuracy of ±1% RH and ±0.05 °C.

The mean air velocity was measured with a hotwire anemometer (DANTEC FLOWMASTER Precision Anemometer Type 54 N 60) positioned in a hole on the chamber roof (Fig. 1).

Prior to inserting a sample, the humidity and temperature in the chamber were allowed to settle to the desired parameters. The mean air velocity was kept constant at 0.58 m/s in all the measurements. Table 1 shows a typical set of experimental conditions. Every experimental run was repeated at least four times for each group of samples. Within each experiment, the uncertainties of ice thickness measurements, cold surface temperature and relative humidity were ±0.014 mm, ±0.2 °C, and ±2% RH, respectively.

Table 1
Typical experimental conditions. The uncertainties for inlet air temperature and velocities represent 95% confidence interval, ambient air temperature is given according to the clean room specifications.

Typical experimental conditions	
Inlet air temperature	17 ± 0.1 °C
Average inlet air velocity (95% confidence interval)	0.578 ± 0.007 m/s
Ambient air temperature in the clean room	24 ± 1 °C

2.3. Ice density measurements

Before the measurements, each sample was weighed on a digital balance placed next to the test chamber. To prevent ice formation between the cold plate and the sample, the cold plate was shortly heated immediately before placing the sample. After placing the sample on the cold plate, the cooling sequence was immediately initiated. At the end of each test, the samples were carefully removed and placed on a digital balance. The accumulated ice mass on top of the sample was determined as the difference between the current and initial mass of the sample.

The density of the ice formed on top of the sample was calculated as

$$\rho_{ice} = \frac{m_{ice}}{S \cdot H_{ice}} \quad (4)$$

where ρ_{ice} is the ice density, S is the sample area, H_{ice} is the measured height of the ice layer, and m_{ice} is the mass of the ice.

2.4. Pattern of water droplet on top of the samples

The patterns of water droplets on top of different surfaces were acquired using STEMI 2000-C ZE 55 Microscope (Carl Zeiss, Germany) with 50× magnification. The microscope was equipped with AxioCam ERc 5s 5 megapixels camera (Carl Zeiss, Germany) and placed in the clean room. The samples were first dried and then quickly cooled down to −10 °C in order to form ice on the surface. Then the cooling was stopped and the process of de-icing was observed with the microscope. The observed patterns of water droplets are shown in Fig. 2. To visualize and quantify the droplet distributions, the original microscope images were converted to black and white using Matlab 2013 and the obtained coverage was calculated by counting black and white pixels.

Table 2
RMS roughness and contact angles for the samples with different surface modifications. The data are shown at a 95% confidence level [28].

Type of sample	RMS roughness (nm)	Contact angle (degree)
Bare aluminum	84 ± 16	78.1° ± 0.7°
Aluminum with PEG coating	98 ± 17	36.9° ± 0.6°
Aluminum with PEG–PFOS coating	85 ± 16	116.1° ± 1.0°
Aluminum with PFOS coating	79 ± 16	123.9° ± 1.4°

3. Results and discussions

The four groups of surface-modified aluminum alloy samples had different surface characteristics such as hydrophobicity, roughness, and contact angle. Table 2 shows RMS roughness and contact angles for the samples of each group according to our previous work [28].

The relation between the surface roughness and the contact angle has been discussed in great detail in our previous work [28]. The present work focuses on the relation between the above mentioned factors and initial ice formation.

It is known (see, e.g., [11]) that the energy barrier for condensation is lower than that for desublimation, hence favoring ice nucleation through the condensation route (i.e. via an intermediate liquid phase). From this perspective, the distribution of water droplets observed upon melting of the incipient ice layer can provide clues about different behavior of differently functionalized surfaces. Moreover it provides important information about uniformity of the wetting properties of the studied surfaces. The patterns of condensed water droplets on the aluminum samples with different surface characteristics are shown in Fig. 2. Although, the size distribution of the droplets formed on the samples is generally not uniform and reflects the heterogeneous nature of nucleation it clearly depends on the functionalization procedure [34]. For instance, hydrophobic substrates (groups 3 and 4) exhibit lower surface coverage, smaller size, and more uniformly distributed droplets. This also correlates with a lower ice growth rate observed for hydrophobic surfaces [35], see also Figs. 3 and 4.

As can be seen in Fig. 2, the area of water–substrate interface is smaller for hydrophobic samples. This leads to reduced heat transfer from the cold surface to the droplets and, as a result, longer freezing time and slower growth kinetics. Moreover, hydrophilic surfaces have a lower energy barrier for nucleation as compared to hydrophobic surfaces, hence leading to a higher nucleation rate of ice [36]. This is in line with our observations presented in Figs. 3 and 4. The rates of ice growth and therefore the ice thickness on the surface of the hydrophilic samples (contact angles of 37° and 24°) are consistently higher than those for the hydrophobic samples at all temperatures investigated (−6, −8, and −10 °C) as shown in Fig. 5. Similar behaviors of the ice thickness on the substrate contact angle have been obtained, e.g., in [37,38].

The wettability characteristics of the hydrophilic surfaces lead to a higher nucleation rate and hence a higher density of nucleation centers during the early stages of ice formation. Therefore, during the early stages of ice formation, both the rate of ice growth and the thickness of the frost formed are higher on the hydrophilic surfaces (bare samples and samples with PEG layer) as compared to the hydrophobic ones (PFOS and PEG–PFOS modified samples), in particular, for lower supercooling.

As can be seen in Figs. 3–5, although the general tendency is that a lower contact angle corresponds to a thicker frost layer (cf. Table 2), the bare aluminum sample falls off the general trend. These results are in line with the observation by Shin et al. [4] and Seki

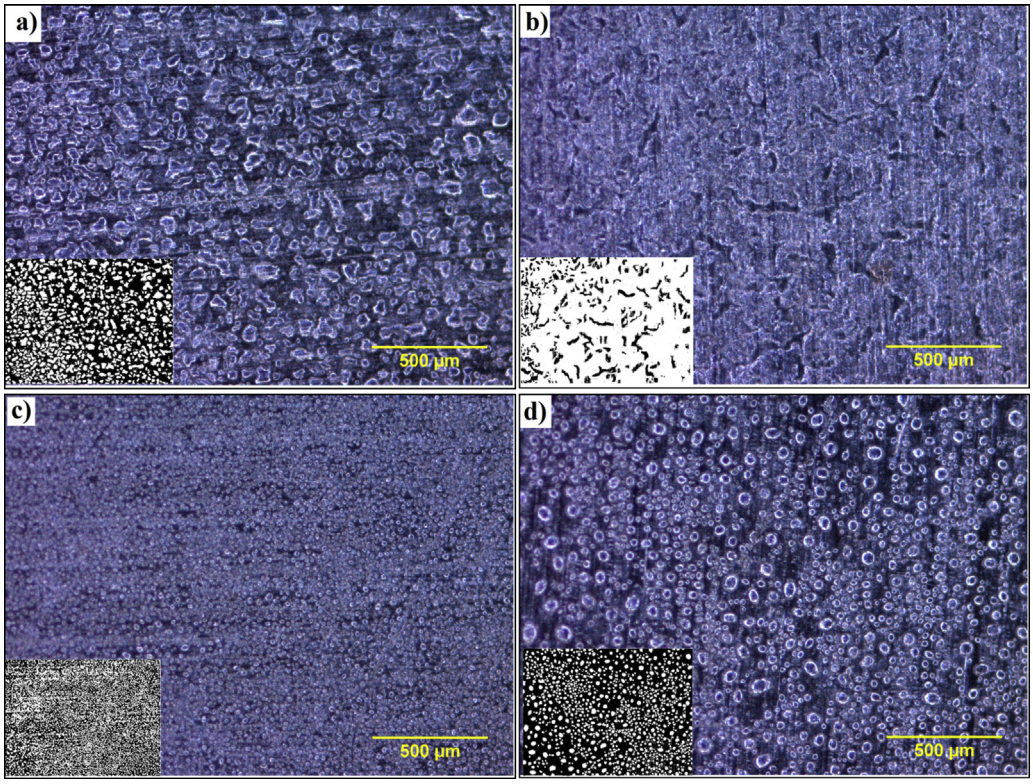

Fig. 2. Pattern of water droplets observed on aluminum samples with different surface modifications after melting the ice formed during one minute of exposure to ambient air of 43% RH at surface temperature −10 °C: (a) bare aluminum (73% ± 4% coverage), (b) PEG-modified aluminum (86% ± 5% coverage), (c) PEG–PFOS-modified aluminum (76% ± 7 coverage), and (d) PFOS-modified aluminum (73% ± 4 coverage). The insets show binary images obtained using Matlab 2013. Black represents the aluminum surface and white is the droplets pattern. The coverage was calculated by counting black and white pixels.

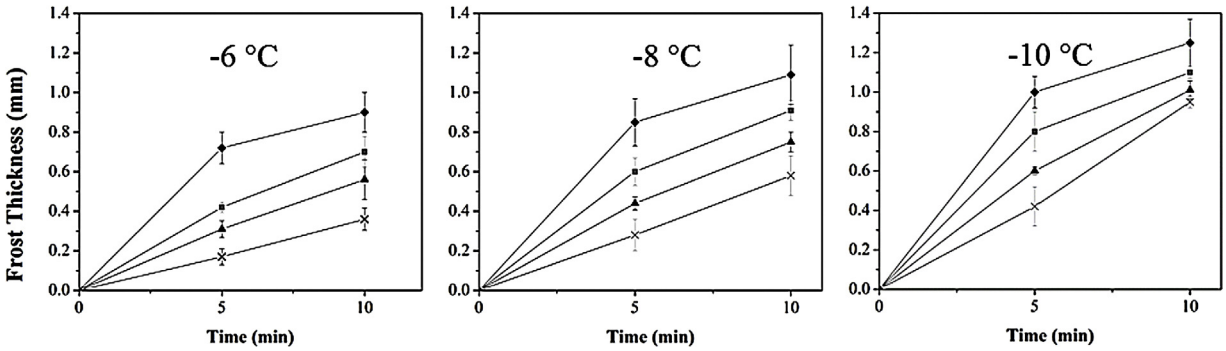

Fig. 3. Growth rate of ice on aluminum samples with different surface treatment at surface temperature of at surface temperature of −6 °C, −8 °C, and −10 °C: ♦—bare, ■—PEG, ▲—PEG-PFOS, and ×—PFOS-modified aluminum. Error bars show 95% confidence interval. The air flow in the chamber had 100% RH at 17 °C.

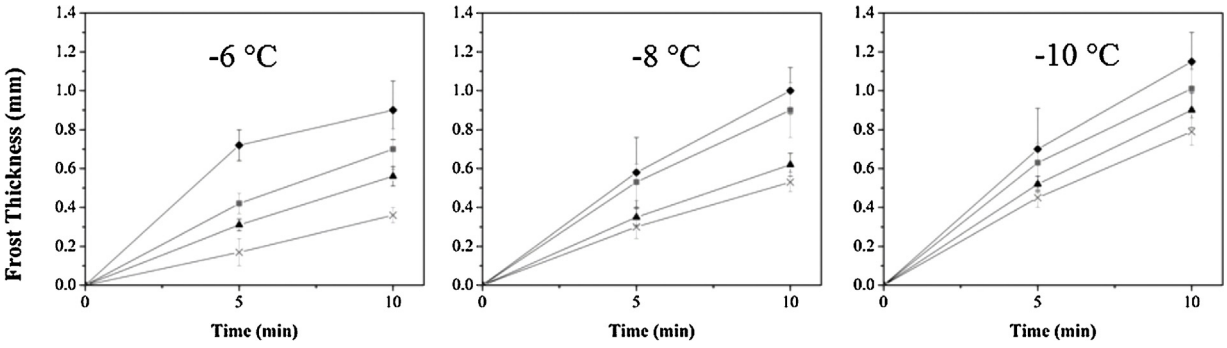

Fig. 4. Growth rate of ice on aluminum samples with different surface treatment at surface temperature of −6 °C, −8 °C, and −10 °C: ♦—bare, ■—PEG, ▲—PEG–PFOS, and ×—PFOS-modified aluminum. Error bars show 95% confidence interval. The air flow in the chamber had 65% RH at 17 °C.

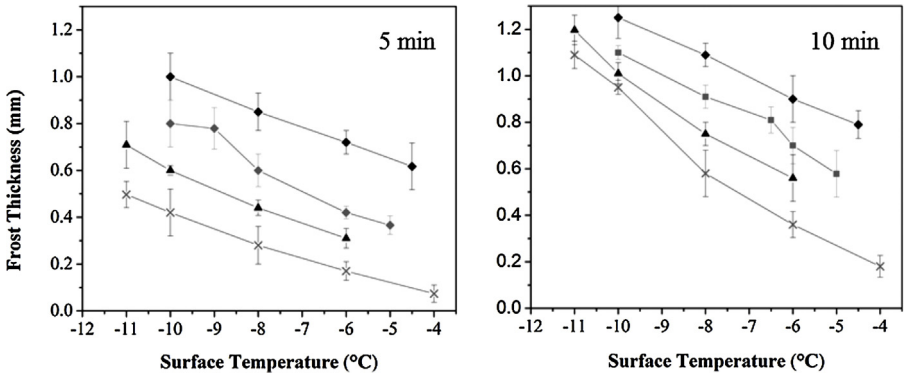

Fig. 5. Frost thickness on aluminum samples with different surface modifications after 5 and 10 min exposure to air of 100% RH at 17 °C plotted as a function of the cold surface temperature. ♦—bare, ■—PEG, ▲—PEG–PFOS, and ×—PFOS-modified aluminum. Error bars show 95% confidence interval.

et al. [3]. To understand these seemingly contradictory results we need to analyze these data in combination with the ice morphology and the distribution of the nucleation centers on the metal surface.

The ice density obtained from the measurements of ice thickness and mass according to Eq. (4) is shown in Fig. 6. As can be seen, the general tendency (except bare aluminum samples) is that the samples with a lower contact angle have a lower ice density. There is a reverse relation between the ice density and the ice thickness (cf. Figs. 5 and 6). The samples with a thicker ice layer exhibit a lower density and vice versa, so the deposited mass is roughly the same for all the samples and grows in time in line with the results of Brian et al. and Shin et al. [4,39]. Thus it may be concluded that the mass transfer coefficient is not a function of contact angle, which is also in line with the finding of Shin et al. [4].

As can be seen in Fig. 6, the ice density on hydrophobic surfaces is generally higher than that on hydrophilic samples, which is in line with earlier observations by Seki et al. [37] and Hoke et al. [40]. Moreover, here again, bare aluminum surface appears to be special and exhibits lower density than hydrophilically modified surfaces with even lower wetting angles, again in line with observation of the above references.

Fig. 7 shows the time evolution of the ice layer morphology on substrates with different hydrophobicity. Again, it can be seen that the morphology of ice, formed at the same psychrometric parameters on bare aluminum is rather different from both hydrophobically and hydrophilically modified samples. While the later exhibit grass-like ice structure, according to the classification by Lee et al. [25], the ice on untreated aluminum surfaces has feather-like structure which was maintained during the whole period of the experiment and at all the psychrometric conditions used in this study. Presence of a feather-like ice layer structure explains the lower density of ice layer observed on bare aluminum.

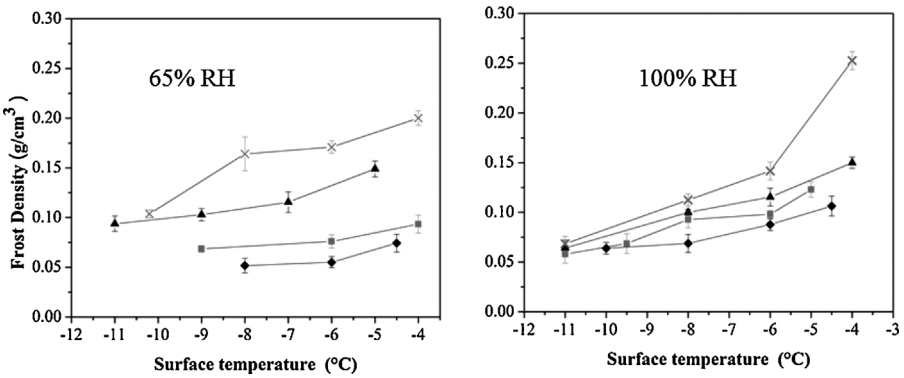

Fig. 6. Density of ice on top of different aluminum samples plotted as a function of the surface temperature for different surface treatment at 65% RH and 100% RH: ♦—bare, ■—PEG, ▲—PEG-PFOS, and ×—PFOS-modified aluminum. Error bars show 95% confidence interval.

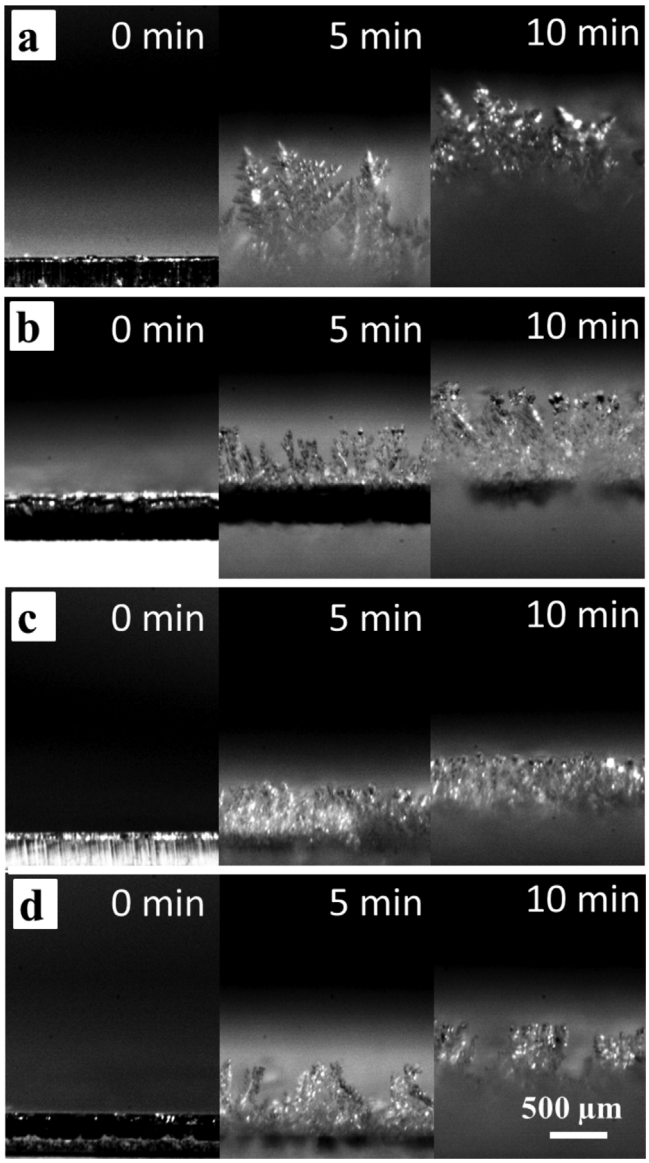

Fig. 7. Side view of the ice morphology formed on differently treated surfaces at 0, 5, and 10 min from the beginning of the experiment at surface temperature of −8 °C: (a) bare aluminum, (b) PEG-modified aluminum, (c) PFOS-modified aluminum, and (d) PEG–PFOS-modified aluminum. Air humidity was 100% RH at 17 °C.

It is known (see, e.g., [41]) that frost formation on a cold plate typically proceeds through the nucleation of liquid droplets, which subsequently solidify [41]. Afterwards an ice tip starts to grow from the center of each droplet, forming an ice column, which subsequently, if space allows, branches. Based on the observed ice crystal morphology we can conclude that bare aluminum is characterized by a significantly larger distance between the tip-growth centers, as compared to both hydrophilically and hydrophobically modified aluminum surfaces. This observation is also corroborated by the observed distribution of droplets on the surface (Fig. 2). We attribute it to significant non-uniformity of bare aluminum surface. Aluminum alloys of the 8000 family are ternary (or more component) alloys [42]. Specifically, 8011 is mainly composed of Al, Fe, and Si. This leads to formation of various intermetallic inclusions (e.g. $FeAl_x$, $FeAl_xSi_y$, etc.), which actually determine the mechanical properties of the material and make it attractive for industrial applications. As a result, the surface structure of these alloys is heterogeneous on the microscopic scale, where the grains of aluminum and different intermetallic compounds are exposed on the surface (see, e.g., [43]). On such materials, a "macroscopic" wetting angle does not provide a complete picture, but only corresponds to averaged (in the Cassie–Baxter sense) surface properties. In reality, such a surface possesses a wide range of nucleation centers of different energy, where some water droplets can start nucleating already at a very small supercooling due to the presence of some high-energy nucleation spots on the surface. On the other hand, if a continuous layer of a surface modifier is present, the native aluminum surface is not accessible to water and the aqueous environment is presented with a uniform surface energy both macroscopically and microscopically. As a result, large amount of nucleation centers are activated at a certain degree of supercooling leading to formation of a denser grass-like structure. Moreover, the surfaces with a higher hydrophobicity produce denser ice morphologies, in line with our density measurements shown in Fig. 6.

4. Conclusion

In the present study, the incipient ice formation was investigated on aluminum surfaces with different chemical modifications: bare surfaces, surfaces with in-situ grown PEG layer, surfaces with a monolayer of PFOS, and surfaces with PFOS-modified PEG layer. Such a choice of treatments provided wide range of contact angles on the same substrate material which was further combined with two different degrees of nano-roughness.

We have found that at the initial stage of ice formation, flat hydrophobic surfaces exhibit the lowest ice formation rate, the smallest thickness and the highest ice density. This translates into lowest thermal resistance as well as less blocking in the air passage

of air to air heat exchanger. It means lowest impact on the air flow capacity of the exchanger, hence making it the treatment of choice for air-to-air heat exchangers without a mechanical ice removal. We should also emphasize here that this type of treatment is carried out in a gas phase making it suitable for the objects of complex geometry.

In line with literature data, we observed faster ice formation and lower ice density on untreated aluminum surfaces, both in comparison with more hydrophobic and more hydrophilic surfaces. Based on the whole set of the obtained data, which also included ice morphology and droplet distribution upon ice melting, we attribute this phenomenon to a highly heterogeneous character of bare aluminum surface, leading to a broad distribution of surface energies on microscopic scale. This leads to nucleation of widely separated water droplets/ice crystals on high-energy nucleation centers upon even minor cooling below the freezing point and formation of low-density feather-like ice structures. On the other hand, both hydrophobic and hydrophilic surface modifications conceal the surface heterogeneity. As a result, a narrower energy distribution of the nucleation centers on treated surfaces leads to instantaneous formation of a large number of embryos resulting in a denser ice structure.

Acknowledgments

We greatly acknowledge the support of EXHAUSTO A/S which contributed with components and materials and the financial support by COWIfonden and Greenland government.

References

[1] H. Chen, L. Thomas, R.W. Besant, Fan supplied heat exchanger fin performance under frosting conditions, Int. J. Refrig. 26 (2003) 140–149.
[2] R.W. Besant, K.S. Rezkallah, A mathematicalmodel for predicting the densification and growth of frost on a flat plate, Int. J. Heat Mass Transf. 36 (1992) 353–363.
[3] N. Seki, S. Fukusako, K. Matsuo, S. Uemura, An analysis of incipient frost formation, Wärme Stoffübertrag. 19 (1985) 9–18.
[4] J. Shin, A.V. Tikhonov, C. Kim, Experimental study on frost structure on surfaces with different hydrophilicity: Density and thermal conductivity, J. Heat Transf. 125 (2003) 84.
[5] S. Jhee, K. Lee, W. Kim, Effect of surface treatments on the frosting/defrosting behavior of a fin-tube heat exchanger, Int. J. Refrig. 25 (2002) 1047–1053.
[6] K.S. Lee, W.S. Kim, T.H. Lee, A one-dimensional model for frost formation on a cold flat surface, Int. J. Heat Mass Transf. 40 (1997) 4359–4365.
[7] R. Ahmed, J. Appelhoff, Frost-protection measures in energy recuperation with multiple counterflow heat exchangers, Rehva 05 (2013) 37–40.
[8] Y.B. Lee, S.T. Ro, Analysis of the frost growth on a flat plate by simple models of saturation and supersaturation, Exp. Therm. Fluid Sci. 29 (2005) 685–696.
[9] K.K. Varanasi, T. Deng, J.D. Smith, M. Hsu, N. Bhate, Frost formation and ice adhesion on superhydrophobic surfaces, Appl. Phys. Lett. 97 (2010) 234102.
[10] C.J.L. Hermes, R.O. Piucco, J.R. Barbosa, C. Melo, A study of frost growth and densification on flat surfaces, Exp. Therm. Fluid Sci. 33 (2009) 371–379.
[11] B. Na, R.L. Webb, A fundamental understanding of factors affecting frost nucleation, Int. J. Heat Mass Transf. 46 (2003) 3797–3808.
[12] G. Heydari, E. Thormann, M. Järn, E. Tyrode, P. Claesson, Hydrophobic surfaces topography effects on wetting by supercooled water and freezing delay, J. Phys. Chem. C 117 (2013) 21752–21762.
[13] H. Wang, L. Tang, X. Wu, W. Dai, Y. Qiu, Fabrication and anti-frosting performance of super hydrophobic coating based on modified nano-sized calcium carbonate and ordinary polyacrylate, Appl. Surf. Sci. 253 (2007) 8818–8824.
[14] Y. Hayashi, A. Aoki, S. Adashi, K. Hori, Study of frost properties correlating with frost formation types, ASME J. Heat Transf. 99 (1977) 239–245.
[15] C.J.L. Hermes, An analytical solution to the problem of frost growth and densification on flat surfaces, Int. J. Heat Mass Transf. 55 (2012) 7346–7351.
[16] R. Tadmor, P. Bahadur, A. Leh, H.E. N'guessan, R. Jaini, L. Dang, Measurement of lateral adhesion forces at the interface between a liquid drop and a substrate, Phys. Rev. Lett. 103 (2009) 266101.
[17] M. He, J. Wang, H. Li, X. Jin, J. Wang, B. Liu, et al., Super-hydrophobic film retards frost formation, Soft Matter 6 (2010) 2396.
[18] M.K. Kwak, H.-E. Jeong, T. Kim, H. Yoon, K.Y. Suh, Bio-inspired slanted polymer nanohairs for anisotropic wetting and directional dry adhesion, Soft Matter 6 (2010) 1849.
[19] H. Butt, K. Graf, M. Kappl, Physics and Chemistry of Interfaces, Wiley-VCH GmbH & Co. KGaA, Weinheim, 2003.
[20] N.H. Fletcher, The Chemical Physics of Ice, 1st ed., Cambridge University Press, Cambridge, 1970.
[21] R.O. Piucco, C.J.L. Hermes, C. Melo, J.R. Barbosa, A study of frost nucleation on flat surfaces, Exp. Therm. Fluid Sci. 32 (2008) 1710–1715.
[22] A.P.G.A.W. Adamson, Physical Chemistry of Surfaces, 6th ed., John Wiley and Sons, New York, 1997.
[23] A.R. Balkenende, H.J.A.P. van de Boogaard, M. Scholten, N.P. Willard, Evaluation of different approaches to assess the surface tension of low-energy solids by means of contact angle measurements, Langmuir 14 (1998) 5907–5912.
[24] K. Kim, K.-S. Lee, Frosting and defrosting characteristics of a fin according to surface contact angle, Int. J. Heat Mass Transf. 54 (2011) 2758–2764.
[25] Z. Liu, X. Zhang, H. Wang, S. Meng, S. Cheng, Influences of surface hydrophilicity on frost formation on a vertical cold plate under natural convection conditions, Exp. Therm. Fluid Sci. 31 (2007) 789–794.
[26] Y. Tao, Y. Mao, R. Besant, Frost growth characteristics on heat exchanger surfaces measurement and simulation studies, ASME Heat Transf. HTD-Vol. 2 (1994) 29–38.
[27] H. Lee, J. Shin, S. Ha, B. Choi, J. Lee, Frost formation on a plate with different surface hydrophilicity, Int. J. Heat Mass Transf. 47 (2004) 4881–4893.
[28] M. Rahimi, P. Fojan, L. Gurevich, A. Afshari, Effects of aluminium surface morphology and chemical modification on wettability, Appl. Surf. Sci. 296 (2014) 124–132.
[29] M. Rahimi, P. Fojan, L. Gurevich, A. Afshari, Aluminium alloy 8011: Surface characteristics, Appl. Mech. Mater. 719–720 (2015) 29–37.
[30] K.S. Lee, S. Jhee, D.-K. Yang, Prediction of the frost formation on a cold flat surface, Int. J. Heat Mass Transf. 46 (2003) 3789–3796.
[31] B. Na, R.L. Webb, New model for frost growth rate, Int. J. Heat Mass Transf. 47 (2004) 925–936.
[32] I. Tokura, H. Saito, K. Kishinami, Study on properties and growth rate of frost layers on cold surface, Trans. ASME, J. Heat Transf. 105 (1983) 895–901.
[33] E. Moallem, L. Cremaschi, D.E. Fisher, S. Padhmanabhan, Experimental measurements of the surface coating and water retention effects on frosting performance of microchannel heat exchangers for heat pump systems, Exp. Therm. Fluid Sci. 39 (2012) 176–188.
[34] K.R. Jensen, P. Fojan, R.L. Jensen, L. Gurevich, Water condensation: A multiscale phenomenon, J. Nanosci. Nanotechnol. 14 (2014) 1859–1871.
[35] R.N. Leach, F. Stevens, S.C. Langford, J.T. Dickinson, Dropwise condensation: experiments and simulations of nucleation and growth of water drops in a cooling system, Langmuir 22 (2006) 8864–8872.
[36] K.K. Varanasi, M. Hsu, N. Bhate, W. Yang, T. Deng, Spatial control in the heterogeneous nucleation of water, Appl. Phys. Lett. 95 (2009) 094101.
[37] N. Seki, S. Fukisako, K. Matsuo, S. Uemura, Incipient phenomena of frost formation, Bull. JSME. 27 (1984) 2476–2482.
[38] J.M. Dyer, B.D. Storey, J.L. Hoke, A.M. Jacobi, J.G. Georgiadis, An experimental investigation of the effect of hydrophobicity on the rate of frost growth in laminar channel flows, ASHRAE Trans. 106 (2000) 143–151.
[39] P.L.T. Brian, R.C. Reid, Y.T. Shah, Frost deposition on cold surfaces, Ind. Eng. Chem. Fundam. 9 (1970) 375–380.
[40] J.L. Hoke, J.G. Georgiadis, A.M. Jacobi, H. Phoenix, The Interaction Between the Substrate and Frost Layer Through Condensate Distribution, General Motors Corporation, 2000, pp. 61801.
[41] J. Iragorry, Y.-X. Tao, S. Jia, A critical review of properties and models for frost formation analysis, HVAC&R Res. 10 (4) (2004) 393–420.
[42] N.J. Luiggi, Metall. Mater. Trans. A 29A (1998) 2669–2677.
[43] A. Korchef, A. Kahoul, Int. J. Corros. 2013 (2013) 983261.

3.1.5 SUMMARY OF '' EFFECT OF ALUMINUM SUBSTRATE SURFACE MODIFICATION ON WETTABILITY AND FREEZING DELAY OF WATER DROPLET AT SUBZERO TEMPERATURES''

In this study, we have investigated the freezing delay of a water droplet on precooled substrates of an aluminum alloy which commonly used for heat-exchanger fins. The surfaces of the substrates were modified to obtain surfaces with different hydrophilicity/hydrophobicity and different surface chemistry but without significantly modifying the surface topography. The freezing delays and water contact angles were measured as a function of the substrate temperature and the results were compared to the predictions of the heterogeneous ice nucleation theory. Although the trends for each sample followed the trend of this theory, the differences in the extents of freezing delays were in apparent disagreement with the predictions. Concretely, a slightly hydrophilic substrate modified by (3-aminopropyl) triethoxysilane (APTES) showed longer freezing delays than both more hydrophilic and more hydrophobic substrates. We suggest that this is because this particular surface chemistry prevents ice formation at the interface of the substrate, prior to the deposition of the water droplet. Based on our results, we suggest that when placing a water droplet on a precooled substrate not only wettability and topography but also the concrete surface chemistry play a significant role in the kinetics of the ice formation process.

Finally, after studying different surface modifications (chemically and mechanically) and their effect on ice formation, structure and wettability, in this paper the effect of chemical surface modifications on ice nucleation and freezing delay is investigated. Moreover, to the knowledge of authors for the first time, the effect of substrate temperatures on the wettability and freezing delay of a water droplet is studied in a wide range of temperatures, from room temperature to subzero temperature. Furthermore, the investigations are done on top of aluminum with different surface characteristics, and the results are illustrated.

The investigation of freezing delay is conducted on top of the four sample groups of bare aluminum alloy group, aluminium with Perfluorooctylsilane (PFOS) coating group, aluminium with organosilane of (3-aminopropyl) triethoxy silane (APTES) coating group and water plasma tretamed aluminum group.

As illustrated in Figure 3-10, the bare aluminum alloy sample group exhibits a continuous decrease in the freezing delay with the decrease of the substrate temperature. The water plasma treated sample group, APTES and PFOS groups show a sudden decrease in the temperature interval between -5°C and -10°C and a slow decrease in freezing delay by the further reduction of the temperature to -20°C.

As Figure 3-10 shows, the magnitude of the delay and their relative changes with the changes in temperature are significantly different for the four groups of samples; for the water-vapor plasma treated and the PFOS modified surfaces, the freezing delays drop to below 10 s at temperatures below -10°C, while the freezing delay stays above 100 s down to -25 °C for the APTES modified surface. In order to better understand the difference in the freezing delay of the groups, the wettability of the surfaces is studied according to the measurement of contact angle and the change in substrate temperature in the interval between +20°C and -25°C.

As the results of contact angle measurement illustrate in Figure 3-11, the contact angle on the bare aluminum and the APTES coated substrate decrease slightly with decreasing temperatures in the interval between +20°C and -25°C. This observation can be explained by the temperature dependency of the surface tension of water.

On the other hand, the contact angle measurement of the water plasma treated sample groups and PFOS group revealed an abrupt increase in the contact angle within the same temperature range while the freezing delays also change dramatically. This observation cannot be explained by the temperature dependency of the surface tension of water. This observation can be argued and explained by sublimation and growth of ice on the cold substrates of the water plasma treated sample groups and PFOS group before the water droplet is placed on the substrate.

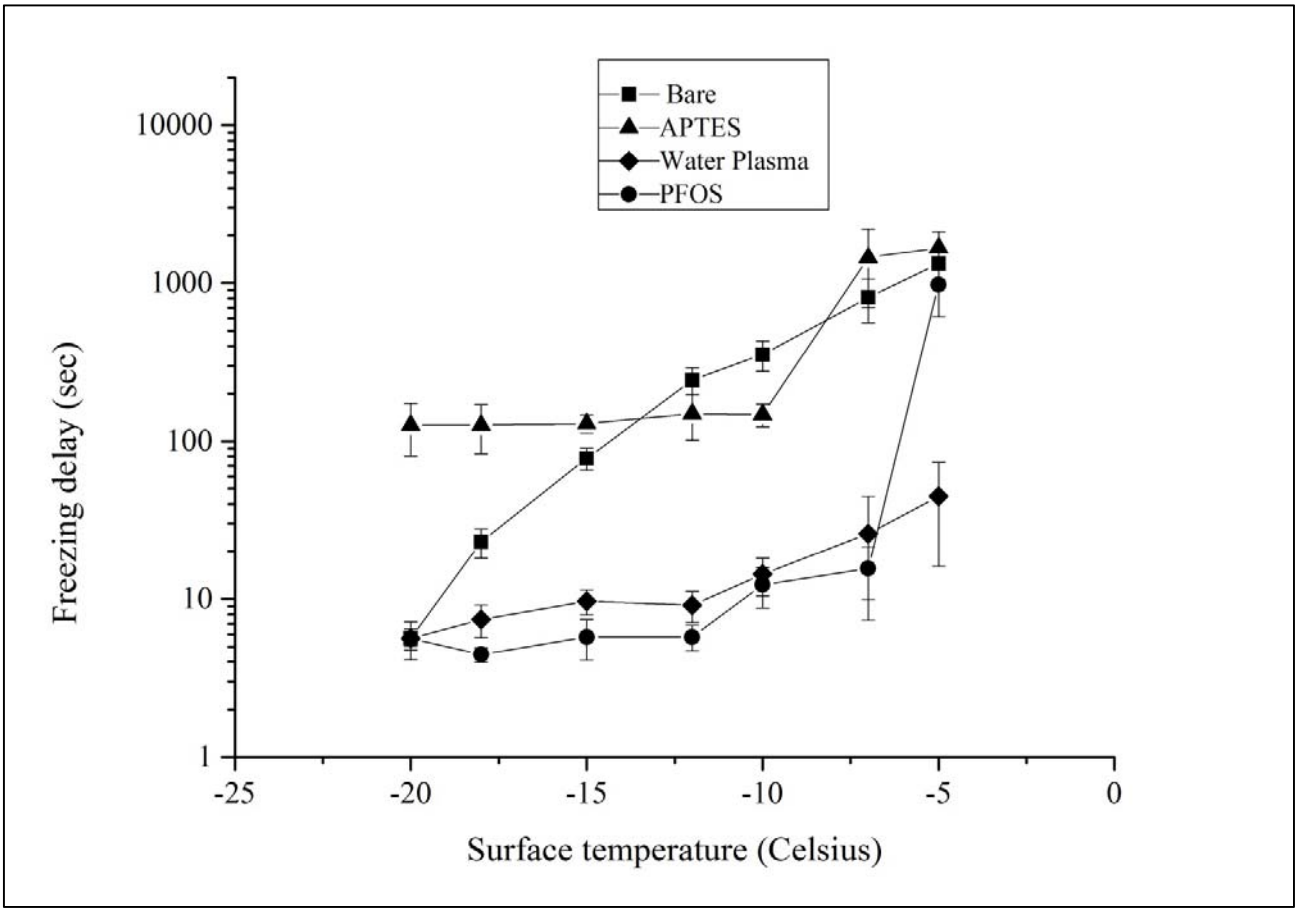

Figure 3-10 Freezing delays of water droplet placed on substrates precooled to temperatures ranging from -5 C° to the -20 C°. The error bars represent a 95% confidence interval.

In order to further investigate the abrupt behavior of freezing delay and wettability of sample groups the observed results are compared to the expectations from nucleation theory and the possible deviations from this theory are discussed.

As Figure 3-12 shows, the energy barrier for the homogeneous nucleation of an ice embryo and for the heterogeneous nucleation on the four different substrates as a function of temperature rapidly decreases when the temperature is decreased from 0°C to −10°C. The reduction in energy barrier of nucleation becomes less noticeable when the temperature is further decreased to -20°C. This observation is thus in qualitative agreement with our results of the modified samples, which show a fast decrease in the freezing delays in the temperature interval between 0°C and −10°C, after which the change in freezing delays becomes moderate.

On the other hand, some of the predictions of high energy barrier for PFOS as compared to APTES and water plasma treated sample groups are in apparent disagreement with our experimental results which showed a longer freezing delay on the APTES-modified samples and shorter and very similar freezing delays on the PFOS- and the water-vapor plasma- modified.

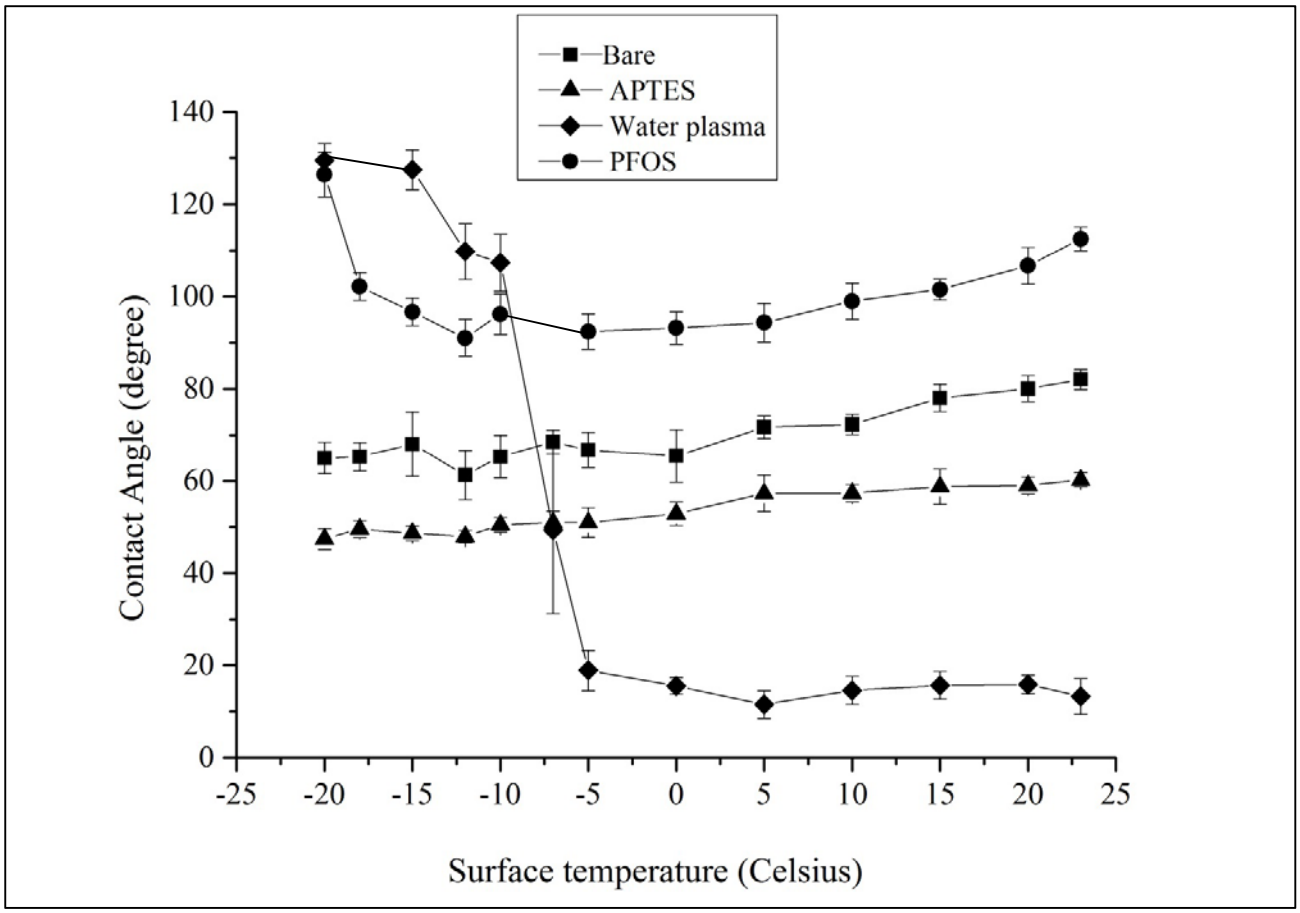

Figure 3-11 Apparent contact angles on the four groups of samples measured in the temperature range from 23 to -20 C°. The error bars represent a 95% confidence interval.

This apparent disagreement with our experimental investigation of the wetting properties of sample groups and their changes in temperature may be explained by the results illustrated in Figure 3-11. As both hydrophilic and hydrophobic sample groups exhibit a sudden increase in the contact angle around −5°C to −10°C, we may conclude that the ice starts to form around this temperature, and the droplet is placed on ice structures instead of directly on the substrate surface.

This occurs due to the fact that according to the previous observations, the water contact angle and its contact angle on ice was increased by decreasing the water droplet temperature [69,92].

According to this discussion, the freezing delay measurement is not representative of the energy barrier of the PFOS and water plasma treated surface.

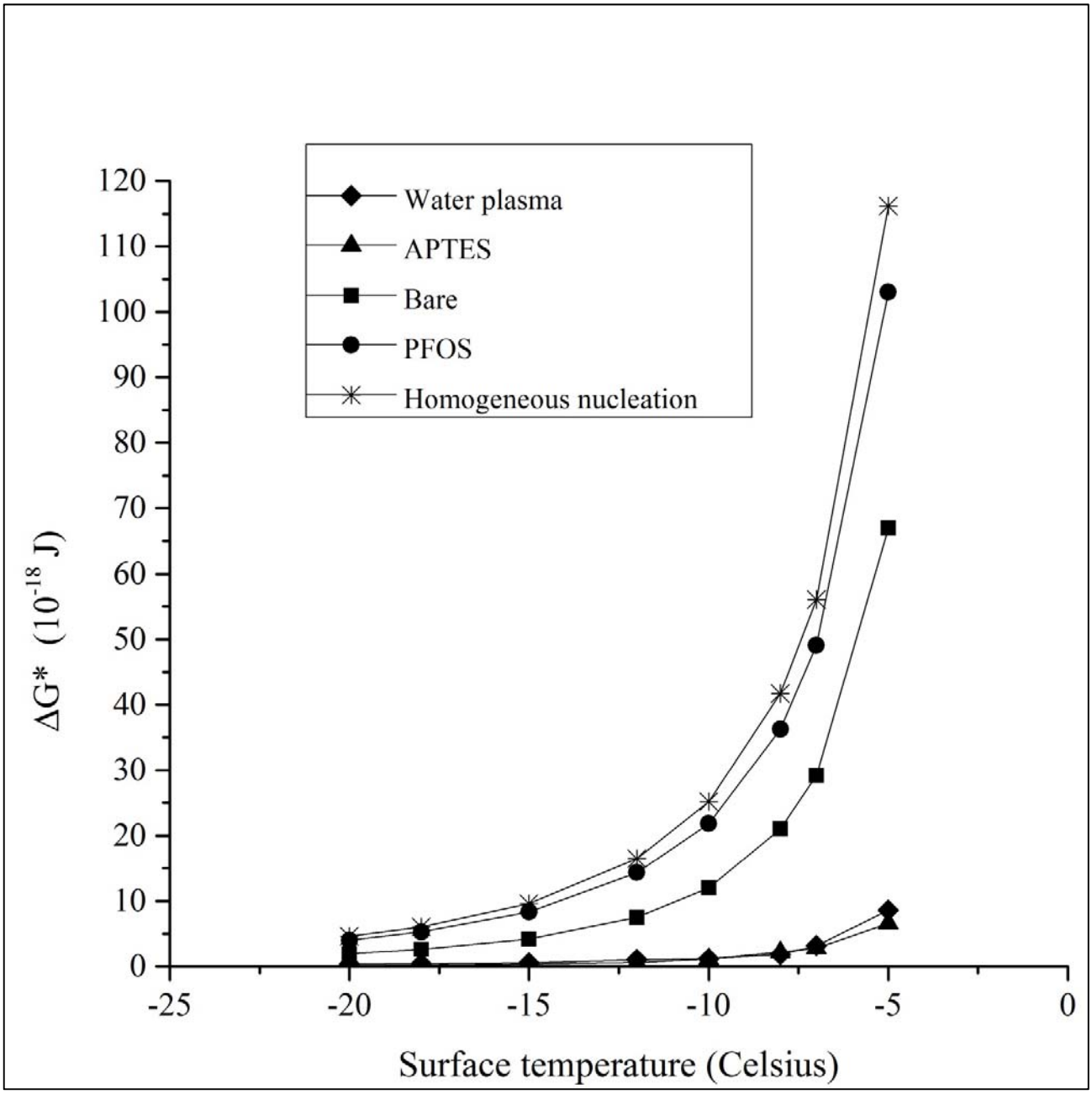

Figure 3-12 The magnitude of energy barrier for the homogeneous nucleation of an ice embryo and for heterogeneous nucleation on the four different substrates as a function of temperature.

The long freezing delay on the APTES surface may be explained by the presence of amino groups which may prevent the formation of an ice layer and ultimately lead to longer freezing delays. This is because at atmospheric conditions, the pH of water will normally be around 5.6 due to dissolution of CO_2 and the pKa-value of surface-bound amino groups has been reported to be around 1. Therefore, in the presence of liquid water the amino groups on the APTES surface are expected to be in acidic form, and the surface will thus have a high surface charge density.

Thus, when condensation occurs on the surface due to the presence of high local ion concentration, the freezing point significantly will suppress proximity to the substrate interface.

At the end of the freezing process, the droplet became fully opaque and a small-sharp pointed protrusion appeared as shown in Figure 3-13. This phenomenon is due to the volume expansion coursed by the freezing transition where a droplet deformation and a protrusion formation take place. This observation are in line with previous reported observations [19,32,93].

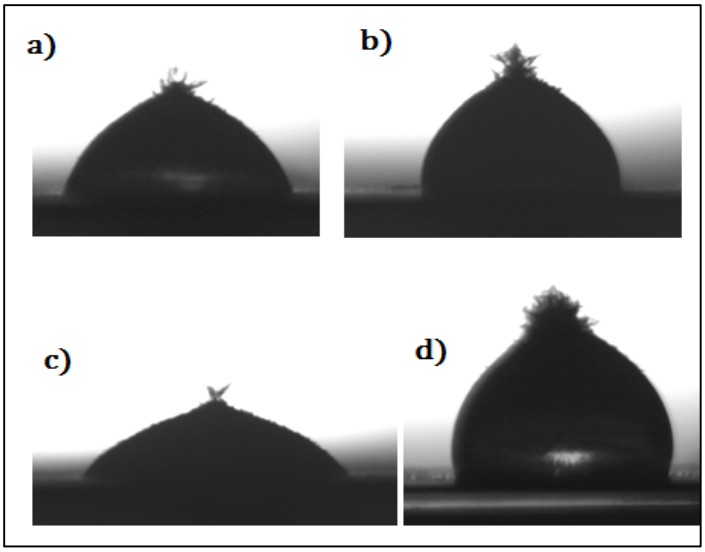

Figure 3-13 Sharp-pointed protrusion on top of the water droplet after 5 minutes from the start of freezing at -20°C for a) Bare sample b) PFOS sample , c) APTES sample and d) water-plasma sample

3.1.5.1 Actual paper V

Effect of Aluminum Substrate Surface Modification on Wettability and Freezing Delay of Water Droplet at Subzero Temperatures

M. Rahimi, A. Afshari, E, Thormann.

ACS applied materials & interfaces Vols, 8(17) (2016) pp 11147–11153

ACS APPLIED MATERIALS & INTERFACES

Research Article

www.acsami.org

Effect of Aluminum Substrate Surface Modification on Wettability and Freezing Delay of Water Droplet at Subzero Temperatures

Maral Rahimi,*[,†] Alireza Afshari,[†] and Esben Thormann[‡]

[†]Department of Energy and Environment, Danish Building Research Institute, Aalborg University, A.C. Meyers Vænge 15, 2450 København SV, Denmark

[‡]Department of Chemistry,Technical University of Denmark, Kemitorvet 207, DK-2800 Kgs Lyngby, Denmark

Supporting Information

ABSTRACT: In this study, we have investigated the freezing delay of a water droplet on precooled substrates of an aluminum alloy that is commonly used for heat-exchanger fins. The surfaces of the substrates were modified to obtain surfaces with different hydrophilicity/hydrophobicity and different surface chemistry but without significantly modifying the surface topography. The freezing delays and water contact angles were measured as a function of the substrate temperature and the results were compared to the predictions of the heterogeneous ice nucleation theory. Although the trends for each sample followed the trend in this theory, the differences in the extents of freezing delays were in apparent disagreement with the predictions. Concretely, a slightly hydrophilic substrate modified by (3-aminopropyl) triethoxysilane (APTES) showed longer freezing delays than both more hydrophilic and more hydrophobic substrates. We suggest that this is because this particular surface chemistry prevents ice formation at the interface of the substrate, prior to the deposition of the water droplet. On the basis of our results, we suggest that not only wettability and topography but also the concrete surface chemistry plays a significant role in the kinetics of the ice formation process when a water droplet is placed on a precooled substrate.

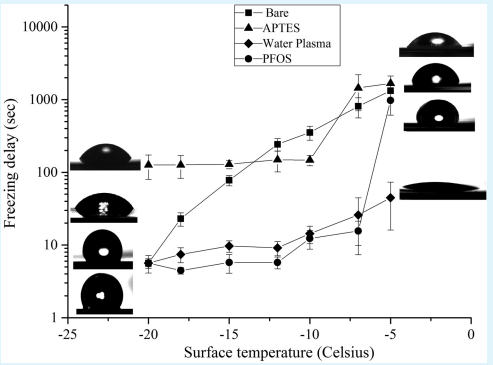

KEYWORDS: *aluminum, surface modification, wettability, freezing delay, ice nucleation, surface chemistry*

INTRODUCTION

Ice formation on solid surfaces can cause lower efficiency, malfunctions, and risks in different industrial applications such as heat exchangers, transmission lines, wind turbines, and aircrafts.[1−3] Several active and passive deicing methods are used to prevent ice formation on solid surfaces. The active methods involve energy consumption and consequently a reduction of the efficiency of the system. Passive deicing methods focus on how surface characteristics such as roughness, chemistry, and wettability influence ice formation and ice adhesion. In the present study we will investigate how the ice formation process can be prolonged by a passive approach.

The first step toward an understanding of how different surface characteristics affect ice formation is in the wetting theories which connect the surface chemistry (surface energy) and the surface topography. Here, we refer to two classical descriptions—the Wenzel model and the Cassie−Baxter model.[4,5] These models are applicable in cases where the droplet size is significantly larger than the wavelength of the surface roughness or chemical inhomogeneity.[6−8] The Wenzel model is based on the ability of a droplet to stay in direct contact with a surface by penetrating the surface features. According to this model, a hydrophilic surface will become more hydrophilic and a hydrophobic surface will become more hydrophobic if the surface roughness is increased.[4] The Cassie−Baxter model elucidates the contact angle of a droplet on a rough surface with trapped air in its surface grooves.[5] This results in the lowest degree of wetting and thus the highest contact angle.

The second step involves an understanding of how wetting and surface topography affect ice nucleation. When a small quantity of water is in contact with a solid surface, it normally does not immediately freeze when the temperature drops below 0 °C. Instead, it exhibits a characteristic freezing delay which is related to a delay in the ice nucleation process. According to the classic theory of nucleation, this can be described by the kinetics of crossing the energy barrier between ice and water. For nucleation in the bulk phase, the magnitude of the energy barrier is only related to the ice−water interfacial tension (which is temperature-dependent) and the magnitude of the difference in Gibbs energy between ice and water.[9] However, if the nucleation takes place at a solid interface, the energy barrier also becomes dependent on the surface topography and the wetting characteristics.[10,9] Several studies have demonstrated the practical implications of the classical ice nucleation theory.

Until now, most investigations regarding freezing delays and ice nucleation are performed under conditions where the droplet is placed on a surface at room temperature and

Received: February 24, 2016
Accepted: April 5, 2016
Published: April 5, 2016

DOI: 10.1021/acsami.6b02321
ACS Appl. Mater. Interfaces 2016, 8, 11147−11153

subsequently cooled to a predetermined temperature below 0 °C,[1,11−13] or alternatively water droplets of different temperatures have been placed to a substrate of a fixed temperature.[14] In the present study, a water droplet was put on substrates precooled to a certain temperature and the apparent contact angles and freezing delay were measured. Subsequently, the experiment was repeated at a new temperature. The apparent contact angle is measured due to the substrates' surface roughness and their chemical heterogeneity.[15] This experimental procedure is believed to mimic the working conditions of many real applications and enables us to study the effect of the substrate temperature of the freezing delay. To our knowledge, no such systematic studies employing substrates precooled to a range of different temperatures have previously been reported.

Aluminum alloys are the main material for air-to-air heat-exchanger fins and this material has shown problems with ice formation during cold winter days.[16] To find a solution to these ice formation problems, samples are prepared from an aluminum alloy sheet received from industry and their surface was modified in four different ways. The first group of samples consisted of bare aluminum which was just moderately cleaned. The second group consisted of aluminum samples exposed to water vapor plasma treatment which removed all surface contaminants. The third group consisted of aluminum samples modified by a monolayer of an organosilane [(3-aminopropyl)-triethoxylsilane, APTES), which gave the surface a hydrophilic character.[17,18] Finally, the fourth group consisted of aluminum samples modified by a monolayer of a perfluorooctylsilane (1H,1H,2H,2H-perfluorooctyltrichlorosilane, PFOS), which gave the surface a hydrophobic character.

EXPERIMENTAL SECTION

Materials. Plates of an aluminum alloy 8011A were received as a gift from Exhausto A/S (Langeskov, Denmark). PFOS, APTES (99%), and toluene (99.5%) were purchased from Sigma-Aldrich (St. Louis).

Sample Preparation. Samples with a size of 10 × 10 mm^2 were cut from the aluminum alloy sheet. Four groups of samples were prepared for the investigations. The first group was the bare aluminum alloys, which were degreased by 10 min of sonication in acetone, 10 min in Milli-Q water, and finally 10 min in ethanol. Subsequently, the samples were dried under a stream of clean compressed air and then kept in an oven at 110 °C overnight. In the second group, the aluminum alloy was treated by water-vapor plasma after degreasing and drying. In the third group, the surface of the aluminum alloys was modified by a monolayer of APTES after degreasing, drying, and plasma treatment. In the fourth group, the surface of the aluminum alloys was modified by a monolayer of PFOS after degreasing, drying, and plasma treatment. The four groups of samples thus represent a partly cleaned sample, a clean and hydrophilic sample, a surface-modified hydrophilic sample, and a surface-modified hydrophobic sample. The four groups of samples further have a very different surface chemistry.

The sample groups 2−4 were activated by water-vapor plasma treatment using a Harrick plasma cleaner. This process cleans the surfaces from any organic contaminations and enriches them by hydroxyl groups.[19] The flow and pressure of the water vapor were controlled by a Harrick flow controller and the plasma treatment was performed at a pressure of 120 Pa and radio frequency power of 30 W. As shown in Figure 1, the contact angle of the surface did not change significantly by plasma time, which indicates that the removal of organic contaminants and the surface activation by hydroxyl groups occur within the first 50 s and that this relatively mild plasma treatment is not leading to significant changes in the surface roughness. To ensure optimal uniformity in the surface functionality, we have in the present study used a plasma time of 200 s for all samples.

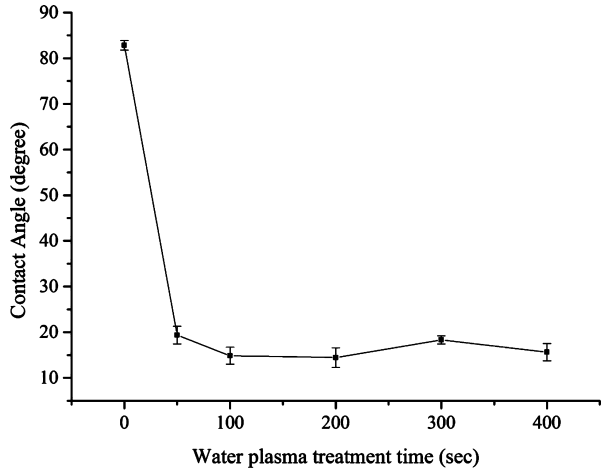

Figure 1. Measured contact angle of bare aluminum samples as a function of the exposure time to the water-vapor plasma. The measurements were performed at room temperature and the error bars represent a 95% confidence interval.

To obtain smooth and reproducible silane layers, chemical vapor deposition was performed by exposing the substrates to vapor of a solution of silane in toluene as previously suggested.[20−22] The aluminum substrates were first activated by the water-vapor plasma and immediately afterward placed in an evacuated desiccator containing a solution of 250 μL of APTES or PFOS in 750 μL of toluene and heated up to 110 °C for 3 h. Next, the samples were removed from the desiccator and sonicated in 99% ethanol and dried under an air stream.

Surface Characterization. *Contact Angle Measurement and Freezing Delay Measurement.* Apparent contact angles (measured in static mode) and freezing delays were measured using an Attension Theta Lite optical tensiometer. The substrate was cooled to the desired temperature prior to the measurement by means of a temperature-controlled sample stage and a thermos-isolated measuring chamber connected to a circulating water/glycerol bath and a MX Temperature Controller (VWR). The sample temperature was measured with a K-type temperature logger (Agilent GUI data logger). When the temperatures became stable, the water droplet with a volume of 6 μL was placed on the substrate and the time and image recording were started simultaneously. Freezing delay times were defined as the time from when the droplet was placed on the precooled substrate to the onset of freezing and was determined by direct imaging with a CCD camera. The onset of freezing coincided with clouding of the water volume, as caused by spontaneous crystallization followed by a volume change.[1,23]

All measurements were conducted at a relative humidity of 26 ± 2% and at a temperature of 21 ± 1 °C inside the measuring chamber. The relative humidity and temperature in the laboratory during the measurements were 30 ± 2% and 23 ± 1 °C. For each group of samples and for each specific temperature, the reported data of freezing delays and contact angles are the average of at least seven measurements.

AFM. Topographical images of the samples were obtained with an atomic force microscope (AFM) (NanoWizard 3, JPK Instruments, Berlin, Germany) operating in tapping mode and employing a NSC36/Cr-Au cantilever (MikroMasch, Sofia, Bulgaria). The acquired AFM images were processed by the JPK data processing software and the root-mean-square, R_q, surface roughness was obtained.

RESULTS

Surface Characterization. Since the surface roughness and the wetting state are expected to play a crucial role in ice nucleation and freezing delay, the four groups of samples were

DOI: 10.1021/acsami.6b02321
ACS Appl. Mater. Interfaces 2016, 8, 11147−11153

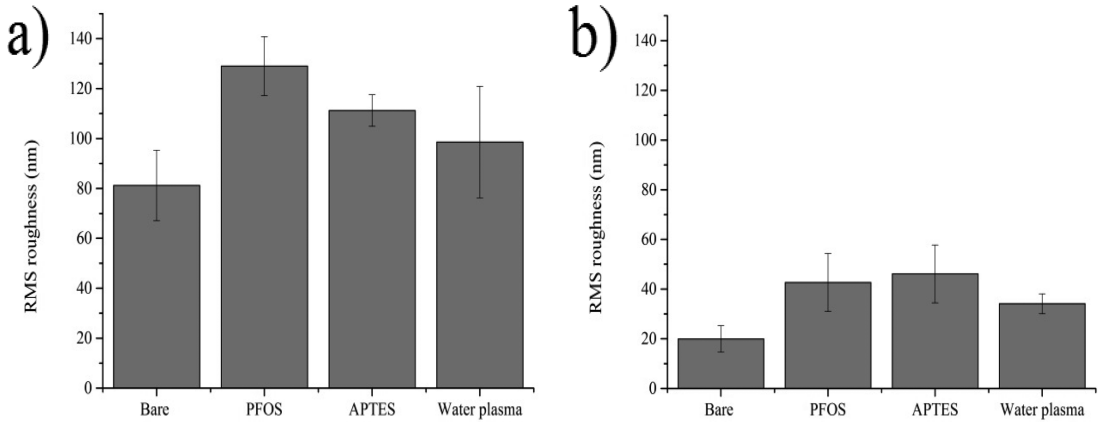

Figure 2. R_q roughness of different samples obtained from AFM images with scan sizes of (a) 50 × 50 μm^2 and (b) 10 × 10 μm^2. The error bars represent a 95% confidence interval.

first characterized with respect to surface roughness and wettability by AFM imaging and contact angle measurements.

As the surface roughness of surfaces with random topographical variations on the nanometer to micrometer scale will depend on the scan size of the AFM image, scans of both 10 × 10 and 50 × 50 μm^2 were obtained and analyzed. The roughness analysis is based on images of three different surface locations for each of the two length scales and the results are presented in Figure 2. It can be observed that within the error bars, the surface roughness is in the same range for the three surface-modified samples, while the bare aluminum sample appears to have a slightly lower degree of roughness. The minor difference between the bare aluminum sample and the modified surface samples is attributed to the removal of organic contaminant by the plasma treatment, while the minor variation within the surface-treated samples can be an effect of the branched structures of APTES and PFOS.

Moreover, to investigate the effect of the extent of the water-vapor plasma treatment on the surface of aluminum, the R_q roughness of samples exposed to water-vapor plasma treatment for different times was measured. The results showed that the roughness did not change significantly by increasing the plasma treatment time which together with the contact angle measurements of the same samples (Figure 1) confirms the assumption that the relative mild plasma treatment removes organic contaminant and activates the surface by hydroxyl groups but does not lead to increased surface roughness.

Next, the contact angle of a water droplet on each of the four groups of samples was measured at room temperature and the results are presented in Figure 3. Aluminum alloys are, like other metals, considered to be a high surface energy material with a low water contact angle. However, in line with previous studies, we observed a high contact angle of 82°, which we believe is due to the presence of hydrophobic contaminants.[22,24] After water-vapor plasma treatment, it is clearly seen that the contaminants can be removed and a hydrophilic surface with a low water contact angle is achieved. The surface treatments with PFOS and APTES are as expected, giving the surfaces a highly hydrophobic and a moderately hydrophilic character, respectively.

Summarizing the surface characterization, we can conclude that we have four groups of samples with different surface chemistry and wettability but with very similar surface topography. This understanding becomes important when the measured freezing delays are going to be compared to the expectations based on ice nucleation theory.

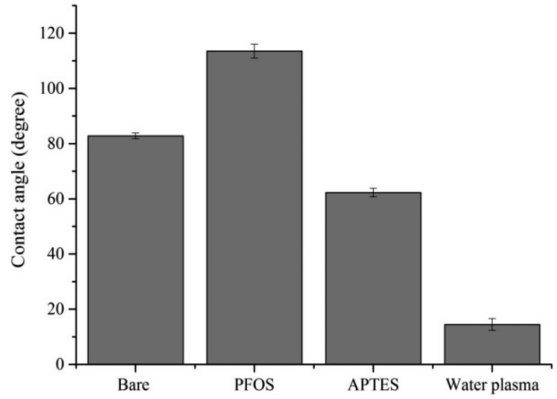

Figure 3. Measured contact angles at room temperature for the four groups of samples. The error bars represent a 95% confidence interval.

Freezing Delays Studies. For all four samples, it is observed that the freezing delay decreases with decreasing substrate temperature (see Figure 4). However, it is also observed that the magnitude of the delay and their relative changes with temperature are significantly different for the four

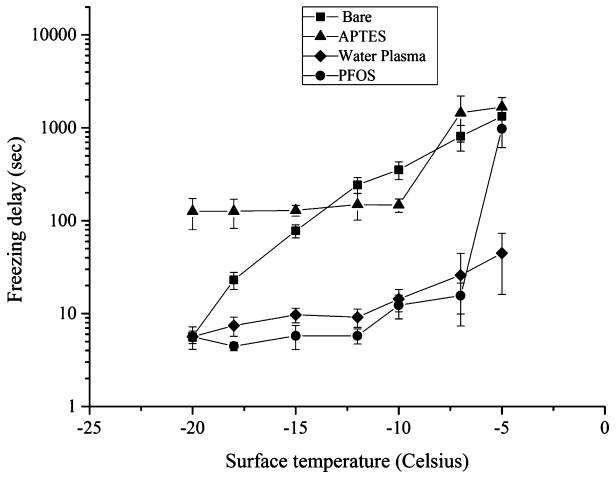

Figure 4. Freezing delays of water droplet placed on substrates precooled to temperatures ranging from −5 to −20 °C. The error bars represent a 95% confidence interval.

DOI: 10.1021/acsami.6b02321
ACS Appl. Mater. Interfaces 2016, 8, 11147−11153

groups of samples. First, in the case of the bare aluminum surface, a continuous decrease in the freezing delay is observed in the entire temperature range. For the APTES- and PFOS-modified surfaces, a rapid decrease in the freezing delay is observed in the temperature interval between −5 and −10 °C, which corresponds to around 98% of the whole freezing delay drop from −5 to −20 °C. Subsequently, the freezing delays only decrease slowly by further reduction in temperature (in the case of the water-vapor plasma-treated sample, the drop in the freezing delay might already have occurred at −5 °C). However, although the change in freezing delays of a water droplet on the three modified samples qualitatively follows a similar trend, major differences in the magnitudes of the freezing delays is observed.

In the cases of water-vapor plasma-treated and the PFOS-modified surfaces, the freezing delays drop to below 10 s at temperatures below −10 °C, while in the case of the APTES-modified surface the freezing delay stays above 100 s down to −25 °C.

A way to understand this different behavior is to monitor how the contact angle of the water droplet is changed by changing the substrate temperature. Such data are presented in Figure 5, where it is seen that the contact angle on the bare aluminum and the APTES-modified substrate exhibits a smooth but weak decrease with decreasing temperature in the interval between +20 and −25 °C. Such a decrease is expected and can be explained by the temperature dependence of the surface tension of water. However, in the case of both the water-vapor plasma-treated and then PFOS-modified sample, an abrupt increase in the contact angle is observed in the same temperature range where the freezing delays also change dramatically. This transition in the wetting behavior is not related to the surface tension of water but can be explained only by a change of the surface energy or in the wetting state. We will return to this issue in the Discussion section.

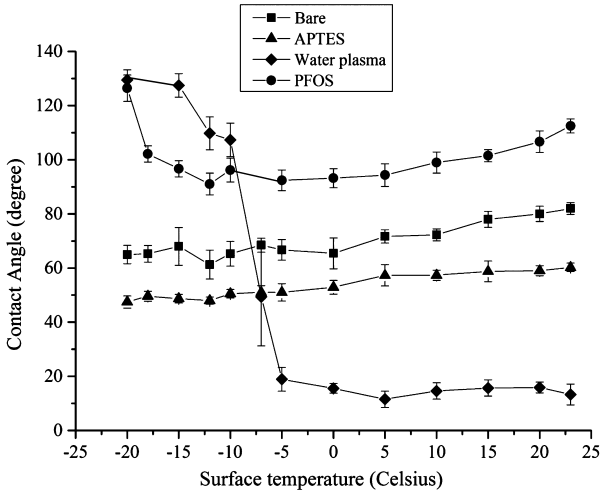

Figure 5. Apparent contact angles on the four groups of samples measured in the temperature range from 23 to −20 °C. The error bars represent a 95% confidence interval.

As an additional note, at the end of the freezing process the droplet becomes fully opaque and a small sharp-pointed protrusion appeared on its top. This is the result of a volume dilatation and change in surface tension due to phase change from liquid to solid. This observation is in line with previous works.[25,2,26] A discussion of this phenomenon is not within the scope of this study but images of this sharp-pointed protrusion on top of the four different samples at −20 °C are presented in the Supporting Information, section B.

DISCUSSION

Previous freezing delay studies have shown different trends and observations on the correlation of the freezing delays and the sample wettability. This is partly due to the fact that the ice formation process is a sensitive phenomenon which goes beyond the surface conditions.[27,13,1,11] The kinetics of the ice formation process and thus the measured freezing delays strongly depends on experimental conditions such as humidity, air temperature, water temperature, and also the droplet size and how the droplet is placed on the surface.[13,28,13,29]

In our analysis we first compare our results to the expectations from nucleation theory and next we discuss the possible deviations from this theory. A thorough description of the relevant nucleation theory and its implications for our measurements is given in the Supporting Information, while only some of the key points are presented in this section.

First, it should be realized that nucleation of a supercooled water droplet can occur either in the bulk phase (homogeneous nucleation) or at the interface of the sample (heterogeneous nucleation).[10,9] Since the energy barrier for nucleation is lower for heterogeneous nucleation than for homogeneous nucleation and since we observe different freezing delays depending on the surface chemistry, we assume that the freezing events in this study should be described by the theory for heterogeneous nucleation. In this case the energy barrier is given by

$$\Delta G^{*}_{\mathrm{hetro}} = \frac{16\pi\gamma_{\mathrm{IW}}^{3}}{3(\Delta G_{\mathrm{V}})^{2}} f(m, x)$$

where γ_{IW} is the ice−water interfacial tension, ΔG_{V} is the free energy difference (per unit of volume) between ice and water, and $f(m,x)$ is a function which is related to the interfacial energies of water, ice, and the substrate (and their temperature dependence), the surface geometry and the surface wetting characteristics. In our case, $f(m,x)$ becomes a function of the contact angle of water on the substrate, the surface roughness, and the temperature (see Supporting Information for more details about the calculation of $f(x,m)$).

Figure 6 presents the values of ΔG^{*} as a function of temperature for our four samples and for the case of homogeneous nucleation. Here, it is observed that the energy barriers in all four cases decrease fast when the temperature is lowered from 0 to −10 °C, where after the decrease it becomes less pronounced when the temperature is further decreased. This observation is thus in qualitative agreement with our results of the modified samples, which show a fast decrease in the freezing delays in the temperature interval between 0 and −10 °C, after which the change in freezing delays becomes moderate. It is, however, also observed that the energy barriers for the hydrophobic PFOS-modified sample is much larger than the energy barriers for the hydrophilic APTES and water-vapor plasma-modified samples. This suggests that the freezing delays should be longest on the PFOS-modified sample. This prediction is thus in apparent disagreement with our experimental result, which showed a longer freezing delay on the APTES-modified samples and shorter and very similar freezing delays on the PFOS- and the water-vapor plasma-modified samples.

DOI: 10.1021/acsami.6b02321
ACS Appl. Mater. Interfaces 2016, 8, 11147−11153

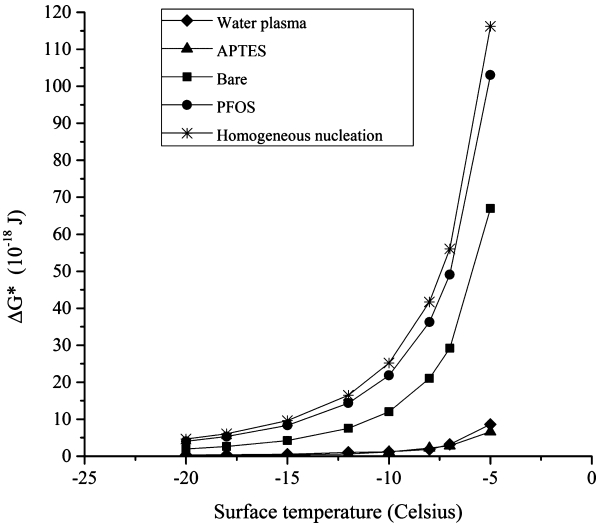

Figure 6. Magnitude of energy barrier for homogeneous nucleation of an ice embryo and for heterogeneous nucleation on the four different substrates as a function of temperature.

To understand this apparent disagreement between the calculated magnitudes of the energy barriers for nucleation and the extent of the freezing delays on the surface-modified samples, one has to consider the change in wettability which for the water-vapor plasma-treated and PFOS-modified samples were observed around −7 °C (see Figure 5). It has previously been observed that highly hydrophobic surfaces can undergo a wetting transition (Wenzel to Cassie−Baxter transition) at decreasing temperature due to condensation of water in nonwetted cavities.[30] In such cases it is observed that the contact angle starts to decrease when the temperature drops below the dew point. However, in the present case where the contact angle suddenly starts to increase by decreasing temperature and where the phenomenon is observed both for a hydrophobic and for a hydrophilic sample, the explanation must be different. Instead, we suggest that this observation is related to sublimation and growth of ice on the cold substrates before the water droplet is placed on the substrate.

If this ice formation starts to take place at temperatures around −5 to −10 °C, it can explain why the contact angles also suddenly change in this temperature range simply because the droplet is being placed on ice structures instead of directly on the substrate surface. The exact temperature at which sublimation and ice formation begins (and also the morphology of a formed ice layer) will depend on surface chemistry, surface structure, and the relative humidity.[31] One question is obviously how the formation of an ice layer will affect the surface wettability. Observations of the contact angle of water on ice have in previous studies shown that it was increasing by decreasing the water droplet temperature. For example, in one study it was observed that when the water temperature decreased from 100 to 0 °C, the contact angle increased from 40° to 90°.[32,33] This result is in line with our observation which shows that the contact angle is increasing by decreasing the temperature after the potential ice structures are formed on the surface.

The next relevant question is why the sublimation and formation of an ice layer apparently do not occur on the APTES-modified sample. One suggestion could be that the high concentration of amino groups prevents ice formation. At atmospheric conditions, the pH of water will normally be around 5.6 due to dissolution of CO_2. The pK_a-value of surface-bound amino groups has previously been reported to be around 10.[34−36] In the presence of liquid water, this means that the amino groups on the APTES surface can be expected to be in acidic form, and the surface will thus have a high surface charge density. If a water film condensates at the surface, it will therefore have a high local ion concentration which can lead to significant freezing point suppression of water in proximity to the interface. This is in line with a number of previous experiments where weaker adhesion of ice and slower ice formation of water condensate to charged interfaces compared to noncharged interfaces has been observed. Here, it was suggested that a liquid-like layer was formed between the ice and the charged interface and that the charged species prevented the freezing of water condensate.[37−39] With this background, we suggest that the presence of amino groups prevents formation of an ice layer and ultimately leads to longer freezing delays.

CONCLUSION

In this study, we have investigated the wetting properties and the freezing delay of a water droplet placed on four differently modified and precooled aluminum substrates. First, a surface characterization at room temperature showed that the four groups of samples exhibited different wetting properties but had similar surface roughness. For all four groups of samples, the studies showed that the extent of the freezing delays were decreasing with decreasing temperatures, in qualitative agreement with the theory for heterogeneous nucleation. However, in apparent disagreement with the ice nucleation theory it was also observed that the hydrophilic APTES-modified surface exhibited longer freezing delays than both the more hydrophilic water-vapor-treated sample and the hydrophobic PFOS-modified sample. To that end, it was also observed that the contact angles of the water-vapor-treated sample and the PFOS-modified sample were showing an unexpected increase with decreasing temperatures. We suggest that an ice layer can spontaneously form on the cold surface exposed to a warmer water-vapor-containing atmosphere and that the formation of such an ice layer can change the wettability as observed in the two cases. However, in the case of the APTES-modified samples, the formation of such an ice layer is apparently avoided. Here we suggest that that the presence of charged surface groups can lead to freezing point suppression, which prevents a condensed water film from freezing. On the basis of the results of this study, we thus suggest that while the surface topography and the surface wettability determine the freezing kinetics of a droplet placed on a precooled sample, the surface chemistry can be used as a tool to control the actual wetting properties of a cold surface in a humid atmosphere. On this basis, we suggest that future studies should focus on how variations in the relative humidity of the surrounding atmosphere affect the surface wettability of samples at subzero temperatures with different surface chemistry.

ASSOCIATED CONTENT

Supporting Information

The Supporting Information is available free of charge on the ACS Publications website at DOI: 10.1021/acsami.6b02321.

Relevant equations from the ice nucleation theory and an illustration of how they relate to our measurements;

DOI: 10.1021/acsami.6b02321
ACS Appl. Mater. Interfaces 2016, 8, 11147−11153

images of the sharp-pointed protrusion of the frozen water droplets (PDF)

AUTHOR INFORMATION

Corresponding Author

*E-mail: mar@sbi.aau.dk.

Notes

The authors declare no competing financial interest.

ACKNOWLEDGMENTS

M. Rahimi and A. Afshari acknowledge financial support from COWIfonden and the Greenland Government. E. Thormann acknowledges financial support from the Swedish Research Council, VR with Grant No. 621-2012-3015. Moreover, we greatly acknowledge the support of Exhausto A/S, who contributed components and materials.

REFERENCES

(1) Hao, P.; Lv, C.; Zhang, X. Freezing of Sessile Water Droplets on Surfaces with Various |Roughness and Wettability. *Appl. Phys. Lett.* **2014**, *104* (16), 161609.

(2) Menini, R.; Ghalmi, Z.; Farzaneh, M. Highly Resistant Icephobic Coatings on Aluminum Alloys, Cold. *Cold Reg. Sci. Technol.* **2011**, *65* (1), 65−69.

(3) Farhadi, S.; Farzaneh, M.; Kulinich, S. a. Anti-icing Performance of Superhydrophobic Surfaces. *Appl. Surf. Sci.* **2011**, *257* (14), 6264−6269.

(4) Wenzel, R. N. Resistance of Solid Surfaces. *Ind. Eng. Chem.* **1936**, *28* (8), 988−994.

(5) Cassie, A. B. D.; Baxter, S. Wettability of Porous Surfaces. *Trans. Faraday Soc.* **1944**, *40* (0), 546−551.

(6) Marmur, A.; Bittoun, E. When Wenzel and Cassie areRight: Reconciling Local and Global Considerations. *Langmuir* **2009**, *25* (3), 1277−1281.

(7) Hansson, P. M.; Swerin, A.; Schoelkopf, J.; Gane, P. a C.; Thormann, E. Influence of Surface Topography on the Interactions Between Nanostructured Hydrophobic Surfaces. *Langmuir* **2012**, *28* (21), 8026−8034.

(8) Hansson, P. M.; Skedung, L.; Claesson, P. M.; Swerin, A.; Schoelkopf, J.; Gane, P. a C.; Rutland, M. W.; Thormann, E. Robust Hydrophobic Surfaces Displaying Different Surface Roughness Scales while Maintaining the Same Wettability. *Langmuir* **2011**, *27* (13), 8153−8159.

(9) Fletcher, N. H. *The Chemical Physics of Ice*, 1st ed.; Cambridge University Press: Cambridge, 1970.

(10) Fletcher, N. H. J. Size Effect in Heterogeneous Nucleation. *J. Chem. Phys.* **1958**, *29* (1958), 572.

(11) Heydari, G.; Thormann, E.; Järn, M.; Tyrode, E.; Claesson, P. Hydrophobic Surfaces Topography Effects on Wetting by supercooled water and freezing delay. *J. Phys. Chem. C* **2013**, *117* (42), 21752−21762.

(12) Singh, D. P.; Singh, J. P. Delayed Freezing of Water Droplet on Silver Nano columnar Thin Film. *Appl. Phys. Lett.* **2013**, *102* (24), 243112.

(13) Ou, J.; Shi, Q.; Wang, Z.; Wang, F.; Xue, M.; Li, W.; Yan, G. Sessile Droplet Freezing and Ice Adhesion on Aluminum with Different Surface Wettability and Surface Temperature. *Sci. China: Phys., Mech. Astron.* **2015**, *58* (7), 1−8.

(14) Mishchenko, L.; Hatton, B.; Bahadur, V.; Taylor, J. A.; Krupenkin, T.; Aizenberg, J. Design of Ice-free Nanostructured Surfaces Based on Repulsion of Impacting Water Droplets. *ACS Nano* **2010**, *4* (12), 7699−7707.

(15) Marmur, A. A Guide to the Equilibrium Contact Angles Maze. *Contact Angle, Wettability and Adhesion*; Brill: Leiden, The Netherlands,2009; Vol. 6, p 18.10.1163/ej.9789004169326.i-400.5

(16) Kragh, J.; Rose, J.; Nielsen, T. R.; Svendsen, S. New Counter Flow Heat Exchanger Designed for Ventilation Systems in Cold Climates. *Energy Build.* **2007**, *39* (11), 1151−1158.

(17) Plueddemann, E. P. *Silane Coupling Agents*; Springer: New York,1982.

(18) Zhang, F.; Sautter, K.; Larsen, A. M.; Findley, D. a.; Davis, R. C.; Samha, H.; Linford, M. R. Chemical Vapor Deposition of Three Aminosilanes on Silicon Dioxide: Surface Characterization, Stability, Effects of Silane Concentration, and Cyanine Dye Adsorption. *Langmuir* **2010**, *26* (18), 14648−14654.

(19) Stratton, G. R.; Bellona, C. L.; Dai, F.; Holsen, T. M.; Thagard, S. M. Plasma-Based Water Treatment: Conception and Application of a New General Principle for Reactor Design. *Chem. Eng. J.* **2015**, *273*, 543−550.

(20) Fiorilli, S.; Rivolo, P.; Descrovi, E.; Ricciardi, C.; Pasquardini, L.; Lunelli, L.; Vanzetti, L.; Pederzolli, C.; Onida, B.; Garrone, E. Vapor-phase Self-assembled Monolayers of Aminosilane on Plasma-activated Silicon Substrates. *J. Colloid Interface Sci.* **2008**, *321* (1), 235−241.

(21) Song, X.; Zhai, J.; Wang, Y.; Jiang, L. Self-assembly of Amino-functionalized Monolayers on Silicon Surfaces and Preparation of Superhydrophobic Surfaces Based on Alkanoic Acid Dual Layers and Surface Roughening. *J. Colloid Interface Sci.* **2006**, *298* (1), 267−273.

(22) Rahimi, M.; Fojan, P.; Gurevich, L.; Afshari, A. Effects of Aluminium Surface Morphology and Chemical Modification on Wettability. *Appl. Surf. Sci.* **2014**, *296*, 124−132.

(23) Jung, S.; Tiwari, M. K.; Doan, N. V.; Poulikakos, D. Mechanism of Supercooled Droplet Freezing on Surfaces. *Nat. Commun.* **2012**, *3*, 615.

(24) Bormashenko, E.; Musin, A.; Zinigrad, M. Evaporation of Droplets on Strongly and Weakly Pinning Surfaces and Dynamics of theTriple Line. *Colloids Surf., A* **2011**, *385* (1−3), 235−240.

(25) Wang, J.; Liu, Z.; Gou, Y.; Zhang, X.; Cheng, S. Deformation of Freezing Water Droplets on a Cold Copper Surface. *Sci. China, Ser. E: Technol. Sci.* **2006**, *49* (5), 590−600.

(26) Huang, L.; Liu, Z.; Liu, Y.; Gou, Y.; Wang, L. Effect of Contact Angle on Water Droplet Freezing Process on a Cold Flat Surface. *Exp. Therm. Fluid Sci.* **2012**, *40*, 74−80.

(27) Boinovich, L.; Emelyanenko, A. M.; Korolev, V. V.; Pashinin, A. S. Effect of Wettability on Sessile Drop Freezing: When Superhydrophobicity Stimulates an Extreme Freezing Delay. *Langmuir* **2014**, *30* (6), 1659−1668.

(28) Alizadeh, A.; Yamada, M.; Li, R.; Shang, W.; Otta, S.; Zhong, S.; Ge, L.; Dhinojwala, A.; Conway, K. R.; Bahadur, V.; Vinciquerra, A. J.; Stephens, B.; Blohm, M. L. Dynamics of Ice Nucleation on Water Repellent Surfaces. *Langmuir* **2012**, *28*, 3180−3186.

(29) Saleema, N.; Farzaneh, M.; Paynter, R. W.; Sarkar, D. K. Prevention of Ice Accretion on Aluminum Surfaces by Enhancing Their Hydrophobic Properties. *J. Adhes. Sci. Technol.* **2011**, *25*, 27−40.

(30) Jo, H.; Hwang, K. W.; Kim, D.; Kiyofumi, M.; Park, H. S.; Kim, M. H.; Ahn, H. S. Loss of Superhydrophobicity of Hydrophobic Micro/Nano Structures During Condensation. *Sci. Rep.* **2015**, *5*, 9901.

(31) Rahimi, M.; Afshari, A.; Fojan, P.; Gurevich, L. The Effect of Surface Modification on Initial Ice Formation on Aluminum Surfaces. *Appl. Surf. Sci.* **2015**, *355*, 327−333.

(32) Makkonen, L. Surface Melting of Ice. *J. Phys. Chem. B* **1997**, *101* (32), 6196−6200.

(33) Friedman, S. R.; Khalil, M.; Taborek, P. Wetting Transition in Water. *Phys. Rev. Lett.* **2013**, *111* (22), 226101.

(34) Kim, J.; Korkmaz, N.; Nam, C. H. Phage Assembly Using ATPES-Conjugation of Major Coated p8 Protein for Possible Scaffolds. *Interdiscip. Bio Cent.* **2012**, *4* (3), 1−7.

(35) Balladur, V.; Theretz, a; Mandrand, B. Determination of the Main Forces Driving DNA Oligonucleotide Adsorption onto Aminated Silica Wafers. *J. Colloid Interface Sci.* **1997**, *194* (2), 408−418.

(36) Dunér, G.; Iruthayaraj, J.; Daasbjerg, K.; Pedersen, S. U.; Thormann, E.; Dėdinaitė, A. Attractive Double-Layer Forces and Charge Regulation Upon Interaction Between Electrografted Amine Layers and Silica. *J. Colloid Interface Sci.* **2012**, *385* (1), 225−234.

DOI: 10.1021/acsami.6b02321
ACS Appl. Mater. Interfaces 2016, 8, 11147−11153

(37) Zhang, Q.; He, M.; Zeng, X.; Li, K.; Cui, D.; Chen, J.; Wang, J.; Song, Y.; Jiang, L. Condensation Mode Determines the Freezing of Condensed Water on Solid Surfaces. *Soft Matter* **2012**, *8* (32), 8285−8288.
(38) Dou, R.; Chen, J.; Zhang, Y.; Wang, X.; Cui, D.; Song, Y.; Jiang, L.; Wang, J. Anti-icing Coating with an Aqueous Lubricating Layer. *ACS Appl. Mater. Interfaces* **2014**, *6* (10), 6998−7003.
(39) Chernyy, S.; Järn, M.; Shimizu, K.; Swerin, A.; Pedersen, S. U.; Daasbjerg, K.; Makkonen, L.; Claesson, P.; Iruthayaraj, J. Superhydrophilic Polyelectrolyte Brush Layers with Imparted Anti-icing Properties: Effect of Counter Ions. *ACS Appl. Mater. Interfaces* **2014**, *6* (9), 6487−6496.

DOI: 10.1021/acsami.6b02321
ACS Appl. Mater. Interfaces 2016, 8, 11147−11153

3.1.5.2 Supporting information of paper V

Supporting Information

Effect of aluminum substrate surface modification on wettability and freezing delay of water droplet at sub-zero temperatures

Maral Rahimi[a,*], Alireza Afshari[a] and Esben Thormann[b]

[a] Department of Energy and Environment, Danish Building Research Institute, Aalborg University, A.C. Meyers Vænge 15, 2450 København SV, Denmark

[b] Technical University of Denmark, Department of Chemistry, Kemitorvet 207, DK-2800 Kgs. Lyngby, Denmark

A. Ice nucleation

According to classical theory of nucleation, a delay in the freezing process can be described by the energy barrier between ice and water. For nucleation in the bulk phase (homogeneous nucleation) the magnitude of the energy barrier is only related to the ice-water interfacial tension (which is temperature dependent) and the magnitude of the difference in Gibbs energy between ice and water.[1] The energy barrier for homogeneous nucleation of an ice embryo with the critical radius, r*, is given as:

$$\Delta G^{*}_{\mathrm{Homo}} = \frac{16\,\pi\,\gamma_{\mathrm{IW}}^{3}}{3(\Delta G_{\mathrm{V}})^{2}} \quad (1)$$

and the critical radius as:

$$r^{*} = -\frac{2\,\gamma_{\mathrm{IW}}}{\Delta G_{\mathrm{V}}} \quad (2)$$

Here ΔG_V is the free energy difference (per unit of volume) between ice and water. This quantity can further be expressed as

$$\Delta G_{\mathrm{V}} = \frac{T_m - T}{T_m}\Delta H_v \quad (3)$$

where T_m is the melting point of ice at 1atm, T is the (sub-zero) temperature, and ΔH_v = 287 MJ/m^3 is the enthalpy of fusion. [2]

γ_{IW} is the ice-water interfacial tension, the temperature dependence of which was calculated by different methods in previous studies.[3,4 5 6] Here we follow the approach of Heydari et al.[5] where the temperature dependence of γ_{IW} is calculated as

$$\gamma_{IW} = 28.0 + 0.25\,(T - 273.15) \quad (4)$$

with γ_{IW} in mJm^{-2} and T in K.

The values of r* , ΔG_V, ΔG^*_{Homo}, and γ_{IW} calculated at different temperatures between -5 °C and -20 °C are shown in Table S1 and Figure S1.

Table S1.

T [°C]	T [K]	ΔG[MJ/m3]	γ IW [mJ/m2]	r*[nm]	ΔG* [J/m3]
-5	268.15	5.25	26.75	10.2	1.16E-17
-7	266.15	7.35	26.25	7.1	5.60E-18
-8	265.15	8.41	26	6.2	4.17E-18
-10	263.15	10.51	25.5	4.9	2.52E-18
-12	261.15	12.61	25	4.0	1.65E-18
-15	258.15	15.76	24.25	3.1	9.62E-19
-18	255.15	18.91	23.5	2.5	6.08E-19
-20	253.15	21.01	23	2.2	4.62E-19

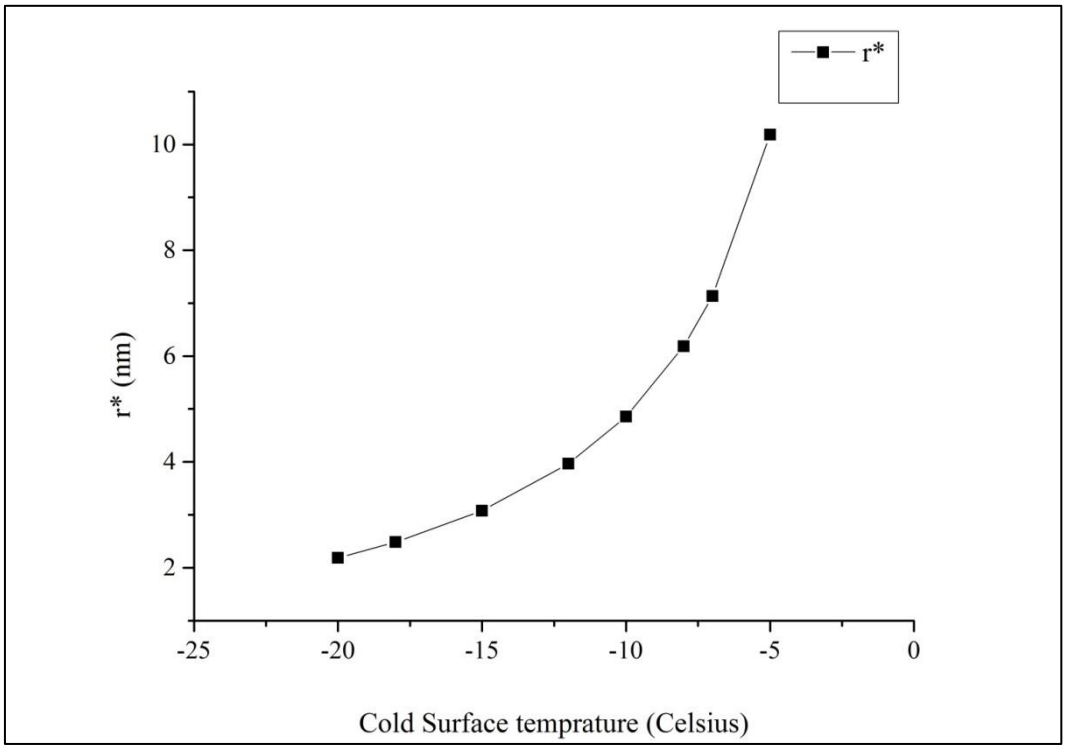

Figure S1. The critical radius, r*, plotted in the temperature range between -5 °C and -20 °C.

In the case where the nucleation takes place at a solid interface (heterogeneous nucleation) the energy barrier also becomes dependent of the surface topography and the wetting characteristics. [7,1] The magnitude of the energy barrier can be written as:

$$\Delta G^{*}_{\mathrm{Hetro}} = \Delta G_{\mathrm{Homo}}{}^{*}\, f(m,x) \qquad (5)$$

where f(m,x) is a function which is related to the interfacial energies of water, ice and the substrate (and their temperature dependence), the surface geometry and the surface wetting characteristics. More specifically, it is expressed as:

$$f(m,x) = \frac{1}{2}\left[1 + \left(\frac{1-mx}{g}\right)^{3} + x^{3}\ \left[2 - 3\left(\frac{x-m}{g}\right) + \left(\frac{x-m}{g}\right)^{3}\right] + [3m^{2}x^{2}(\frac{x-m}{g} - 1)]\right] \qquad (6)$$

Here m=cos $\theta_{IS,}$ where θ_{IS} is the contact angle of an ice embryo on the nucleating substrate in water. According to Young's equation and by assuming the contact angle of ice and super cooled water to be the same, m can now be expressed as:[8]

$$m = \cos\theta_{IW} = \frac{\gamma_I - \gamma_W}{\gamma_{IW}} \cos\theta \quad (7)$$

Here γ_{IW} is ice-water interfacial tension which is temperature dependent and can be calculated at different temperature according to Equation (4). θ is the contact angle of water on the substrate. γ_I is the surface energy of ice which is assumed to be constant. The value of γ_I is widely considered to be in the range 105-109 mJ/m2, but it should be mentioned that a value as low as 73 mJ/m2 has also been suggested.[5,9,10] In this work, we have used γ_I = 109 mJ/m^2. γ_W is the surface energy of super cooled water (see Table S2).

x=r/r* is the relation between the radius of an ice nucleus and the critical radius. In our calculations, we follow the common approach in the literature suggesting that x≈R/r* where R is the surface roughness. The g-function is defined as:

$$g = (1 + x^2 - 2mx)^{\frac{1}{2}} \quad (8)$$

with the meaning of x and m as described above.

Table S2. Surface energy of super cooled water at different temperatures. The data are extracted and extrapolated from work by Floriano and Angell, 1990.[3]

T [°C]	γ_W [mJ/m2]
-5	76
-7	76.5
-8	77.24
-10	77.37
-12	77
-15	78
-18	78.3
-20	78.82

On the basis of the values in Tables S1 and S2, f(x,m) is calculated in the temperature range between -5 °C and -20 °C for the four groups of samples (see Figure S2)

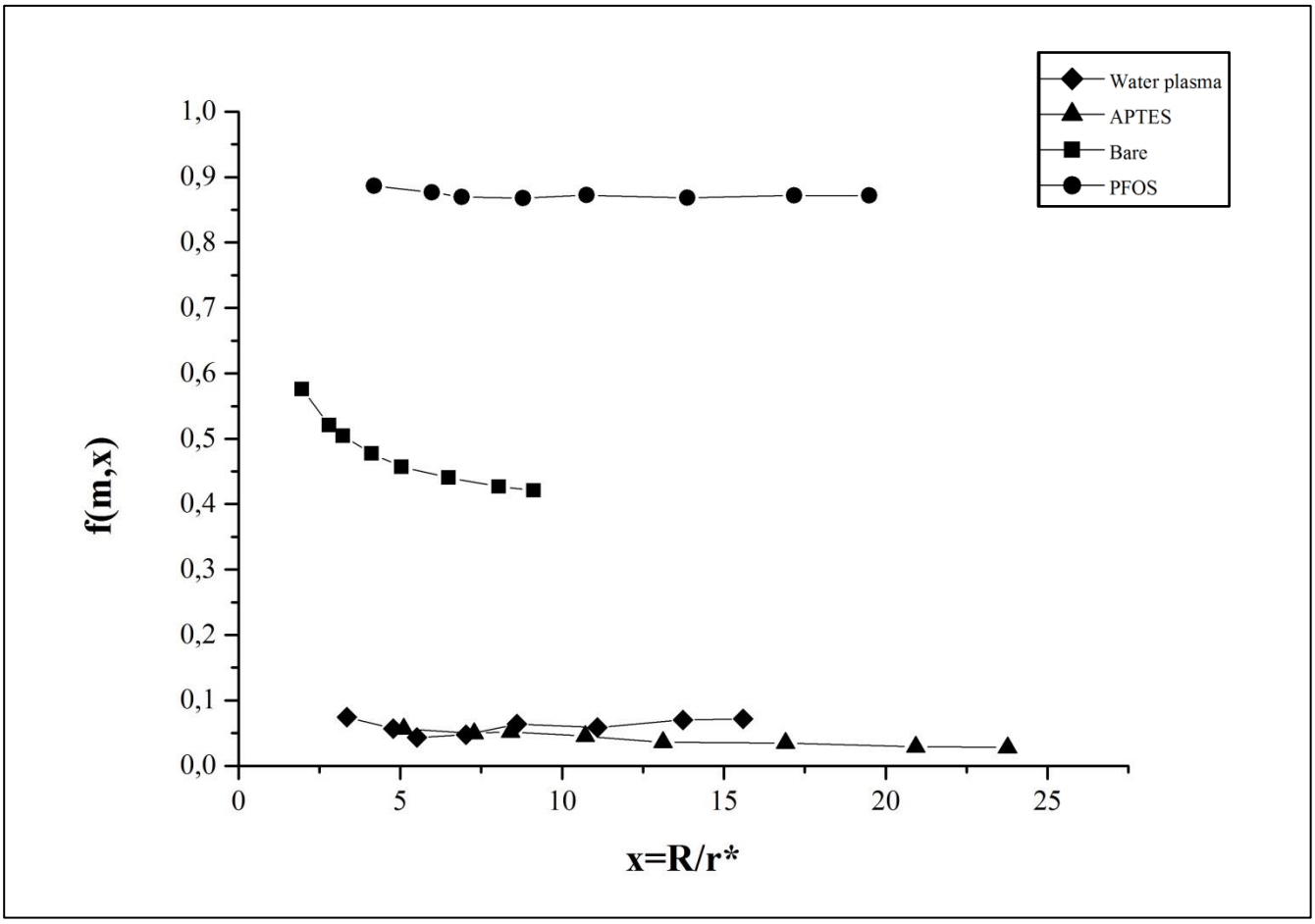

Figure S2. The geometrical factor f(m,x) vs the roughness parameter x

B. Sharp-pointed protrusion

At the end of the freezing process, the droplet became fully opaque and a small-sharp pointed protrusion appeared as shown in Figure S3. This phenomenon is due to the volume expansion coursed by the freezing transition where a droplet deformation and a protrusion formation take place. This observation are in line with previous reported observations.[11, 12,13]

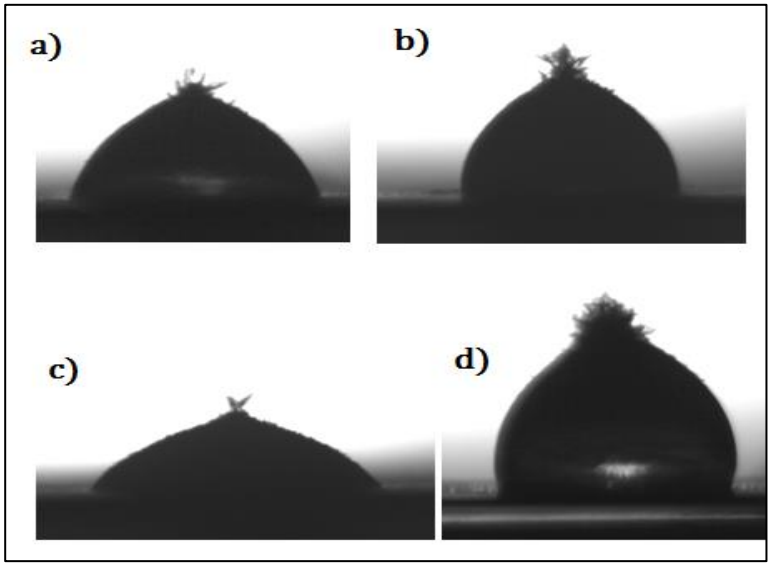

Figure S3. Sharp-pointed protrusion on top of the water droplet after 5 minutes from the start of freezing at -20°C for a) Bare sample b) PFOS sample , c) APTES sample and d) water-plasma sample

References

(1) Fletcher, N. H. *The Chemical Physics of Ice*, 1st ed.; Press, C. U., Ed.; Cambridge, **1970**.

(2) Hao, P.; Lv, C.; Zhang, X. , Freezing of sessile water droplets on surfaces with various roughness and wettability, *Appl. Phys. Lett.* **2014**, *104* , 161609.

(3) Floriano, M. a.; Angell, C. a. , Surface Tension and Molar Surface Free Energy and Entropy of Water to -27.2 °C, *The Journal of Physical Chemistry*. **1990**, 94, 4199–4202.

(4) Leyendekkers, J. V.; Hunter, R. J. , Thermodynamic properties of water in the subcooled region. II, *J. Chem. Phys.* **1985**, *82*, 1440.

(5) Heydari, G. ; Thormann, E. ; Järn, M. ; Tyrode, E. ;; Claesson, P. , Hydrophobic Surfaces Topography Effects on Wetting by supercooled water and freezing delay, *J. Phys. Chem. Part C Nanomater. Interfaces* **2013**, *117*, 21752–21762.

(6) Pruppacher, H. R.; Klett, J. D.; Wang, P. K. Microphysics of Clouds and Precipitation; **1998**; 28, 381-382.

(7) Fletcher, N. H. , Size effect in heterogeneous nucleation, *J. Chem. Phys.* **1958**, *29*, 572.

(8) Jung, S.; Dorrestijn, M.; Raps, D.; Das, A.; Megaridis, C. M.; Poulikakos, D. , Are Superhydrophobic Surfaces Best for Icephobicity, *Langmuir* **2011**, *27*, 3059–3066.

(9) Kloubek, J. , Calculation of surface free energy components of ice according to its wettability by water, chlorobenzene, and carbon disulfide, *J. Colloid Interface Sci.* **1974**, *46*, 185–190.

(10) Makkonen, L. , Surface Melting of Ice, *J. Phys. Chem. B* **1997**, *101*, 6196–6200.

(11) Wang, J.; Liu, Z.; Gou, Y.; Zhang, X.; Cheng, S. , Deformation of freezing water droplets on a cold copper surface, *Sci. China, Ser. E Technol. Sci.* **2006**, *49*, 590–600.

(12) Menini, R.; Ghalmi, Z.; Farzaneh, M. , Highly resistant icephobic coatings on aluminum alloys, *Cold Reg. Sci. Technol.* **2011**, *65*, 65–69.

(13) Huang, L.; Liu, Z.; Liu, Y.; Gou, Y.; Wang, L. , Effect of contact angle on water droplet freezing process on a cold flat surface, *Exp. Therm. Fluid Sci.* **2012**, *40*, 74–80.

3.2 DISCUSSION

After the in-depth study of the ice formation problems on heat exchangers' fins in cold working days, all current and common techniques and methods for its formation prevention and control are evaluated.

Since the passive ice control methods used in air to air heat exchangers can prevent and control the ice formation without requiring energy and leading to a reduction in the efficiency of the system, they have been the subject of recent research and of this PhD study. The passive method is dependent on the surface characteristics of the substrate that the ice is willing to form on it. Therefore, the focus of this PhD study is the effect of surface characteristics on ice nucleation and formation and freezing delay.

Due to its special characteristics such as its relatively low cost, light weight, high heat conductivity and proper corrosion resistance, the main material for heat exchanger production is aluminum alloy. Therefore, the substrate selected for all experiments and investigations of this study is aluminum alloy 8011, which came from the production line of heat exchanger' fins.

The high surface roughness and inhomogeneous surface of aluminum alloy renders it almost impossible to measure the receding contact angle on its surface, this is due to the pinning phenomenon and the continuous reduction of the contact angle caused by evaporation. Moreover, aluminum alloy has a higher contact angle than expected from a metal surface with a high surface energy of 78 degrees. This is due to the fact that, even in a short term exposure to atmosphere, any clean hydrophilic surface will be contaminated by hydrophobic organic contamination and consequently, its water contact angle on the surface will increase.

For the surface modification different mechanical and chemical methods were applied in order to study the effect of surface modification on the wetting properties and consequently, on the icing problem. Polishing and coating techniques for changing the surface morphology and chemical composition of the surface was chosen for further investigations. The coating technique is an effective method for modifying the surfaces by keeping the substrate as an aluminum alloy. This is due to the fact that the surface will adopt the surface properties of the coated material. The results showed that the chemical and mechanical surface modification of bare aluminum can change the contact angle and wettability from 15° to 124° degree and the surface roughness of initial aluminum surface from 84 nm to 15 nm or up to 99 nm. The change in the surface roughness upon mechanical polishing causes wetting regime transition from Cassie–Baxter's to Wenzel's regime.

The surface characteristics have an impact on ice nucleation, formation and growth rate and on the density in the initial stage of ice nucleation and formation. The study of the patterns of condensed water droplets on the aluminum samples with different surface characteristics showed that the hydrophilic sample group of brushed hyperbranched polyethylene glycol (PEG) has the highest surface coverage and the hydrophobic sample group with fluorinated silane coat has the lowest surface coverage by droplet. Also the droplet pattern was smaller in size, and the more uniformly distributed droplets correlated with a lower ice growth rate for this group as compared to others. Due to the low surface coverage, small size droplet and more uniformly distributed droplet on top of the modified hydrophobic sample surfaces (samples with fluorinated silane coat and samples with fluorinated silane coat on top of hydrophilic coat of brushed hyperbranched polyethylene glycol), they exhibit a lower heat transfer rate and consequently, slower ice growth kinetics and growth rate.

According to nucleation theory, the hydrophilic sample group with a coating layer of PEG and with a lower contact angle will also have a lower energy barrier for nucleation, and according to the investigation, it will have a higher surface coverage of around 86% ± 5% of the total surface. These lead to the high density of the nucleation center during the early stage of ice formation caused by mass transfer from humid air and higher ice thickness and growth rate.

There is a relation between the contact angle and formed ice density. The lower surface contact angle has the lower formed ice density on the surface; expect the bare aluminum samples which do not follow the trend of this study.

Therefore, in order to explain the difference in the density of formed ice on top of the different surfaces, the ice layer structure of all sample groups with different surface characteristics are investigated and compared and validated with other previous studies.

The bare aluminum sample group had rather different ice morphology compared to the other groups of hydrophilic and hydrophobic samples. Compared to the other groups, bare aluminum had a feather-like structure in all psychrometric experimental conditions with a larger distance between the ice tip-growth centers. This ice morphology and structure was caused by the significant non uniformity of the surfaces of the bare aluminum samples due to the presence of different intermetallic inclusion in this alloy chemical structure and surface. This observation may explain the observation of a lower ice density on top of the bare aluminum as compared to the other groups.

The investigation of the ice structure on top of the sample groups showed that all sample groups expect the bare aluminum exhibited a grass-like ice structure with closer ice tip-growth centers and a denser ice structure.

It may then be concluded that on such a heterogeneous surface structure, a wetting angle does not provide a complete picture, it only corresponds to average (in the Cassie-Baxter sense) surface properties.

Moreover, in order to study the role of surface chemistry on the ice formation, ice nucleation and freezing delay, four groups of samples with different surface chemistry were prepared with the substrate as aluminum alloy 8011. For studying the effect of the surface chemistry, different coating materials were applied to have almost same surface topography but different surface chemistry and consequently different wettability.

The freezing delay of a water droplet on precooled substrates of an aluminum alloy was investigated. The freezing delays and water contact angles were measured as a function of the substrate temperature, and the results were compared to the predictions of the heterogeneous ice nucleation theory.

In order to activate the aluminum surface for the further chemical surface modification and for preparing a clean aluminum surface, the water-vapor plasma treatment method was chosen. According to the measurements in this activation technique, the surface roughness remains almost in a same range with bare aluminum alloy. The water-vapor plasma treated aluminum samples showed low contact angles and hydrophilic characteristics due to hydrophobic contaminants removal from bare aluminum samples.

Hydrophilic and hydrophobic samples were prepared through the application of coating surface modification technique prior to activating the bare aluminum oxide layer by water-vapor plasma treatment. The coating method applied in the previous investigation of this study is applied for the preparation of the hydrophobic samples; this method is molecular vapor deposition of fluorinated silane. The hydrophilic samples are also prepared prior to the surface activation by the molecular vapor deposition of (3-aminopropyl) triethoxy silane (APTES).

For all four groups of samples, it is observed that the freezing delay of a water droplet placed on a precooled substrate from -5°C to -20°C decreases with the decreasing substrate temperature. However, it is also observed that the magnitude of the delay and the relative changes in temperature differ significantly for the four groups of samples.

The results of freezing delay in the temperature range of -5°C to -20°C showed that the freezing delay of the bare aluminum sample group constantly decrease when the temperature decreases. APTES and the PFOS-modified sample group exhibited a rapid decrease in freezing delay (around 98% of the entire freezing delay drop from -5°C to -20°C) in the temperature interval between -5°C and-10°C and then a slow decrease with further reductions in temperature. Moreover, for the water-vapor plasma treated sample group, the freezing delay dropped at -5°C and the freezing delay dropped to below 10 s at temperatures below -10°C; the same applied to the PFOS sample group, however, the APTES sample group showed a freezing delay of more than 100 s down to -25°C.

In this study, the observation of freezing delay is in qualitative agreement with the calculation of the energy barrier for the heterogeneous nucleation of an ice embryo for all four different sample groups as a function of temperature. Calculations show a sudden decrease in the energy barrier of nucleation in a temperature range of 0°C to -10°C, and the decrease becomes less pronounced when the temperature is further decreased.

Moreover, in order to understand and clarify the differences in freezing delay and how it changes, the wettability of different sample surfaces was investigated. This was done by measuring the changes in the contact angles of the modified surfaces in the temperature range of +25°C to -20°C.

The investigation results showed that the contact angles on the surfaces of the bare aluminum and the APTES-modified sample group exhibited a smooth and slight decrease with decreasing temperatures in the interval between +20°C and -25°C. Such a decrease is expected and can be explained by the temperature dependence of the surface tension of water.

In addition, the results showed that the water-vapor plasma treated and PFOS-modified sample groups exhibited an abrupt increase in the contact angle in the temperature ranges in which the freezing delays also change dramatically. This transition in the wetting behavior cannot be related to the surface tension of water.

The contact angles of these groups of sample are changing suddenly in temperature range around -5°C to -10°C which the ice can form. It can be explain by the sublimation and growth of ice on the cold substrates before the water droplet is placed on the substrate. The ice formation on the surface changes the wettability of the surface. The contact angle of water on ice has been measured in previous studies by other researchers, and these have shown that the contact angle increases when the water droplet temperature is decreased. This is in line with the observations of this study for PFOS and water plasma treated samples.

Beyond all investigations and studies of ice formation and its relation to the surface characteristics, it is obvious that the ice formation process is a sensitive phenomenon which goes beyond the surface conditions. Consequently, according to the experimental conditions such as humidity, air temperature, water temperature and also the droplet size and how the droplet is placed on the surface, the kinetics of the ice formation process and thus, the measured freezing delays and other factors related to the ice formation may differ.

CHAPTER 4. CONCLUSIONS AND FUTURE WORK

As explained in the introduction, this study aimed to find an innovative and pragmatic solution for the ice formation problem of aluminum alloy surfaces and make suggestions for future research. Aluminum alloy 8011 was chosen as the main material and substrate for this study. This is due to the fact that aluminum alloys are the main material used for the production of heat exchanger and many other industrial applications with the ice formation problem. In this chapter, the main conclusions of this study are described and explained. Moreover, future research directions are suggested which may provide the next steps along the path to finding a practical and widely applicable solution for the ice formation problem.

4.1 CONCLUSIONS

The aim of this PhD study was to find a solution for the control and prevention of ice formation on air to air heat exchangers by focusing on the energy saving perspective. The study and review of the existing methods for ice formation control and prevention showed that two types of methods for ice control and prevention in air to air heat exchangers are currently used: active and passive methods. The active methods require energy for the prevention and control of ice formation, and the passive methods focus on the surface characteristics of heat exchanger fins for preventing and controlling the ice formation for certain duration of time without requiring energy. Since, as previously mentioned, the aim of this PhD study was to find an energy saving method, the passive methods came into focus in this PhD study.

Moreover, as the passive methods are based on changing the surface characteristics of heat exchanger fins and the main material for heat exchangers production is aluminum alloy, aluminum alloy was chosen as the main material and substrate for the investigations.

The effect of tailoring surface characteristics and morphology on the wettability and roughness of different aluminum alloy substrates: aluminum alloy as received from the production line, polished one and aluminum foil surface were investigated.

The results showed that the wettability of the aluminum samples was increased by changing the surface morphology through the formation of a hydrophilic PEG layer by surface-initiated polymerization. The PEG layer increased the roughness of the samples and led to the lower contact angles. Moreover, the large increase was observed upon forming PEG on top of the samples with a higher initial surface roughness. On the contrary, the aluminum samples became hydrophobic by molecular vapor deposition of low surface energy perfluorooctylsilane on their surface.

Since the hydrophobicity of the hydrophobic samples (PFOS samples) are increased with increasing the surface roughness, it can be concluded that they followed the Wenzel model and the bare unpolished and unpolished PEG samples followed the Cassie–Baxter model due to their high roughness and the presence of air pockets in their structure. It can be concluded that changing the surface roughness upon mechanical polishing and mechanical surface modification in aluminum samples leads to a transition from the Cassie–Baxter's to Wenzel's regime.

The results showed another interesting wetting characteristic for aluminum alloy 8011, such as a rather high contact angle of 78°. This observation can be explained by the effect of organic contamination on its surface caused by the exposure to atmosphere and its high roughness and presence of air pockets on its grooves. It should be noted that the rough and inhomogeneous surface of aluminum rendered it impossible to measure the receding contact angle on its surface due to the pinning phenomenon.

Moreover, the effect of psychrometric parameters, such as air humidity and cold surface temperature together with the effects of surface chemical modification on the ice formation thickness, structure, ice density and ice deposition on top of the aluminum alloy 8011 was investigated experimentally in an attempt to increase the knowledge of this alloy and its application in heat exchangers.

The results of the distribution of water droplets observed upon melting of the incipient ice layer showed that, in general, the size distribution of the droplets formed on the samples was not uniform and thus reflected the heterogeneous nature of nucleation. For instance, hydrophobic substrates with PFOS on top exhibited a lower surface coverage, smaller size, and more uniformly distributed droplets. This also correlates with the lower ice growth rate observed for these hydrophobic surfaces due to smaller area of water–substrate interface and lower heat transfer from the cold surface to the droplets and slower growth kinetics.

On the other hand, the hydrophilic surface samples (bare samples and samples with PEG layer) have a lower energy barrier for nucleation as compared to hydrophobic surfaces and higher rates of ice growth and therefore, the ice thickness on the surface of the hydrophilic samples at all temperatures were investigated (−6, −8, and −10 ◦C).

The investigation showed that, during the early stages of ice formation, both the rate of ice growth and the thickness of the formed ice are higher on the hydrophilic surfaces as compared to the hydrophobic ones.

The mass of ice deposited in identical time intervals was almost identical for all samples, which may be interpreted as indecency of mass transfer coefficient to surface wettability and contact angle. This led to a reverse relation between the obtained ice density from measurements and ice thickness. The samples with a thicker ice layer exhibited a lower density and vice versa.

The high dependency of freezing delay to the substrate chemistry was investigated. Moreover, for the first time, the dependency of the wettability of different types of surfaces on the substrate temperature for a wide range of substrates was investigated in this study, and this investigation showed interesting results.

The contact angle on the bare aluminum and the APTES coated substrate decreases slightly with decreasing temperatures in the interval between +20°C and -25°C which can be explained by the temperature dependency of the surface tension of water; however, within the same temperature range, the abrupt increase in the contact angle for water plasma treated sample groups and the PFOS group cannot be explained by the temperature dependency of the surface tension of water. This observation can be argued and explained by the sublimation and growth of ice on the cold substrates of the water plasma treated sample groups and the PFOS group before the water droplet is placed on the substrate. This is due to the fact that, according to previous observations, the contact angle of water on ice was increased with decreasing the temperature.

The bare aluminum alloy sample group exhibited a continuous decrease in freezing delay with decreasing the substrate temperature. On the other hand, the freezing delay for water-plasma treated samples, as well as APTES and PFOS groups showed a sharp drop in the temperature interval between -5°C and -10°C followed by a slow decrease in freezing delay upon a further reduction of the temperature to -20°C. The magnitude of the delay and their relative temperature changes differed significantly for the four groups of samples: for the water-vapor plasma treated and the PFOS modified surfaces, the freezing delays dropped to below 10 s at temperatures below -10°C, while in the case of the APTES modified surface the freezing delay stayed above 100 s down to -25°C. The observed results of the freezing delay were compared to the expectations from nucleation theory and possible deviations from this theory were discussed.

The calculation of the energy barrier for the homogeneous nucleation of an ice embryo and for the heterogeneous nucleation on four different substrates as a function of temperature showed a fast decrease when the temperature was lowered from 0°C to −10°C. The reduction in the energy barrier of nucleation became less pronounced when the temperature was further decreased to -20°C. This observation was thus in qualitative agreement with our results from the modified samples, which showed a fast decrease in the freezing delay in the temperature interval between 0°C and −10°C; after this point the change in the freezing delay became moderate. On the other hand, some of the predictions of a high energy barrier for the PFOS group as compared to the APTES and water plasma treated sample groups is in apparent disagreement with our experimental results, which showed a longer freezing delay on the APTES-modified samples and shorter and very similar freezing delays on the PFOS- and the water-vapor plasma-modified samples.

The long freezing delay on the APTES surface may be explained by the presence of high local ion concentration of amino groups which can prevent the formation of an ice layer and ultimately lead to longer freezing delays.

The results of this study indicate that hydrophobic surfaces may not offer the best choice for the design and production of anti-freezing applications, as many researches are focuses previously.

These new observations can give insights to and help us understand the specific mechanisms and the dependency of freezing and icing on surface morphology, chemistry and to the operation. This can be helpful for the design and practical application of anti-icing systems, such as heat exchangers.

4.2 SUGGESTIONS FOR FUTURE WORK

In this work, the effect of surface modifications on the formed ice thickness and density is studied. Since thermal conductivity is another crucial ice property that may affect the performance of heat exchangers, it is suggested that the effect of the surface modification on thermal conductivity of formed ice on the modified surface be investigated and studied.

Moreover, as the presence of a high local ion concentration on the aluminum modified surface with APTES coating exhibited a suppression of the freezing point, it is suggested that other ionic coatings with different ion type and concentrations are investigated in terms of how these may affect the freezing delay.

Future works may also focus on applying these acquired results of surface modification on aluminum surfaces to full-scale heat exchanger modeling in order to better understand their effect on the performance of real size heat exchangers in real working conditions.

REFERENCE

[1] D. Danish Government, Strategy for energy renovation of buildings, 2014.

[2] International Energy Agency, Energy Efficiency Requirements in Building Codes, Energy Efficiency Policies for New Buildings, (2008). http://www.iea.org/g8/2008/Building_Codes.pdf.

[3] R. Mohammad, K. Miklos, G.. Gaoming, S. Carey J, Evaluation of defrosting methods for air-to-air heat/energy exchangers on energy consumption of ventilation, Appl. Energy. 151 (2015) 32–40.

[4] Air-to-Air Energy Recovery, in: ASHRAE Syst. Equip. Handb., 2003: p. 44.-44.19.

[5] C.J.L. Hermes, An analytical solution to the problem of frost growth and densification on flat surfaces, Int. J. Heat Mass Transf. 55 (2012) 7346–7351. doi:10.1016/j.ijheatmasstransfer.2012.06.070.

[6] A. Alizadeh, M. Yamada, R. Li, W. Shang, S. Otta, S. Zhong, et al., Dynamics of Ice Nucleation on Water Repellent Surfaces, Langmuir. 28 (2012) 3180–3186.

[7] N. Saleema, M. Farzaneh, R.W. Paynter, Prevention of Ice Accretion on Aluminum Surfaces by Enhancing Their Hydrophobic Properties, J. Adhes. Sci. Technol. 25 (2011) 27–40.

[8] J. Kragh, J. Rose, T.R. Nielsen, S. Svendsen, New counter flow heat exchanger designed for ventilation systems in cold climates, Energy Build. 39 (2007) 1151–1158. doi:10.1016/j.enbuild.2006.12.008.

[9] E.G. Phillips, R.E. Chant, D.R. Fisher, B.C. Bradley, D.R. Fisher, Comparison of Freezing Control Strategies for Residential Air-to-Air Heat Recovery Ventilators, ASHRAE Trans. 95 (1989) 484–490.

[10] R. Ahmed, J. Appelhoff, Frost-protection measures in energy recuperation with multiple counterflow heat exchangers, Rehva. 5 (2013) 37–40.

[11] H. Chen, L. Thomas, R.W. Besant, Fan supplied heat exchanger fin performance under frosting conditions, Int. J. Refrig. 26 (2003) 140–149.

[12] B.J.F. Straube, D. Ph, Moisture in Buildings, (2002) 15–19.

[13] M. Rahimi, A. Afshari, Control and prevention of ice formation and accretion on heat exchangers for ventilation systems, in: Heal. Build. Conf. Eur. 2015, Eindhoven, 2015.

[14] P.T. Ninomura, R. Bhargava, Heat recovery ventilators in multifamily resi-dences in the arctic, ASHRAE Trans. 101 (95AD) 961–966.

[15] M. Rafati, M. Fauchoux, R.W. Besant, C.J. Simonson, A review of frosting in air-to-air energy exchangers, Renew. Sustain. Energy Rev. 30 (2014) 538–554. doi:10.1016/j.rser.2013.10.038.

[16] J. Kragh, J. Rose, S. Svendsen, Mechanical ventilation with heat recovery in cold climates, Proc. Seventh Nord. Symp. Build. Phys. Nord. Countries, Tech. Univ. Denmark. (2005) 1–8.

[17] M. Rahimi, A. Afshari, P. Fojan, L. Gurevich, The effect of surface modification on initial ice formation on aluminum surfaces, Appl. Surf. Sci. 355 (2015) 327-333. doi:10.1016/j.apsusc.2015.06.201.

[18] K. Kim, K.-S. Lee, Frosting and defrosting characteristics of a fin according to surface contact angle, Int. J. Heat Mass Transf. 54 (2011) 2758–2764. doi:10.1016/j.ijheatmasstransfer.2011.02.065.

[19] R. Menini, Z. Ghalmi, M. Farzaneh, Highly resistant icephobic coatings on aluminum alloys, Cold Reg. Sci. Technol. 65 (2011) 65–69. doi:10.1016/j.coldregions.2010.03.004.

[20] Z. Qi, Water retention and drainage on air side of heat exchangers—A review, Renew. Sustain. Energy Rev. 28 (2013) 1–10. doi:10.1016/j.rser.2013.07.014.

[21] M.A. Rahman, A.M. Jacobi, Drainage of frost melt water from vertical brass surfaces with parallel microgrooves, Int. J. Heat Mass Transf. 55 (2012) 1596–1605. doi:10.1016/j.ijheatmasstransfer.2011.11.015.

[22] M. Rahimi, P. Fojan, L. Gurevich, A. Afshari, Effects of aluminium surface morphology and chemical modification on wettability, Appl. Surf. Sci. 296 (2014) 124–132. doi:10.1016/j.apsusc.2014.01.059.

[23] H. Lee, J. Shin, S. Ha, B. Choi, J. Lee, Frost formation on a plate with different surface hydrophilicity, Int. J.

Heat Mass Transf. 47 (2004) 4881–4893. doi:10.1016/j.ijheatmasstransfer.2004.05.021.

[24] Z. Liu, X. Zhang, H. Wang, S. Meng, S. Cheng, Influences of surface hydrophilicity on frost formation on a vertical cold plate under natural convection conditions, Exp. Therm. Fluid Sci. 31 (2007) 789–794. doi:10.1016/j.expthermflusci.2006.08.004.

[25] M.K. Kwak, H.-E. Jeong, T. Kim, H. Yoon, K.Y. Suh, Bio-inspired slanted polymer nanohairs for anisotropic wetting and directional dry adhesion, Soft Matter. 6 (2010) 1849. doi:10.1039/b924056j.

[26] L. Cao, A.K. Jones, V.K. Sikka, J. Wu, D. Gao, Anti-icing superhydrophobic coatings., Langmuir. 25 (2009) 12444–8. doi:10.1021/la902882b.

[27] S. Farhadi, M. Farzaneh, S. a. Kulinich, Anti-icing performance of superhydrophobic surfaces, Appl. Surf. Sci. 257 (2011) 6264–6269. doi:10.1016/j.apsusc.2011.02.057.

[28] S. a. Kulinich, S. Farhadi, K. Nose, X.W. Du, Superhydrophobic surfaces: are they really ice-repellent?, Langmuir. 27 (2011) 25–9. doi:10.1021/la104277q.

[29] M. Nosonovsky, V. Hejazi, Why superhydrophobic surfaces are not always icephobic., ACS Nano. 6 (2012) 8488–91. doi:10.1021/nn302138r.

[30] L. Oberli, D. Caruso, C. Hall, M. Fabretto, P.J. Murphy, D. Evans, Condensation and freezing of droplets on superhydrophobic surfaces, Adv. Colloid Interface Sci. 210 (2014) 47–57. doi:10.1016/j.cis.2013.10.018.

[31] S. Jung, M. Dorrestijn, D. Raps, A. Das, C.M. Megaridis, D. Poulikakos, Are Superhydrophobic Surfaces Best for Icephobicity, Langmuir. 27 (2011) 3059–3066. doi:10.1021/la104762g.

[32] J. Wang, Z. Liu, Y. Gou, X. Zhang, S. Cheng, Deformation of freezing water droplets on a cold copper surface, Sci. China, Ser. E Technol. Sci. 49 (2006) 590–600. doi:10.1007/s11431-006-2017-y.

[33] K. Prolss, G. Schmitz, Modeling of Frost Growth on Heat Exchanger Surfaces, Proc. 5th Model. Conf. (2006) 509–516.

[34] C.-H. Cheng, C.-C. Shiu, Frost formation and frost crystal growth on a cold plate in atmospheric air flow, Int. J. Heat Mass Transf. 45 (2002) 4289–4303. doi:10.1016/S0017-9310(02)00134-5.

[35] Y. Tao, Y. Mao, R. Besant, Frost growth characteristics on heat exchanger surfaces measurement and simulation studies, ASME HEAT Transf. HTD—Vol. 2 (1994) 29–38.

[36] Y. Hayashi, A. Aoki, S. Adashi, K. Hori, Study of frost properties correlating with frost formation types, ASME J. Heat Transf. 99 (1977) 239–245.

[37] R. LE Gall, J.M. Grillot, C. Jallut, Modelling of frost growth and densification, 40 (1997) 3177–3187.

[38] C.J.L. Hermes, R.O. Piucco, J.R. Barbosa, C. Melo, A study of frost growth and densification on flat surfaces, Exp. Therm. Fluid Sci. 33 (2009) 371–379. doi:10.1016/j.expthermflusci.2008.10.006.

[39] Y.-X. Tao, R.W. Besant, Y. Mao, Characteristics of Frost Growth on a Flat Plate During the Early Growth Period, ASHRAE Trans. 99 (1993) 746–753.

[40] B. Na, R.L. Webb, New model for frost growth rate, Int. J. Heat Mass Transf. 47 (2004) 925–936. doi:10.1016/j.ijheatmasstransfer.2003.09.001.

[41] Y.B. Lee, S.T. Ro, Analysis of the frost growth on a flat plate by simple models of saturation and supersaturation, Exp. Therm. Fluid Sci. 29 (2005) 685–696. doi:10.1016/j.expthermflusci.2004.11.001.

[42] Y. Hayashi, K. Aoki, H. Yuhura, Study of Frost Formation Based on a Theoretical Model of the Frost Layer, Trans. Japan Soc. Mech. Eng. 40 (1976) 885–899.

[43] R.O. Piucco, C.J.L. Hermes, C. Melo, J.R. Barbosa, A study of frost nucleation on flat surfaces, Exp. Therm. Fluid Sci. 32 (2008) 1710–1715. doi:10.1016/j.expthermflusci.2008.06.004.

[44] G.; Heydari, E.; Thormann, M.; Järn, E.; Tyrode, P. Claesson, Hydrophobic Surfaces Topography Effects on Wetting by supercooled water and freezing delay.pdf, J. Phys. Chem. Part C Nanomater. Interfaces. 117 (2013) 21752–21762.

[45] M. Rahimi, A. Afshari, E. Thormann, E ff ect of Aluminum Substrate Surface Modi fi cation on Wettability and Freezing Delay of Water Droplet at Subzero Temperatures, ACS Appl. Mater. Interfaces. 8 (2016)

11147–11153. doi:10.1021/acsami.6b02321.

[46] H. Butt, K. Graf, M. Kappl, Physics and Chemistry of Interfaces, WILEY-VCH GmbH & Co . KGaA, 2003.

[47] R. Tadmor, Line energy and the relation between advancing, receding, and young contact angles., Langmuir. 20 (2004) 7659–64. doi:10.1021/la049410h.

[48] Y. Yuan, T.R. Lee, Surface Science Techniques, Springer Berlin Heidelberg, Berlin, Heidelberg, 2013. doi:10.1007/978-3-642-34243-1.

[49] R.N. Wenzel, Resistance of solid surfaces, Ind. Eng. Chem. 28 (1936) 988–994.

[50] A.B.D. Cassie, S. Baxter, Wettability of porous surfaces, Trans. Faraday Soc., Trans. Faraday Soc. 40 (1944) 546–551.

[51] A. Marmur, E. Bittoun, When Wenzel and Cassie are right: reconciling local and global considerations., Langmuir. 25 (2009) 1277–81. doi:10.1021/la802667b.

[52] C. Dorrer, J. Rühe, Drops on microstructured surfaces coated with hydrophilic polymers: Wenzel's model and beyond, Langmuir. 24 (2008) 1959–64. doi:10.1021/la7029938.

[53] N.J. Shirtcliffe, G. McHale, M. I. Newton, The superhydrophobicity of polymer surfaces: Recent developments, J. Polym. Sci. Part B Polym. Phys. 49 (2011) 1203–1217. doi:10.1002/polb.22286.

[54] J. Drelich, E. Chibowski, D.D. Meng, K. Terpilowski, Hydrophilic and superhydrophilic surfaces and materials, Soft Matter. 7 (2011) 9804–9828. doi:10.1039/c1sm05849e.

[55] S. a. Kulinich, M. Farzaneh, Ice adhesion on super-hydrophobic surfaces, Appl. Surf. Sci. 255 (2009) 8153–8157. doi:10.1016/j.apsusc.2009.05.033.

[56] C. Bourg, M.E.R. Shanahan, Influence of Evaporation on Contact Angle, Int. J. Adhes. Adhes. 14 (1995) 2820–2829.

[57] M. Miwa, A. Nakajima, A. Fujishima, K. Hashimoto, Effects of the Surface Roughness on Sliding Angles of Water Droplets on Superhydrophobic Surfaces, 1998 (2000) 5754–5760.

[58] M.E.R. Shanahan, C. Bourg, Effects of evaporation on contact angles on polymer surfaces, Int. J. Adhes. Adhes. 14 (3) (1994) 201–205.

[59] E. Bormashenko, Wetting transitions on biomimetic surfaces., Philos. Trans. A. Math. Phys. Eng. Sci. 368 (2010) 4695–711. doi:10.1098/rsta.2010.0121.

[60] E. Bormashenko, A. Musin, M. Zinigrad, Evaporation of droplets on strongly and weakly pinning surfaces and dynamics of the triple line, Colloids Surfaces A Physicochem. Eng. Asp. 385 (2011) 235–240. doi:10.1016/j.colsurfa.2011.06.016.

[61] K.R. Jensen, P. Fojan, R.L. Jensen, L. Gurevich, Water Condensation: A Multiscale Phenomenon, J. Nanosci. Nanotechnol. 14 (2014) 1859–1871. doi:10.1166/jnn.2014.9108.

[62] W. Possart, H. Kamusewitz, Wetting and scanning force microscopy on rough polymer surfaces: Wenzel's roughness factor and the thermodynamic contact angle, Appl. Phys. A Mater. Sci. Process. 76 (2003) 899–902. doi:10.1007/s00339-002-1972-9.

[63] N.H. Fletcher, The Chemical Physics of Ice, 1st ed., Cambridge, 1970. doi:http://dx.doi.org/10.1017/CBO9780511735639.

[64] P. Hao, C. Lv, X. Zhang, Freezing of sessile water droplets on surfaces with various roughness and wettability, Appl. Phys. Lett. 104 (2014) 161609. doi:10.1063/1.4873345.

[65] M. a. Floriano, C. a. Angell, Surface Tension and Molar Surface Free Energy and Entropy of Water to -27.2 °C, J. Phys. Chem. 94 (1990) 4199–4202. doi:10.1021/j100373a059.

[66] J. V. Leyendekkers, R.J. Hunter, Thermodynamic properties of water in the subcooled region. I, J. Chem. Phys. 82 (1985) 1440. doi:10.1063/1.448417.

[67] H.R. Pruppacher, J.D. Klett, P.K. Wang, Microphysics of Clouds and Precipitation, 1998. doi:10.1080/02786829808965531.

[68] N.H. Fletcher, Size effect in heterogeneous nucleation, J. Chem. Phys. 29 (1958) 572.

doi:10.1063/1.1744540.

[69] L. Makkonen, Surface Melting of Ice, J. Phys. Chem. B. 101 (1997) 6196–6200. doi:10.1021/jp963248c.

[70] S. Jung, M. Dorrestijn, D. Raps, A. Das, C.M. Megaridis, D. Poulikakos, Supporting Information Are Are superhydrophobic surfaces best for icephobicity?, Langmuir. 27 (2011) 3059–3066. doi:10.1021/la104762g.

[71] B. Na, R.L. Webb, A fundamental understanding of factors affecting frost nucleation, Int. J. Heat Mass Transf. 46 (2003) 3797–3808. doi:10.1016/S0017-9310(03)00194-7.

[72] A.R. Balkenende, H.J.A.P. van de Boogaard, M. Scholten, N.P. Willard, Evaluation of different approaches to assess the surface tension of low-energy solids by means of contact angle measurements, Langmuir. 14 (1998) 5907–5912. doi:10.1021/la9801110.

[73] J. Shin, A. V. Tikhonov, C. Kim, Experimental Study on Frost Structure on Surfaces With Different Hydrophilicity: Density and Thermal Conductivity, J. Heat Transfer. 125 (2003) 84. doi:10.1115/1.1518496.

[74] N. Seki, S. Fukusako, K. Matsuo, S. Uemura, An analysis of incipient frost formation, Wärme- Und Stoffübertragung. 19 (1985) 9–18. doi:10.1007/BF01682542.

[75] L. Mishchenko, B. Hatton, V. Bahadur, J.A. Taylor, T. Krupenkin, J. Aizenberg, Design of ice-free nanostructured surfaces based on repulsion of impacting water droplets, ACS Nano. 4 (2010) 7699–7707. doi:10.1021/nn102557p.

[76] D.P. Singh, J.P. Singh, Delayed freezing of water droplet on silver nanocolumnar thin film, Appl. Phys. Lett. 102 (2013) 243112. doi:10.1063/1.4811751.

[77] H. Wang, G. He, Q. Tian, Effects of nano-fluorocarbon coating on icing, Appl. Surf. Sci. 258 (2012) 7219–7224. doi:10.1016/j.apsusc.2012.04.043.

[78] M. Khan, W.T.S. Huck, Hyperbranched Polyglycidol on Si / SiO 2 Surfaces via Surface-Initiated Polymerization, 46 (2003) 5088–5093.

[79] G.R. Stratton, C.L. Bellona, F. Dai, T.M. Holsen, S.M. Thagard, Plasma-based water treatment: Conception and application of a new general principle for reactor design, Chem. Eng. J. 273 (2015) 543–550. doi:10.1016/j.cej.2015.03.059.

[80] N.A. Alcantar, E.S. Aydil, J.N. Israelachvili, Polyethylene glycol – coated biocompatible surfaces, J. Biomed. Mater. Res. 51 (2000) 343–351.

[81] S. Fiorilli, P. Rivolo, E. Descrovi, C. Ricciardi, L. Pasquardini, L. Lunelli, et al., Vapor-phase self-assembled monolayers of aminosilane on plasma-activated silicon substrates, J. Colloid Interface Sci. 321 (2008) 235–241. doi:10.1016/j.jcis.2007.12.041.

[82] X. Song, J. Zhai, Y. Wang, L. Jiang, Self-assembly of amino-functionalized monolayers on silicon surfaces and preparation of superhydrophobic surfaces based on alkanoic acid dual layers and surface roughening, J. Colloid Interface Sci. 298 (2006) 267–273. doi:10.1016/j.jcis.2005.11.048.

[83] F. Zhang, K. Sautter, A.M. Larsen, D. a. Findley, R.C. Davis, H. Samha, et al., Chemical vapor deposition of three aminosilanes on silicon dioxide: Surface characterization, stability, effects of silane concentration, and cyanine dye adsorption, Langmuir. 26 (2010) 14648–14654. doi:10.1021/la102447y.

[84] A. Yadav, R. Sriram, J. Carter, B. Miller, Comparative Study of Solution Phase and Vapor Phase Deposition of Aminosilanes on Silicon Dioxide Surfaces, Mater Sci Eng C Mater Biol Appl. (2014) 283–290. doi:10.1016/j.msec.2013.11.017.Comparative.

[85] F. Zhang, Chemical Vapor Deposition of Silanes and Patterning on Silicon, Brigham Young University, 2010.

[86] I. Horcas, R. Fernández, J.M. Gómez-Rodríguez, J. Colchero, J. Gómez-Herrero, a M. Baro, WSXM: a software for scanning probe microscopy and a tool for nanotechnology., Rev. Sci. Instrum. 78 (2007) 13705. doi:10.1063/1.2432410.

[87] K.S. Lee, S. Jhee, D.-K. Yang, Prediction of the frost formation on a cold flat surface, Int. J. Heat Mass Transf. 46 (2003) 3789–3796. doi:10.1016/S0017-9310(03)00195-9.

[88] I. Tokura, H. Saito, K. Kishinami, Study on properties and growth rate of frost layers on cold surface.pdf,

Trans. ASME,J. Heat Transf. 105 (1983) 895–901.

[89] E. Moallem, L. Cremaschi, D.E. Fisher, S. Padhmanabhan, Experimental measurements of the surface coating and water retention effects on frosting performance of microchannel heat exchangers for heat pump systems, Exp. Therm. Fluid Sci. 39 (2012) 176–188. doi:10.1016/j.expthermflusci.2012.01.022.

[90] S. Jung, M.K. Tiwari, N.V. Doan, D. Poulikakos, Mechanism of supercooled droplet freezing on surfaces, Nat. Commun. 3 (2012) 615. doi:10.1038/ncomms1630.

[91] P.L.T. Brian, R.C. Reid, Y.T. Shah, Frost Deposition on Cold Surfaces, Ind. Eng. Chem. Fundam. 9 (1970) 375–380. doi:10.1021/i160035a013.

[92] S.R. Friedman, M. Khalil, P. Taborek, Wetting transition in water, Phys. Rev. Lett. 111 (2013) 1–5. doi:10.1103/PhysRevLett.111.226101.

[93] L. Huang, Z. Liu, Y. Liu, Y. Gou, L. Wang, Effect of contact angle on water droplet freezing process on a cold flat surface, Exp. Therm. Fluid Sci. 40 (2012) 74–80. doi:10.1016/j.expthermflusci.2012.02.002.

SUMMARY

In cold climates, mechanical ventilation systems with heat recovery, e.g. air-to-air exchangers, are often used to reduce energy demand for heating by recovering the heat from the exhausted air. This, however, creates a risk of ice accretion on the fins of the heat exchanger as warm and humid exhausted air cools down. Due to the reduction in heat exchanger efficiency due to ice formation, this phenomenon has been studied for many decades. There are two approaches to controlling ice formation on heat exchangers: active and passive. The active methods, e.g. bypass, recirculation, preheating etc., require energy and consequently reduce the overall efficiency of the system. They are not addressed in this work and have already been studied extensively by many researchers. The passive methods, which are related to the surface characteristics of the heat exchanger fins and their effect on the initial phases of ice formation, are the main focus of this PhD study. Since aluminum alloys are commonly used to build air-to-air heat exchangers, their surface characteristics play a crucial role in ice nucleation, formation and accretion. This study is specifically focused on aluminum alloy 8011. Aluminum and its alloys are expected to possess a high energy surface; however, measurements show that the actual surface exhibits a rather high contact angle of about 78 degrees, which is presumably related to surface contamination. In this PhD study, several types of surface modifications were developed that allowed us to obtain stable hydrophilic and hydrophobic surfaces with the contact angles varying from 12° to more than 120°. The effects of these modifications on surface morphology and wettability—the main parameters determining ice nucleation, formation, accretion and freezing delay—were studied comprehensively. In particular, it was found in the first part of study that flat hydrophobic surfaces exhibit slower ice growth and denser ice layers, making this type of treatment preferable for aluminum heat exchangers. Moreover, observations show that the bare aluminum surfaces are characterized by faster ice growth and less dense ice layer as compared to hydrophilically and hydrophobically modified aluminum surfaces. This commonly observed phenomenon can be attributed to the heterogeneous character of bare aluminum surfaces, leading to a broad distribution of surface energies on the microscopic scale. Upon even minor cooling below the freezing point, this leads to the nucleation of widely separated water droplets/ice crystals on high-energy nucleation centers and the formation of low-density feather-like ice structures, hence this significantly deteriorates the performance of heat exchangers with aluminum fins.

Furthermore, the freezing delay and wettability of chemically modified aluminum surface as a function of the substrate temperature was studied. Comparison of the observed behavior with the predictions of the heterogeneous ice nucleation theory showed that a slightly hydrophilic substrate modified with (3-aminopropyl) triethoxy silane (APTES) exhibited longer freezing delays as compared to both more hydrophilic and more hydrophobic substrates. This is attributed to a particular surface chemistry of the APTES modification that prevents ice formation at the interface of the substrate due to presence of high local ion concentration (amino groups), hence leading to significant freezing point suppression. Furthermore, the results suggest that surface topography and wettability determine the freezing kinetics of a droplet placed on a precooled sample. Therefore, surface chemistry which may change these surface characteristics can be used as a tool to control the actual wetting properties of a cold surface in a humid atmosphere.

On the basis of the findings and observations of this study, we find that tailoring the surface characteristics through the application of different chemical or mechanical methods is an effective method for changing the icing properties of a surface. Future studies might focus on studying the effect of different surface coatings with ion concentration on ice formation kinetics.

ISSN (online): 2246-1248
ISBN (online): 978-87-7112-845-1

AALBORG **UNIVERSITY PRESS**